UPPSALA
UNIVERSITET

Digital Comprehensive Summaries of Uppsala Dissertations from the Faculty of Science and Technology 936

Correlated Electronic Structure of Materials

Development and Application of Dynamical Mean Field Theory

PATRIK THUNSTRÖM

ACTA
UNIVERSITATIS
UPSALIENSIS
UPPSALA
2012

ISSN 1651-6214
ISBN 978-91-554-8376-0
urn:nbn:se:uu:diva-173300

Dissertation presented at Uppsala University to be publicly examined in Polhemsalen, Ångströmlaboratoriet, Lägerhyddsvägen 1, Uppsala, Thursday, June 7, 2012 at 09:15 for the degree of Doctor of Philosophy. The examination will be conducted in English.

Abstract
Thunström, P. 2012. Correlated Electronic Structure of Materials: Development and Application of Dynamical Mean Field Theory. Acta Universitatis Upsaliensis. *Digital Comprehensive Summaries of Uppsala Dissertations from the Faculty of Science and Technology* 936. 84 pp. Uppsala. ISBN 978-91-554-8376-0.

This thesis is dedicated to the development, implementation and application of a combination of Density Functional Theory and Dynamical Mean Field Theory. The resulting program is shown through several examples to be a powerful and flexible tool for calculating the electronic structure of strongly correlated materials. The main part of this work is focused on the development and implementation of three methods for solving the effective impurity model arising in the Dynamical Mean Field Theory: Hubbard-I approximation (HIA), Exact Diagonalization (ED), and Spin-Polarized T-matrix Fluctuation-exchange (SPTF). The Hubbard-I approximation is limited to systems where the hybridization between the 4f-orbitals and the rest of the material can be completely neglected, and can therefore not capture any Kondo physics. It has been used to study the atomic-like multiplet spectrum of the strongly localized 4f-electrons in the Lanthanide compounds $YbInCu_4$, YbB_{12}, Yb_2Pd_2Sn, $YbPd_2Sn$, SmB_6, $SmSn_3$, and $SmCo_5$. The calculated spectral properties are shown to be in excellent agreement with experimental direct and inverse photoemission data, clearly affirming the applicability of the Hubbard-I approximation for this class of systems if we are not focusing on Kondo physics. Full self-consistence in both self-energy and electron density is shown to be of key importance in the extraction of the magnetic properties of the hard permanent magnet $SmCo_5$. The Exact Diagonalization solver is implemented as an extension of the Hubbard-I approximation. It takes into account a significant part of the hybridization between the correlated atom and the host through the use of a few effective bath orbitals. This approach has been applied to the long-standing problem of the electronic structure of NiO, CoO, FeO, and MnO. The resulting spectral densities are favorably compared to photoemission spectroscopy. Apart from predicting the correct spectral properties, the Exact Diagonalization solver also provides full access to the many-body density operator. This feature is used to make an in-depth investigation of the correlations in the electronic structure, and two measures of the quantum entanglement of the many-body ground-states are presented. It is shown that CoO possesses the most intricate entanglement properties, due to a competition between crystal field effects and Coulomb interaction, and such a mechanism likely carries over to several classes of correlated electron systems. The Exact Diagonalization solver has also been applied to the prototypical dilute magnetic semiconductor Mn doped GaAs, a material of great importance in the study of future spintronics applications. The problem of Fe impurities in Cs has been used to study the dependence of the spectral properties on the local environment. Finally, the Spin-polarized T-matrix Fluctuation-exchange solver has been implemented and applied to more delocalized electron systems where the effective impurity problem can be solved as a perturbation with respect to the strength of the local Coulomb interaction. This approach has been used to study the magnetic and spectral properties of the late transition metals, Fe, Co and Ni, and NiS.

Keywords: DFT, DMFT, correlation, entanglement

Patrik Thunström, Uppsala University, Department of Physics and Astronomy, Materials Theory, Box 516, SE-751 20 Uppsala, Sweden.

ISSN 1651-6214
ISBN 978-91-554-8376-0
urn:nbn:se:uu:diva-173300 (http://urn.kb.se/resolve?urn=urn:nbn:se:uu:diva-173300)

till mina schegnojer

List of papers

This thesis is based on the following papers, which are referred to in the text by their Roman numerals.

I **Multiplet effects in the electronic structure of intermediate valence compounds**
P. Thunström, I. Di Marco, A. Grechnev, S. Lebègue, M.I. Katsnelson, A. Svane, and O. Eriksson
Phys. Rev. B 79, 165104 (2009)

II **High-resolution photoelectron spectroscopy study of Kondo metals: $SmSn_3$ and $Sm_{0.9}La_{0.1}Sn_3$**
H. Yamaoka, P. Thunström, I. Jarrige, K. Shimada, N. Tsujii, M. Arita, H. Iwasawa, H. Hayashi, J. Jiang, T. Habuchi, D. Hirayama, H. Namatame, M. Taniguchi, U. Murao, S. Hosoya, A. Tamaki, and H. Kitazawa
Phys. Rev. B 85, 115120 (2012)

III **Study of electronic structures on Yb_2Pd_2Sn and $YbPd_2Sn$ by photoelectron and x-ray emission spectroscopies**
H. Yamaoka, P. Thunström, N. Tsujii, I. Jarrige, K. Shimada, M. Arita, H. Iwasawa, H. Hayashi, H. Namatame, M. Taniguchi, N. Hiraoka, H. Ishii, K.D. Tsuei, M. Giovannini, and E. Bauer
In Manuscript

IV **Charge self-consistent dynamical mean-field theory based on the full-potential linear muffin-tin orbital method: Methodology and applications**
O. Grånäs, I. Di Marco, P. Thunström, L. Nordström, O. Eriksson, T. Björkman, J.M. Wills
Comp. Mat. Sci. 55, 295 (2012)

V **Electronic entanglement in late transition metal oxides**
P. Thunström, I. Di Marco, and O. Eriksson
Submitted to PRL

VI **Spectral properties of Mn doped GaAs: experiment and correlated electronic structure theory**
I. Di Marco, P. Thunström, M.I. Katsnelson, J. Sadowski, K. Karlsson, S. Lebegue, J. Kanski, and O. Eriksson
In Manuscript

VII **Correlated electronic structure of Fe in Cs**
M. Costa, P. Thunström, I. Di Marco, A. Bergman, A. Burlamaqui Klautau, and O. Eriksson
In Manuscript

VIII **An LDA+DMFT study of the orbital magnetism and total energy properties of the late transition metals: conserving and non-conserving approximations**
I. Di Marco, P. Thunström, O. Grånäs, L. Pourovskii, M.I. Katsnelson, L. Nordström, and O. Eriksson
In Manuscript

IX **A charge self-consistent LDA+DMFT study of the spectral properties of NiS**
S. K. Panda, P. Thunström, I. Di Marco, R. Lizárraga, A. Delin, I. Dasgupta, O. Eriksson, and D. D. Sarma
In Manuscript

Reprints were made with permission from the publishers.

Publications not included in this thesis

- **Adiabatic approximation for weakly open systems**
  P. Thunström, J. Åberg, and E. Sjöqvist
  Phys. Rev. A 72, 022328 (2005)

- **Electronic structure of Co doped ZnO: Theory and experiment**
  B. Sanyal, O. Grånäs, R. Knut, V. A. Coleman, P. Thunström, D. M. Iusan, O. Karis, O. Eriksson, and G. Westin
  J. Appl. Phys. 103, 07D130 (2008)

Contents

1. Introduction

The aim of this thesis is to investigate the role of correlations in the electronic structure of materials. The following chapters contain an introduction to the subject, starting from the Dirac equation and ending with the Dynamical Mean Field Theory. However, for those of you who are asking yourself right now what electronic structure even means, and if these correlations are any useful, this small chapter is for you.

One can think of a piece of material as a giant ballroom, and the electrons as a group of graceful but very shy and indistinguishable dancers. When you look the other way they will dance around like waves, but as soon as you even take a glimpse of what they are doing they will stop. The dance is called the electronic structure of the material, and the dance steps are guided by the Schrödinger equation. As in real life, the most important rule is to avoid to bump into each other. The Coulomb interaction makes sure that the electrons do not lose track of each other and keep their distance. The Coulomb interaction is also responsible for the important quantum effect called entanglement. This effect can arise in confined areas where two or more electrons really have to correlate their movement to make sure that everyone has enough space.

It is unfortunately not possible to directly calculate the true electronic structure of a material due to the huge number of interacting electrons. The trick is to replace the well-mannered electrons with rude quasi-particles which do not really care if they invade the space of the others. This allows us to treat each quasi-particle separately without considering exactly where the other particles are, which leads to great simplifications and a method called Kohn-Sham Density Functional Theory (KS-DFT). This approach works well, except for the confined areas where the electrons become entangled. In these areas we need to go back to the proper way of describing the electrons, and one of the best methods to do this is called Dynamical Mean Field Theory (DMFT).

So, before we stretch this analogy too thin let us go back to the important question at hand, namely how can all these dancing electrons influence your everyday life? Hard permanent magnets, like $SmCo_5$ studied in Paper IV, are key components in the generators which produce the electricity you use at home. The transition metal oxides in Paper V make your life less gray, as they are used as pigments in paint and glazes. MnO puts food on your table as it also serves as a fertilizer. Dilute magnetic semiconductors, like Mn doped GaAs in Paper VI, can potentially be used to greatly improve the next generation of computers, and thereby allow you to update your Facebook status at least twice as fast! Finally, we are just beginning to understand the role

of entanglement in the electronic structure, so the most important discoveries are still to be made. This thesis will hopefully bring us a bit closer to those discoveries.

1.1 Notation

A list of the notation and commonly used symbols is found in Table 1.1. This includes the notation used for the various representations of an operator A. The one-electron representation $\tilde{A}$ acts on the single-particle state vector $|q_i\rangle$. The many-body representation $\widehat{A}$ acts on the many-body state vector $|\nu_i\rangle$.

Table 1.1. *List of symbols*

$\Re(a)$	real part of the number a
$\Im(a)$	imaginary part of the number a
$\|q_i\rangle$	single-particle state vector
$\|\nu_i\rangle$	many-body state vector
$\mathbf{a}$	vector or matrix of the quantity a
$\tilde{A}$	one-electron representation of operator A
$\tilde{\mathrm{A}}$	matrix representation of $\tilde{A}$
$\tilde{\mathrm{A}}_{ij}$	matrix element ij of $\tilde{\mathrm{A}}$
$\widehat{A}$	many-body representation of operator A
$\widehat{\mathrm{A}}$	matrix representation of $\widehat{A}$
$\widehat{\mathrm{A}}_{ij}$	matrix element ij of $\widehat{\mathrm{A}}$

2. Single particle physics

2.1 Relativistic states

Let us consider a single isolated electron in a time-independent external potential $V(\tilde{\mathbf{r}})$, where $\tilde{\mathbf{r}}$ is the position operator. In the energy range most commonly found in solid state physics, this system can be fully described by a four-component spinor [1, 2, 3]:

$$|\chi(t)\rangle = \begin{bmatrix} |\chi^A\rangle \\ |\chi^B\rangle \end{bmatrix} \equiv \begin{bmatrix} |\chi^1\rangle \\ |\chi^2\rangle \\ |\chi^3\rangle \\ |\chi^4\rangle \end{bmatrix}. \tag{2.1}$$

The $|\chi^1\rangle$ ($|\chi^2\rangle$) component describes an electron with spin up (down), while the $|\chi^3\rangle$ ($|\chi^4\rangle$) component describes a positron with spin up (down). The state vector $|\chi(t)\rangle$ evolves in time according to the Dirac equation

$$i\hbar\frac{d}{dt}|\chi(t)\rangle = \tilde{H}|\chi(t)\rangle \equiv \begin{bmatrix} V(\tilde{\mathbf{r}})+mc^2 & c\tilde{\boldsymbol{\sigma}}\cdot\tilde{\mathbf{p}} \\ c\tilde{\boldsymbol{\sigma}}\cdot\tilde{\mathbf{p}} & V(\tilde{\mathbf{r}})-mc^2 \end{bmatrix} \begin{bmatrix} |\chi^A\rangle \\ |\chi^B\rangle \end{bmatrix}, \tag{2.2}$$

where m is the mass, c is the speed of light, $\tilde{\mathbf{p}}$ is the momentum operator, $\tilde{\boldsymbol{\sigma}} = (\tilde{\sigma}_1, \tilde{\sigma}_2, \tilde{\sigma}_3)$, and $\tilde{\sigma}_i$ is a Pauli operator.

The eigenstates $\{|\chi_i\rangle\}_i$ of $\tilde{H}$ constitute a complete basis of the system, and are obtained from the equation

$$\begin{bmatrix} V(\tilde{\mathbf{r}})+mc^2 & c\tilde{\boldsymbol{\sigma}}\cdot\tilde{\mathbf{p}} \\ c\tilde{\boldsymbol{\sigma}}\cdot\tilde{\mathbf{p}} & V(\tilde{\mathbf{r}})-mc^2 \end{bmatrix} \begin{bmatrix} |\chi_i^A\rangle \\ |\chi_i^B\rangle \end{bmatrix} = E_i \begin{bmatrix} |\chi_i^A\rangle \\ |\chi_i^B\rangle \end{bmatrix}, \tag{2.3}$$

where E_i is the eigenvalue corresponding to $|\chi_i\rangle$. Solving Eq. (2.3) with respect to $|\chi_A\rangle$ gives

$$\left[\tilde{K}(E_i) - c^2(\tilde{\boldsymbol{\sigma}}\cdot\tilde{\mathbf{p}})\left(\tilde{K}(E_i)+2mc^2\right)^{-1}(\tilde{\boldsymbol{\sigma}}\cdot\tilde{\mathbf{p}})\right]|\chi_i^A\rangle = 0, \tag{2.4}$$

where $\tilde{K}(E_i) = E_i - mc^2 - V(\tilde{\mathbf{r}})$. Eq. (2.4) describes the fully relativistic electronic problem.

2.2 Non-relativistic limit

If the energy of the electron is close to its rest mass mc^2, the relativistic effects are rather small. The non-relativistic limit of Eq. (2.4) is obtained by

expanding $[\tilde{K}(E_i)+2mc^2]^{-1}$ in powers of $\tilde{K}(E_i)/2mc^2$. Keeping the lowest order terms yields

$$\left(\tilde{K}(E_i)+2mc^2\right)^{-1} \approx \frac{-1}{4m^2c^4}\left(\tilde{K}(E_i)-2mc^2\right). \tag{2.5}$$

Substituting Eq. (2.5) into (2.4) gives

$$\left[\tilde{K}(E_i)-\frac{\tilde{p}^2}{2m}+\frac{1}{4m^2c^2}(\tilde{\sigma}\cdot\tilde{\mathbf{p}})\tilde{K}(E_i)(\tilde{\sigma}\cdot\tilde{\mathbf{p}})\right]|\chi_i^A\rangle = 0. \tag{2.6}$$

The third term in Eq. (2.6) can be written as

$$(\tilde{\sigma}\cdot\tilde{\mathbf{p}})\tilde{K}(E_i)(\tilde{\sigma}\cdot\tilde{\mathbf{p}}) = \tilde{K}(E_i)\tilde{p}^2 + i\hbar\nabla V(\tilde{\mathbf{r}})\cdot\tilde{\mathbf{p}} - \hbar\tilde{\sigma}\cdot[\nabla V(\tilde{\mathbf{r}})]\times\tilde{\mathbf{p}}, \tag{2.7}$$

where we have used the identity $(\tilde{\sigma}\cdot\tilde{A})(\tilde{\sigma}\cdot\tilde{B}) = \tilde{A}\cdot\tilde{B} + i\tilde{\sigma}\cdot\tilde{A}\times\tilde{B}$ and $[\tilde{\mathbf{p}},A(\tilde{\mathbf{r}})] = -i\hbar\nabla A(\tilde{\mathbf{r}})$. It is important to note that the first and the second term on the right hand side in Eq. (2.7) are not hermitian, but that their sum is [4]. To take this observation into account we expand $\tilde{K}(E_i)\tilde{p}^2$ in a symmetric and antisymmetric part

$$\tilde{K}(E_i)\tilde{p}^2 = \frac{1}{2}\left\{\tilde{K}(E_i),\tilde{p}^2\right\} + \frac{1}{2}\left[\tilde{K}(E_i),\tilde{p}^2\right]. \tag{2.8}$$

The antisymmetric part gives

$$\begin{aligned}\frac{1}{2}\left[\tilde{K}(E_i),\tilde{p}^2\right] &= \frac{1}{2}(\tilde{\mathbf{p}}\cdot[\tilde{\mathbf{p}},V(\tilde{\mathbf{r}})] + [\tilde{\mathbf{p}},V(\tilde{\mathbf{r}})]\cdot\tilde{\mathbf{p}}) \\ &= \frac{1}{2}[\tilde{\mathbf{p}}\,[\tilde{\mathbf{p}},V(\tilde{\mathbf{r}})]] + [\tilde{\mathbf{p}},V(\tilde{\mathbf{r}})]\cdot\tilde{\mathbf{p}} \\ &= -\frac{\hbar^2}{2}\nabla^2 V(\tilde{\mathbf{r}}) - i\hbar\nabla V(\tilde{\mathbf{r}})\cdot\tilde{\mathbf{p}}. \end{aligned} \tag{2.9}$$

The second term on the last line of Eq. (2.9) cancels the non-hermitian part in Eq. (2.7). Neglecting the third term in Eq. (2.6) gives $\tilde{K}(E_i)\approx\tilde{p}^2/2m$ for all eigenstates $|\chi_i^A\rangle$. Substituting this approximation into the symmetric part of Eq. (2.8) yields

$$\frac{1}{2}\left\{\tilde{K}(E_i),\tilde{p}^2\right\} \approx \frac{\tilde{p}^4}{2m}. \tag{2.10}$$

Substituting Eq. (2.8), (2.9), (2.10), and (2.7) into Eq. (2.6) finally yields,

$$\tilde{H}|\chi_i^A\rangle = E_i|\chi_i^A\rangle \tag{2.11}$$

where

$$\begin{aligned}\tilde{H} = \Bigg[&mc^2 + \frac{\tilde{p}^2}{2m} + V(\tilde{\mathbf{r}}) - \frac{\tilde{p}^4}{8m^3c^2} \\ &+ \frac{\hbar^2}{8m^2c^2}\nabla^2 V(\tilde{\mathbf{r}}) + \frac{\hbar}{4m^2c^2}\tilde{\sigma}\cdot[\nabla V(\tilde{\mathbf{r}})]\times\tilde{\mathbf{p}}\Bigg]. \end{aligned} \tag{2.12}$$

The first term in the Hamiltonian $\tilde{H}$ in Eq. (2.12) gives the rest mass energy of the electron. The second and third terms constitute the non-relativistic kinetic energy and potential energy of the Hamiltonian. The fourth term can be seen as a relativistic correction to the kinetic energy. The fifth term is called the Darwin term [5] and is a relativistic correction to the potential. The last term in $\tilde{H}$ corresponds to a generalized form of the spin-orbit interaction.

If V is a central potential, its gradient is given by

$$\nabla V(\tilde{\mathbf{r}}) = \frac{dV}{dr}\frac{\tilde{\mathbf{r}}}{\tilde{r}}, \tag{2.13}$$

where $\tilde{r} = |\tilde{\mathbf{r}}|$. One can then write the spin-orbit interaction term in a more familiar form

$$\frac{\hbar}{4m^2c^2}\tilde{\boldsymbol{\sigma}} \cdot [\nabla V(\tilde{\mathbf{r}})] \times \tilde{\mathbf{p}} = -\frac{1}{2m^2c^2}\frac{1}{\tilde{r}}\frac{dV}{dr}(\tilde{r})\,\tilde{\mathbf{l}} \cdot \tilde{\mathbf{s}}, \tag{2.14}$$

where $\tilde{\mathbf{l}} = \tilde{\mathbf{r}} \times \tilde{\mathbf{p}}$, and $\tilde{\mathbf{s}} = (\hbar/2)\tilde{\boldsymbol{\sigma}}$.

2.2.1 Periodic potential

Crystal structures are characterized by a periodic arrangement of atoms [6]. The external potential $V(\tilde{\mathbf{r}})$ in Eq. (2.12) is therefore periodic in space, and there exist some lattice vectors $\mathbf{a}_1$, $\mathbf{a}_2$, and $\mathbf{a}_3$ such that

$$V(\tilde{\mathbf{r}}) = V(\tilde{\mathbf{r}} + \mathbf{R}_{i_1 i_2 i_3}), \tag{2.15}$$

$$\mathbf{R}_{i_1 i_2 i_3} = i_1\mathbf{a}_1 + i_2\mathbf{a}_2 + i_3\mathbf{a}_3, \tag{2.16}$$

for all integers i_2, i_2, and i_3. The integers i_1, i_2, and i_3 can be extracted from $\mathbf{R}$ by taking the scalar product with the reciprocal lattice vectors $\mathbf{b}_1$, $\mathbf{b}_2$, and $\mathbf{b}_3$. These are defined as

$$\mathbf{b}_1 = \frac{2\pi}{v}\mathbf{a}_2 \times \mathbf{a}_3, \tag{2.17}$$

$$\mathbf{b}_2 = \frac{2\pi}{v}\mathbf{a}_3 \times \mathbf{a}_1, \tag{2.18}$$

$$\mathbf{b}_3 = \frac{2\pi}{v}\mathbf{a}_1 \times \mathbf{a}_2, \tag{2.19}$$

$$\tag{2.20}$$

where $v_{cell} = \mathbf{a}_1 \cdot (\mathbf{a}_2 \times \mathbf{a}_3)$ is the volume of the unit cell spanned by $\mathbf{a}_1$, $\mathbf{a}_2$, and $\mathbf{a}_3$. The reciprocal lattice vectors fulfill the relation

$$\mathbf{R}_{i_1 i_2 i_3} \cdot \mathbf{b}_j = (i_1\mathbf{a}_1 + i_2\mathbf{a}_2 + i_3\mathbf{a}_3) \cdot \mathbf{b}_j = 2\pi i_j. \tag{2.21}$$

The full Hamiltonian $\tilde{H}$ in Eq. (2.12) depends on the position operator $\tilde{\mathbf{r}}$ only through the potential $V(\tilde{\mathbf{r}})$. We can write $V(\tilde{\mathbf{r}})$ in the momentum basis

$$|\mathbf{k}\rangle \equiv \Omega^{-1/2}\int |\mathbf{r}\rangle e^{i\mathbf{r}\cdot\mathbf{k}} d\mathbf{r}, \tag{2.22}$$

where the normalization constant $\Omega = \sum_{\mathbf{R}} v_{cell}$ is the volume of the crystal. Then we get

$$\begin{aligned}\langle \mathbf{k}|V(\tilde{\mathbf{r}})|\mathbf{k}'\rangle &= \sum_{\mathbf{R}} \int_{cell} \langle \mathbf{k}|\mathbf{R}+\mathbf{r}\rangle \tilde{H}[V(\mathbf{r})]\langle \mathbf{R}+\mathbf{r}|\mathbf{k}'\rangle d\mathbf{r} \\ &= \frac{1}{\Omega}\int_{cell} V(\mathbf{r}) e^{-i\mathbf{r}\cdot(\mathbf{k}-\mathbf{k}')} d\mathbf{r} \sum_{\mathbf{R}} e^{-i\mathbf{R}\cdot(\mathbf{k}-\mathbf{k}')} \\ &= \sum_{\mathbf{K}} \delta(\mathbf{K}-\mathbf{k}+\mathbf{k}') V_{\mathbf{K}}, \end{aligned} \tag{2.23}$$

where $\mathbf{K} = j_1\mathbf{b}_1 + j_2\mathbf{b}_2 + j_3\mathbf{b}_3$ and

$$V_{\mathbf{K}} = \frac{1}{v_{cell}} \int_{cell} V(\mathbf{r}) e^{-i\mathbf{r}\cdot\mathbf{K}} d\mathbf{r}. \tag{2.24}$$

Substituting Eq. (2.24) into Eq. (2.12) shows that the one-electron Hamiltonian $\tilde{H}$ is block diagonal in the momentum basis $\{|\mathbf{k}\rangle\}$ for a periodic potential. Within each block the $\mathbf{k}$-vectors are related by a reciprocal lattice vector $\mathbf{K}$. All eigenstates $|q_i^{\mathbf{k}}\rangle$ of $\tilde{H}$ can be made to belong to some $\mathbf{k}$-block which means that their position representation can be written as

$$\langle \mathbf{r}|q_i^{\mathbf{k}}\rangle = \int \langle \mathbf{r}|\mathbf{k}'\rangle\langle \mathbf{k}'|q_i^{\mathbf{k}}\rangle d\mathbf{k}' = e^{i\mathbf{r}\cdot\mathbf{k}} \sum_K e^{i\mathbf{r}\cdot\mathbf{K}} \langle \mathbf{k}+\mathbf{K}|q_i^{\mathbf{k}}\rangle. \tag{2.25}$$

This means that the electronic wave-function in a crystal can be expressed as a plane-wave $e^{i\mathbf{r}\cdot\mathbf{k}}$ times a function $u_{\mathbf{k}}(\mathbf{r}) = \sum_K e^{i\mathbf{r}\cdot\mathbf{K}}\langle \mathbf{k}+\mathbf{K}|q_i^{\mathbf{k}}\rangle$ which has the same periodicity of the lattice. Equation (2.25) can be restated in a more familiar form, known as Bloch's theorem [6]:

$$\langle \mathbf{r}+\mathbf{R}|q_i^{\mathbf{k}}\rangle = e^{i\mathbf{k}\cdot\mathbf{R}}\langle \mathbf{r}|q_i^{\mathbf{k}}\rangle. \tag{2.26}$$

2.2.2 Quantum numbers

One of the corner stones of quantum mechanics is that any measurable quantity of a system can be represented by a hermitian operator, called an observable. For any system there exists a maximal set $\mathscr{Q}$ of observables that commute with each other. $\mathscr{Q}$ can be constructed by sequentially adding observables that commute with the rest of the observables in $\mathscr{Q}$, until no more observables can be added. Since the observables in $\mathscr{Q}$ commute with each other, they share a common orthonormal eigenbasis $\{|q_i\rangle\}_i$, where the index q_i is a list of the corresponding eigenvalues. For a free electron, $\mathscr{Q}$ could for example contain the momentum operator $\tilde{\mathbf{p}}$ and the spin operator $\tilde{s}_z$, and $q = (\mathbf{k}, s_z)$. Each index q_i represents a unique list of values, which means that they can be given an order

$$q_1 < q_2 < q_3 < \cdots. \tag{2.27}$$

The possibility to define an order will be of importance in the construction of the many-body basis presented in the next chapter.

3. Many-body physics

3.1 Non-interacting fermions

3.1.1 Many-body basis

Let us start by considering a system consisting of two identical non-interacting fermions. It can be tempting to construct a two-particle basis $\{\psi_{ij}\}$ by (implicitly) labeling the particles and then indexing them like two single particle states vectors,

$$|\psi_{ij}\rangle = |q_i\rangle \otimes |q_j\rangle. \tag{3.1}$$

However, the state vector $|\psi_{ij}\rangle$ in Eq. (3.1) is incompatible with the Pauli principle, which for fermions states that an interchange of two particle labels will result in a change of sign of the state vector, i.e.,

$$|\psi_{ij}\rangle = -|\psi_{ji}\rangle. \tag{3.2}$$

The definition of the state in (3.1) can be made antisymmetric, thereby conforming to the Pauli principle, by writing out the particle labels explicitly and taking the determinant of the one particle state vectors. The antisymmetric definition gives

$$|\psi_{ij}\rangle = \frac{1}{\sqrt{2}}(|q_i\rangle \otimes |q_j\rangle - |q_j\rangle \otimes |q_i\rangle) \equiv \frac{1}{\sqrt{2}} \begin{vmatrix} |1,q_i\rangle & |2,q_i\rangle \\ |1,q_j\rangle & |2,q_j\rangle \end{vmatrix}. \tag{3.3}$$

The state vectors $|\psi_{ij}\rangle$ and $|\psi_{ji}\rangle$ correspond to the same state as they are equal up to a phase factor. This means that only one of them should be included in the two-particle basis. There is a convention which states that only state vectors with indices sorted according to Eq. (2.27) should be included in the basis. If an operation yields an unordered state vector, one has to do some changes of the rows in the Slater determinant in Eq. (3.3) to obtain the ordered state vector. The same construction can be used for an N-particle system, which gives the basis $\{|\psi_{i_1,i_2,\cdots,i_N}\rangle\}$ [7].

The many-body basis $\{|\psi_{i_1,i_2,\cdots,i_N}\rangle\}$ grows very rapidly as a function of the available one-particle states,

$$|\{|\psi_{i_1,i_2,\cdots,i_N}\rangle\}| = \binom{M}{N}. \tag{3.4}$$

where M is the number of single-particle states and N is the number of electrons. Since the computational resources needed to solve a problem numerically grow at least linearly with the size of the basis, the number of available

single-particle states must be severely restricted. In a standard solid state problem, one often tries to limit the number of orbitals explicitly included in the many-body basis. Some orbitals are therefore assumed to be always occupied or unoccupied, so their effect can be integrated out and added as an external potential.

3.1.2 Operators and occupation number formalism

The one-particle Hamiltonian $\tilde{H}$ in Eq. (2.12) can be generalized to an N-particle system as a sum of one-particle operators,

$$\widehat{H} = \sum_{j=1}^{N} \tilde{H}^j = \sum_{j=1}^{N} \sum_{k,l} \tilde{\mathrm{H}}^j_{kl} |j,q_k\rangle\langle j,q_l|, \tag{3.5}$$

where the index j runs over the particle labels, and $\tilde{\mathrm{H}}^j_{kl} = \langle j,q_k|\tilde{H}^j|j,q_l\rangle$. Since $\tilde{H}^j$ only acts on particle j, its matrix elements $\tilde{\mathrm{H}}^j$ do not depend on the states of the other particles. The N-particle Hamiltonian $\widehat{H}$ obtained in this way can therefore only describe non-interacting particles. For identical particles $\tilde{\mathrm{H}}^j_{kl}$ is independent of the particle label and can be written as $\tilde{\mathrm{H}}_{kl}$. The N-particle operator $\widehat{H}$ can hence be written as

$$\widehat{H} = \sum_{k,l} \tilde{\mathrm{H}}_{kl} \sum_{j=1}^{N} |j,q_k\rangle\langle j,q_l| \equiv \sum_{k,l} \tilde{\mathrm{H}}_{kl} \widehat{Q}_{kl}. \tag{3.6}$$

The operator $\widehat{Q}_{kl}$ acts on the state $|\psi_{i_1,i_2,\cdots,i_N}\rangle$ as

$$\widehat{Q}_{kl}|\psi_{i_1,i_2,\cdots,i_N}\rangle = \sum_{j=1}^{N} \delta_{i_j l} \widehat{Q}_{kl} |\psi_{i_1,i_2,\cdots,l,\cdots,i_N}\rangle = \sum_{j=1}^{N} \delta_{i_j l} |\psi_{i_1,i_2,\cdots,k,\cdots,i_N}\rangle. \tag{3.7}$$

If $|\psi_{i_1,i_2,\cdots,k,\cdots,i_N}\rangle$ contains two copies of the single-particle state index k, the antisymmetric properties of the wave function makes it zero. The new list of indices $[i_1,i_2,\cdots,k,\cdots,i_N]$ in the right hand side of Eq. (3.7) is generally not sorted in the conventional order. The reordering process of $|\psi_{i_1,i_2,\cdots,k,\cdots,i_N}\rangle$ interchanges a number of rows in the Slater determinant. Each row change multiplies the state vector with a factor of (-1). The number of row changes is given by

$$\gamma_{kl} = \sum_{s} n_s, \tag{3.8}$$

where the index s runs over all integers between k and l, and $n_s \in \{0,1\}$ is the occupation number of the single-particle state indexed by q_s. The state vector on the right hand side of Eq. (3.7) can hence be written as

$$\sum_{j=1}^{N} \delta_{i_j l} |\psi_{i_1,i_2,\cdots,k,\cdots,i_N}\rangle = (\delta_{n_k 0} + \delta_{kl}) \delta_{n_l 1} (-1)^{\gamma_{kl}} |\psi_{\sigma(i_1,i_2,\cdots,k,\cdots,i_N)}\rangle, \tag{3.9}$$

where σ sorts the indices according to the conventional order.

As seen in Eq. (3.9), all the properties of Q_{kl} and $|\psi_{i_1,i_2,\cdots,i_j,\cdots,i_N}\rangle$ are captured by the occupation numbers. A common way of denoting the state vector $|\psi_{i_1,i_2,\cdots,i_j,\cdots,i_N}\rangle$ is therefore a sorted list of the occupation numbers. The state vector $|\psi_{24}\rangle$, having one electron in state $|q_2\rangle$ and one in $|q_4\rangle$, can for example be written like

$$|\psi_{24}\rangle = |n_1, n_2, \cdots\rangle = |0,1,0,1,0,\cdots\rangle, \tag{3.10}$$

and Eq. (3.7) becomes

$$\widehat{Q}_{kl}|\cdots, n_k, \cdots, n_l, \cdots\rangle = (\delta_{n_k 0} + \delta_{kl})\delta_{n_l 1}(-1)^{\gamma_{kl}}|\cdots, 1, \cdots, 0, \cdots\rangle. \tag{3.11}$$

The expectation value of the operator $\widehat{Q}_{kk}$ gives the occupation number for the state indexed by q_k,

$$\langle \widehat{n}_k \rangle = \langle \cdots, n_k, \cdots | \widehat{Q}_{kk} | \cdots, n_k, \cdots \rangle = n_k. \tag{3.12}$$

3.1.3 Creation and annihilation operators

It is a straightforward exercise to show that the operator $\widehat{Q}_{kl}$ can be written as a product of two operators

$$\widehat{Q}_{kl} = \widehat{c}_k^\dagger \widehat{c}_l, \tag{3.13}$$

where $\widehat{c}_k^\dagger$ is called "creation" operator and $\widehat{c}_l$ is called "annihilation" operator. They are defined as

$$\widehat{c}_k^\dagger |\cdots, n_k, \cdots\rangle = \delta_{n_k 0}(-1)^{\sum_{s=1}^{k-1} n_s}|\cdots, 1, \cdots\rangle, \tag{3.14}$$

$$\widehat{c}_l |\cdots, n_l, \cdots\rangle = \delta_{n_l 1}(-1)^{\sum_{s=1}^{l-1} n_s}|\cdots, 0, \cdots\rangle. \tag{3.15}$$

The occupation number operator $\widehat{n}_k$ becomes

$$\widehat{n}_k = \widehat{c}_k^\dagger \widehat{c}_k. \tag{3.16}$$

As seen from the definitions in Eq. (3.14) and (3.15) the (fermionic) creation and annihilation operators follow the anti-commutation relations

$$\left\{\widehat{c}_k^\dagger, \widehat{c}_l^\dagger\right\} \equiv \widehat{c}_k^\dagger \widehat{c}_l^\dagger + \widehat{c}_l^\dagger \widehat{c}_k^\dagger = 0, \tag{3.17}$$

$$\left\{\widehat{c}_k, \widehat{c}_l\right\} \equiv \widehat{c}_k \widehat{c}_l + \widehat{c}_l \widehat{c}_k = 0, \tag{3.18}$$

$$\left\{\widehat{c}_k^\dagger, \widehat{c}_l\right\} \equiv \widehat{c}_k^\dagger \widehat{c}_l + \widehat{c}_l \widehat{c}_k^\dagger = \delta_{kl}. \tag{3.19}$$

3.1.4 Field operators

Substituting $\widehat{Q}_{kl}$ from Eq. (3.13) into Eq. (3.6) gives

$$\widehat{H} = \sum_{kl} \tilde{\mathrm{H}}_{kl} \hat{c}_k^\dagger \hat{c}_l = \left(\sum_k \hat{c}_k^\dagger \langle q_k | \right) \tilde{H} \left(\sum_l |q_l\rangle \hat{c}_l \right) = \widehat{\Psi}^\dagger \tilde{H} \widehat{\Psi}. \tag{3.20}$$

The operator $\widehat{\Psi}$ is called field operator, and is a very useful tool in the theoretical treatment of many-body physics. One can interpret the action of $\widehat{\Psi}$ as taking a particle from an occupied single-particle state in the many-body system and putting it into an empty system, which then becomes a single-particle system. $\widehat{\Psi}^\dagger$ does the opposite, that is, it takes the particle from the one-particle system and puts it into the same single-particle state but in the many-body system. Since the sum in Eq. (3.20) runs over all single-particle states, all particles will be treated.

The way the many-body Hamiltonian in Eq. (3.20) is written has a quite natural interpretation. First $\widehat{\Psi}$ takes a particle from an occupied single-state in the many-body system and adds it to a single-particle system. In this single-particle system the particle is operated upon by the single-particle Hamiltonian $\tilde{H}$. Finally, the particle is put back into the many-body system by $\widehat{\Psi}^\dagger$.

3.1.5 The ground state of a system of non-interacting particles

At zero Kelvin the ground state $|gs\rangle$ of a system of N non-interacting particles governed by the Hamiltonian in Eq. (3.20), can be obtained by diagonalizing the matrix representation of the Hamiltonian in some many-body basis $\{|\nu_i\rangle\}_i$,

$$\widehat{H} = \sum_{ij} \widehat{\mathrm{H}}_{ij} |\nu_i\rangle\langle\nu_j| = \sum_l E_l^{(N)} |\nu_l'\rangle\langle\nu_l'|, \tag{3.21}$$

where $\{|\nu_i'\rangle\}$ is the N-particle eigenbasis of $\widehat{H}$ and $\{E_i^{(N)}\}_i$ are the eigenvalues. The ground state corresponds to the eigenstate $|\nu_i'\rangle$ with the lowest energy. However, diagonalizing the matrix $\widehat{\mathrm{H}}_{ij}$ directly is very computationally demanding since almost all realistic problems yield an enormous many-body basis.

An alternative approach is based on the less demanding diagonalization of the corresponding single-particle Hamiltonian $\tilde{H}$,

$$\tilde{H} = \sum_{ij} \tilde{\mathrm{H}}_{ij} |q_i\rangle\langle q_j| = \sum_i E_i^{(1)} |q_i'\rangle\langle q_i'|, \tag{3.22}$$

where $\{|q_i'\rangle\}$ is the single-particle eigenbasis of $\tilde{H}$ and $\{E_i^{(1)}\}$ are the eigenvalues. The idea is to use the single-particle eigenstates, ordered according to energy, as the single-particle states used in the construction in Eq. (3.3) of

the many-body basis $\{|\nu_i\rangle\}_i$. Thus, when the field operator $\widehat{\Psi}$ acts on $|\nu_i\rangle$, it can take a particle from one of these single-particle eigenstates $|q'_j\rangle$, without affecting the other particles, and let that state be acted upon by $\tilde{H}$. Since $|q'_j\rangle$ is an eigenstate to $\tilde{H}$, it will only be multiplied with the eigenvalue $E_j^{(1)}$ and then returned back by $\widehat{\Psi}^\dagger$. This implies that $|\nu_i\rangle$ is in fact already an eigenvector of $\widehat{H}$,

$$\begin{aligned}
\widehat{\Psi}^\dagger \tilde{H} \widehat{\Psi} |\nu_i\rangle &= \widehat{\Psi}^\dagger \tilde{H} \sum_j |q'_j\rangle \delta_{n_j 1} (-1)^{\sum_{s=1}^{j-1} n_s} |\cdots, n_j = 0, \cdots\rangle \\
&= \widehat{\Psi}^\dagger \sum_j E^{(1)_j} |q'_j\rangle \delta_{n_j 1} (-1)^{\sum_{s=1}^{j-1} n_s} |\cdots, n_j = 0, \cdots\rangle \\
&= \sum_j E_j^{(1)} \delta_{n_j 1} (-1)^{2\sum_{s=1}^{i-1} n_s} |\cdots, n_j = 1, \cdots\rangle \\
&= \sum_j E_j^{(1)} \delta_{n_j 1} |\nu_i\rangle, \qquad (3.23)
\end{aligned}$$

with an eigenvalue $E_i^{(N)} = \sum_j E_j^{(1)} \delta_{n_i j}$. Finding the ground state is now a trivial task. It corresponds to the many-body state in which N of the single-particle eigenstates of lowest eigenvalue are occupied. As the single-particle basis was ordered according to energy the N-particle ground state $|gs\rangle$ can be written as

$$|gs\rangle = |\underbrace{1, 1, \cdots, 1}_{\text{N times}}, 0, \cdots\rangle. \qquad (3.24)$$

3.2 Thermal effects

Up to now we have not discussed any thermal effects, except for the statement that the ground state $|gs\rangle = |1, 1, \cdots, 1, 0, \cdots\rangle$ is valid for zero Kelvin. To understand the thermal effects it is important to remember that temperature is a measure of the average kinetic energy of particles moving randomly in a sample. The motion of the particles is still governed by a Hamiltonian, so that the total energy is conserved. However, only knowing the average kinetic energy of the system does not identify its state, since the Hamiltonian of a many-body system often has large degenerate eigenspaces. Due to the lack of information the best we can do is to work with probabilities, and look at the resulting statistical properties of the system.

3.2.1 Density operator

Suppose we have a statistical system which has a probability P_n of being in the state $|\nu_n\rangle$. To calculate the expectation value of the observable $\widehat{O}$ we need

to consider each state $|\nu_n\rangle$ separately, and then weight each outcome with the probability P_n,

$$\langle \widehat{O} \rangle = \sum_n P_n \langle \nu_n | \widehat{O} | \nu_n \rangle = \mathrm{Tr}\left(\sum_n P_n |\nu_n\rangle\langle\nu_n| \widehat{O} \right) = \mathrm{Tr}(\widehat{\rho}\widehat{O}), \tag{3.25}$$

where $\widehat{\rho} \equiv \sum_n P_n |\nu_n\rangle\langle\nu_n|$ is called the density operator [8]. The density operator is a generalization of the state vector description of a system since it also can describe statistical systems. Just like the state contains all the physically significant information we possibly can obtain about a non-statistical system, the density operator does the same for the statistical system in question. In addition to the relation in Eq. (3.25) the density operator is Hermitian and its trace is one:

$$\widehat{\rho} = \widehat{\rho}^\dagger \tag{3.26}$$

$$\mathrm{Tr}(\widehat{\rho}) = \sum_n P_n \mathrm{Tr}(|\nu_n\rangle\langle\nu_n|) = \sum_n P_n = 1. \tag{3.27}$$

3.2.2 Ensembles

When talking about probabilities it is often fruitful to use the concept of statistical ensemble [8]. An ensemble is an infinite collection of systems prepared according to some known recipe. The systems are not allowed to interact with each other which means that the ensemble does not have to exist as a whole at a given time. In practice there is always a state preparation machine, which creates each system right before the system is used. It is important to note that the order in which the systems are produced is unimportant. Two ensembles are equivalent as long as the total probability to obtain a certain outcome of a measurement is the same. A good illustration of the concept is a beam of electrons (the ensemble) coming out of a linear accelerator (the state preparation machine). In theory one can of course consider an ensemble of any system, even the universe[1].

Suppose again that we have a statistical system which has a probability P_n of being in the state $|\nu_n\rangle$, described by the density operator $\widehat{\rho} = \sum_n P_n |\nu_n\rangle\langle\nu_n|$. To calculate what happens if we probe the system with some measurement apparatus $A[\cdot]$ we need to consider the effect on each state $|\nu_n\rangle$ separately, and then weight each outcome with the probability P_n,

$$A[\widehat{\rho}] = \sum_n P_n A[|\nu_n\rangle\langle\nu_n|] = \sum_n P_n A_n. \tag{3.28}$$

Another way of doing the same thing is to consider X copies of the system (an ensemble), with $P_n X$ copies having the density operator $\widehat{\rho}_n = |\nu_n\rangle\langle\nu_n|$.

[1]The existence and uniqueness of a universe state preparation machine has long been the topic of heated debate, and has given rise to several major world religions.

Instead of measuring only on a single system we perform the measurement on each system in the ensemble and normalize the outcome with the number of systems. Schematically everything looks the same,

$$\frac{A[\widehat{X}]}{X} \equiv \frac{\sum_n P_n X A[|\nu_n\rangle\langle\nu_n|]}{X} = \sum_n P_n A_n, \tag{3.29}$$

where $\widehat{X} = X\widehat{\rho}$ represents the entire ensemble. The two ways of representing a statistical system, with probabilities and with an ensemble, are equivalent. The ensemble picture, however, has the advantage that it describes a physical entity, a collection of systems, onto which we can apply all our previously derived formalism.

3.2.3 Quantum statistical mechanics

By using ensembles to represent the state of a statistical system we can answer the following two fundamental questions:

1. What is the probability that a random preparation procedure produces a certain density operator $\widehat{\rho} = \sum_n P_n|\nu_n\rangle\langle\nu_n|$ instead of another density operator $\widehat{\rho}'$?
2. What density operator has the largest probability to be prepared by the random procedure, for a given energy $E = \mathrm{Tr}(\widehat{H}\widehat{\rho})$ and number of particles $N = \mathrm{Tr}(\widehat{n}\widehat{\rho})$?

We will consider the grand canonical ensemble, where both particles and energy may be transfered between the systems and a reservoir. This is the most general type of ensemble that can describe an open system. The random preparation procedure can be described as a preparation machine controlled by a random number generator. The probability that the preparation machine will produce a certain ensemble is then proportional to the total number of ways Ω it can prepare the individual systems and still get the same ensemble [9],

$$\Omega = \frac{X!}{X_1!X_2!X_3!\cdots}, \tag{3.30}$$

where X is the number of systems in the ensemble and $X_n \equiv P_n X$ is the number of systems in state $|\nu_n\rangle$. Eq. (3.30) can be simplified for large X by applying Stirling's approximation

$$\ln(X!) \approx X\ln X - X, \tag{3.31}$$

giving

$$\Omega = \exp\left[X\ln X - \sum_n X_n \ln X_n\right]. \tag{3.32}$$

In terms of probabilities this simplifies further to

$$\Omega = \exp\left[-X\sum_n P_n \ln P_n\right] = \exp\left[-X\,\mathrm{Tr}(\widehat{\rho}\ln\widehat{\rho})\right]. \tag{3.33}$$

The probability to obtain $\widehat{\rho}$ instead of $\widehat{\rho}'$ is simply

$$p = \frac{\Omega}{\Omega + \Omega'}, \tag{3.34}$$

where Ω' corresponds to $\widehat{\rho}'$.

To answer the second question we need to maximize Ω under the constrain that it should be a stationary point with respect to energy ($\delta[\mathrm{Tr}(\widehat{H}\widehat{\rho})] = 0$), number of electrons ($\delta[\mathrm{Tr}(\widehat{n}\widehat{\rho})] = 0$), and probability ($\delta[\mathrm{Tr}(\widehat{\rho})] = 0$). Maximizing Ω corresponds to maximizing $-\mathrm{Tr}(\widehat{\rho}\ln\widehat{\rho})$, and the constraints can be enforced by using Lagrangian multipliers. By choosing the multipliers $-\beta$ for $\delta[\mathrm{Tr}(\widehat{H}\widehat{\rho})]$, $\mu\beta$ for $\delta[\mathrm{Tr}(\widehat{n}\widehat{\rho})]$, and λ for $\delta[\mathrm{Tr}(\widehat{\rho})]$ we get

$$\frac{\delta}{\delta\widehat{\rho}}\left[-\mathrm{Tr}(\widehat{\rho}\ln\widehat{\rho}) - \beta\mathrm{Tr}(\widehat{H}\widehat{\rho}) + \mu\beta\mathrm{Tr}(\widehat{n}\widehat{\rho}) - \lambda\mathrm{Tr}(\widehat{\rho})\right] = 0. \tag{3.35}$$

Resolving the functional derivatives in Eq. (3.35) yields

$$\ln\widehat{\rho} + 1 + \beta\widehat{H} - \mu\beta\widehat{n} + \lambda = 0. \tag{3.36}$$

Eq. (3.36) is solved by

$$\widehat{\rho} = \frac{1}{Z}e^{-\beta(\widehat{H}-\mu\widehat{n})}, \tag{3.37}$$

where $Z \equiv e^{\lambda+1}$. Using $\mathrm{Tr}(\widehat{\rho}) = 1$ in Eq. (3.37) gives,

$$Z = \mathrm{Tr}\left(e^{-\beta(\widehat{H}-\mu\widehat{n})}\right). \tag{3.38}$$

The remaining Lagrangian multipliers β and μ correspond to the inverse temperature of the system, $\beta = 1/k_B T$, and the chemical potential, respectively. The energy of the ensemble can be adjusted by tuning β, and the number of particles by shifting μ. If the number of particles $\mathrm{Tr}(\widehat{n}\widehat{\rho})$ is not an integer the ground state is called an intermediate valence state. In the following chapters the operator $\widehat{H} - \mu\widehat{n}$ will often be encountered. To lighten the notation we will denote it just as $\widehat{H}$.

3.3 Interacting fermions

Going from a single-particle system to a system of identical non-interacting fermions required some new notation, but the dynamics was still governed by the single-particle Hamiltonian, as shown in Eq. (3.20). The dynamics of a system of interacting fermions is fundamentally different from the single-particle dynamics. In fact, due to the interaction with other particles, generally there exists no single-particle state $|q_i\rangle$ that remains occupied or unoccupied over time,

$$\left[\widehat{H}, \widehat{n}_i\right] = \left[\widehat{H}, \widehat{c}_i^{\dagger}\widehat{c}_i\right] \neq 0. \tag{3.39}$$

3.3.1 Coulomb interaction

The Hamiltonian of a system of particles can always be divided into two parts, $\widehat{H}_0 = \widehat{\Psi}^\dagger \tilde{H} \widehat{\Psi}$ with $\tilde{H}$ from Eq. (2.12), and $\widehat{H}_I$ which contains the two-particle operators giving the interaction between the particles [9]. The Hamiltonian of a system of electrons can be written as

$$\widehat{H} = \widehat{H}_0 + \widehat{H}_I = \widehat{\Psi}^\dagger \tilde{H}_0 \widehat{\Psi} + \widehat{U}, \tag{3.40}$$

where $\tilde{H}_0$ is taken from Eq. (2.12) and the Coulomb interaction between the electrons is given by $\widehat{U}$. The Coulomb interaction acts on pairs of electrons and is inversely proportional to their relative distance. Instead of starting from a sum of two-particle operators

$$\widehat{U} = \sum_i^N \sum_{i \neq j}^N \widehat{U}^{i,j}, \tag{3.41}$$

and proceeding in the same way as with the one-particle Hamiltonian in Eq. (3.5), we will save time and derive the form of $\widehat{U}$ using some simple but less rigorous arguments. Let us start by looking at a system containing two distinguishable particles with state vector $|q_i\rangle \otimes |q_j\rangle$. In this case the operator $\tilde{U}$ can be written as

$$\tilde{U} = \frac{1}{\left|\tilde{\mathbf{r}} \otimes \tilde{1} - \tilde{1} \otimes \tilde{\mathbf{r}}\right|}, \tag{3.42}$$

where $\tilde{\mathbf{r}}$ is the one-particle position operator. Inspired by the form of Eq. (3.20) we can generalize the definition of the field operators from one-particle states

$$|q_i\rangle \rightarrow \widehat{\Psi} \equiv \sum_i |q_i\rangle \widehat{c}_i \tag{3.43}$$

to two-particle states

$$|q_i\rangle \otimes |q_j\rangle \rightarrow \widehat{\Psi}^{(2)} \equiv \sum_{ij} |q_i\rangle \otimes |q_j\rangle \widehat{c}_i \widehat{c}_j, \tag{3.44}$$

and write

$$\widehat{U} \equiv \frac{1}{2} \widehat{\Psi}^{(2)\dagger} \tilde{U} \widehat{\Psi}^{(2)} = \frac{1}{2} \widehat{\Psi}^{(2)\dagger} \left(\frac{1}{\left|\tilde{\mathbf{r}} \otimes \tilde{1} - \tilde{1} \otimes \tilde{\mathbf{r}}\right|} \right) \widehat{\Psi}^{(2)}. \tag{3.45}$$

The factor 1/2 is introduced to compensate that the interactions between the particles are counted twice in the product with the field operators. Expanding the operator $\tilde{\mathbf{r}}$ in Eq. (3.45) in a single-particle position basis $\{|\mathbf{r}\rangle\}$ gives the standard expression [10]

$$\widehat{U} = \frac{1}{2} \int \widehat{\Psi}^\dagger(\mathbf{r}) \widehat{\Psi}^\dagger(\mathbf{r}') \frac{1}{|\mathbf{r} - \mathbf{r}'|} \widehat{\Psi}(\mathbf{r}') \widehat{\Psi}(\mathbf{r}) d\mathbf{r} d\mathbf{r}'. \tag{3.46}$$

3.4 Correlation effects

To be able to discuss the effects of the interaction between the electrons in a material we need to introduce the concepts of pure, mixed, separable and entangled states.

The state of a system is called pure if it can be represented by a state vector. If a density operator is required to describe the state it is called a mixed state. This means that all diagonal representations of a density operator representing a mixed state must have at least two non-zero terms. A mixed state is also said to be classically correlated, as the correlation between the states is of statistical nature. The thermal density operator in Eq. (3.37) describes in general a mixed state as long as the temperature is non-zero.

A state vector is called separable if it can be written as a single Slater determinant, i.e. a single vector in the occupation number formalism $|\nu\rangle = |n_1, n_2, \cdots\rangle$, for some one-particle states $\{|q_i'\rangle\}_i$. A general state is called separable if its density operator has a diagonal representation that only contains separable terms. A state that is not separable but must be represented in one way or another through a superposition of several Slater determinants is said to be entangled or quantum correlated. In section 3.1.5 we saw that the Hamiltonian of a system of non-interacting particles has only pure and separable eigenstates. Hence, an entangled state can not be described as a convex sum of the eigenstates of a single-particle Hamiltonian. This means that the density operator in Eq. (3.37) is always separable if $\widehat{H}$ is given by a single-particle Hamiltonian.

These definitions can be succinctly summarized for an N-electron state as

$$\left.\begin{aligned} |\Psi'_{\mathbf{i}}\rangle &= \widehat{\Lambda}^\dagger|0\rangle \equiv \prod_p^N \widehat{c}^\dagger_{\mathbf{i}_p}|0\rangle \ \text{pure separable} \end{aligned}\right\} \text{uncorrelated}$$

$$\left.\begin{aligned} |\Psi_{\mathbf{i}}\rangle &= \sum_{\mathbf{j}} a_{\mathbf{ij}} \prod_p^N \widehat{c}^\dagger_{\mathbf{j}_p}|0\rangle \ \text{pure entangled} \\ \widehat{\rho}' &= \sum_{\mathbf{i}} p'_{\mathbf{i}} |\Psi'_{\mathbf{i}}\rangle\langle\Psi'_{\mathbf{i}}| \ \text{mixed separable} \\ \widehat{\rho} &= \sum_{\mathbf{i}} p_{\mathbf{i}} |\Psi_{\mathbf{i}}\rangle\langle\Psi_{\mathbf{i}}| \ \text{mixed entangled} \end{aligned}\right\} \text{correlated}$$

where $|0\rangle$ is the vacuum state. Here $p_{\mathbf{i}}$ and $p'_{\mathbf{i}}$ are sets of probabilities normalized to one, and $a_{\mathbf{ij}}$ are expansion coefficients. The vectorial indices $\mathbf{i}$ and $\mathbf{j}$ are composed of the ordered components $\mathbf{i}_p$ and $\mathbf{j}_p$ referring to a generic one-particle basis. For example the state $\widehat{c}^\dagger_1\widehat{c}^\dagger_3\widehat{c}^\dagger_7|0\rangle$ corresponds to a many body index $\mathbf{i} = (1,3,7)$.

Classical correlations can derive from physical processes, e.g. thermal decoherence, but also be induced by a local projection upon some set of orbitals, e.g. the d- or f-orbitals of single atom in a solid. To see the effect of a local projection, let us consider a set orbitals $\mathscr{A}$ labelled by the indices in $A = \{j; |q_j\rangle \in \mathscr{A}\}$. A set of 3d-orbitals could for example have

$A = \{21, 22, \cdots, 30\}$ where the orbitals indexed by $1, \cdots, 20$ could be s- and p-orbitals. The corresponding Fock-subspaces[11] are given by

$$\mathscr{A}' = \left\{ \widehat{A}^\dagger = \sum_{\mathbf{j} \in A} a_{\mathbf{j}} \prod_p^{N_{\mathbf{j}}} \widehat{c}^\dagger_{\mathbf{j}_p}; \sum_{\mathbf{j}} |a_{\mathbf{j}}|^2 = 1 \right\}, \tag{3.47}$$

$$\mathscr{B}' = \left\{ \widehat{B}^\dagger = \sum_{\mathbf{j} \notin A} b_{\mathbf{j}} \prod_p^{N_{\mathbf{j}}} \widehat{c}^\dagger_{\mathbf{j}_p}; \sum_{\mathbf{j}} |b_{\mathbf{j}}|^2 = 1 \right\}, \tag{3.48}$$

where $\mathbf{j} \in A$ is defined as $\mathbf{j}_p \in A$ for $p = 1, \cdots, N_{\mathbf{j}}$. The full Hilbert space $\mathscr{H}$ can be bipartitioned as

$$\mathscr{H} = \mathscr{A}'' \otimes \mathscr{B}'' \equiv \left\{ \sum_{\mathbf{ij}} \alpha_{\mathbf{ij}} \widehat{A}^\dagger_{\mathbf{i}} \widehat{B}^\dagger_{\mathbf{j}} |0\rangle; \widehat{A}^\dagger_{\mathbf{i}} \in \mathscr{A}', \widehat{B}^\dagger_{\mathbf{j}} \in \mathscr{B}' \right\}, \tag{3.49}$$

where

$$\mathscr{A}'' = \left\{ \widehat{A}^\dagger |0\rangle; \widehat{A}^\dagger \in \mathscr{A}' \right\}, \tag{3.50}$$

$$\mathscr{B}'' = \left\{ \widehat{B}^\dagger |0\rangle; \widehat{B}^\dagger \in \mathscr{B}' \right\}. \tag{3.51}$$

The local projection of a pure state $|\Psi\rangle \in \mathscr{A}'' \otimes \mathscr{B}''$ upon the orbitals in $\mathscr{A}$ is obtained by taking the partial trace over $\mathscr{B}''$:

$$\widehat{\rho}^A = \sum_{\mathbf{ij}} \widehat{\rho}^A_{\mathbf{ij}} \widehat{A}^\dagger_{\mathbf{i}} |0\rangle \langle 0| \widehat{A}_{\mathbf{j}}, \tag{3.52}$$

where $\widehat{\rho}^A_{\mathbf{ij}} = \sum_{\mathbf{k}} \alpha_{\mathbf{ik}} \alpha^*_{\mathbf{jk}}$. The locally projected state $\widehat{\rho}^A$ is therefore a mixed state, unless $\widehat{\rho}^A$ happens to be idempotent.

Quantum correlations can stem from pair-wise particle interactions, e.g. Coulomb interaction between electrons, or be induced by a non-local projection. To illustrate these effects let us consider a system with one spin-up electron and one spin-down electron in two degenerate orbitals. If the exchange interaction matrix element $\widehat{\mathrm{U}}_{1221}$ between the two orbitals is positive (negative) the ground state $|gs-\rangle$ ($|gs+\rangle$) can be written as

$$|gs\pm\rangle = \frac{1}{\sqrt{2}} ((\widehat{c}^\dagger_{1\uparrow} \widehat{c}^\dagger_{2\downarrow} \pm \widehat{c}^\dagger_{1\downarrow} \widehat{c}^\dagger_{2\uparrow}) |0\rangle. \tag{3.53}$$

The state vector $|gs-\rangle$ ($|gs+\rangle$) cannot be written as a separable state vector, which makes it entangled. If both electrons have the same spin then one needs at least four orbitals and a non-zero pair-hopping element of the form $\widehat{\mathrm{U}}_{1234}$ to get an entangled state. This situation is artistically depicted on the front page of this thesis for a set of d-orbitals.

A non-local projection is qualitatively different from a local projection in that it projects onto a set of many-body states, and not a set of orbitals. A

non-local projection can therefore easily lead to entanglement. For example, the non-local projection operator

$$\widehat{P} = \widehat{c}^{\dagger}_{1\uparrow}\widehat{c}^{\dagger}_{2\downarrow}|0\rangle\langle 0|\widehat{c}_{2\downarrow}\widehat{c}_{1\uparrow} + \widehat{c}^{\dagger}_{1\downarrow}\widehat{c}^{\dagger}_{2\uparrow}|0\rangle\langle 0|\widehat{c}_{2\uparrow}\widehat{c}_{1\downarrow}, \tag{3.54}$$

turns the pure separable spin-coherent state $(1/2)(\widehat{c}^{\dagger}_{1\uparrow}+\widehat{c}^{\dagger}_{1\downarrow})(\widehat{c}^{\dagger}_{2\uparrow}\pm\widehat{c}^{\dagger}_{2\downarrow})|0\rangle$ into the entangled state $|gs\pm\rangle$. It should be noted that $\widehat{P}$ projects onto two separable states, and that the non-local projection used in this example in fact corresponds to a simple Stern-Gerlach experiment on a beam of spin-1 particles, with a single slit to remove the spin ± 1 components of the beam.

Considering that the electrons are constantly interacting with each other it is perhaps surprising that many systems with delocalized one-electron states are in fact well described by separable states. There are, however, processes which at least heuristically can explain this observation. One important factor is decoherence in an open quantum system. If an electron in an entangled state is subject to a measurement of a one-electron observable $\tilde{O}$, the entangled state will partially collapse and the electron will end up in a (separable) one-electron eigenstate of $\tilde{O}$. The more a state is susceptible to measurements from the surrounding, the less chance it has to stay entangled. Furthermore, a delocalized electron interact with a large number of other delocalized electrons. There are now two main scenarios, either the entanglement between the electrons add up in a constructive way to lower the energy of the state, or the entanglement is frustrated and the ground state becomes a superposition between a large number of slightly different many-body states. You can for example think of this as a growing magnetic domain in the first case, and a spin-glass-like behavior in the second. In the first case the entanglement spreads throughout the system on a macroscopic scale. As the number of entangled electrons grows the risk that one of them will be detected by a probe increases dramatically, resulting in the collapse into a separable state. In the second case the large number of superpositioned many-body states, and the small energy differences involved, makes the total effect smaller and less distinct. These heuristic arguments might explain the success of the effective potential approaches described in the next chapter.

4. Single particle approximations

The many-body eigenbasis of $\widehat{H}$ in Eq. (3.40) can not be constructed simply from occupying the single-particle eigenstates, like in Eq. (3.23), due to the interaction term $\widehat{U}$. To find the eigenvalues and eigenstates of $\widehat{H}$ one has to diagonalize its matrix representation $\widehat{\mathrm{H}}$ in the full many-body basis. Due to the rapid growth of the basis with the increase in the number of particles and available one-particle states, see Eq. (3.4), this problem becomes intractable for anything but the smallest systems. Much effort has therefore been devoted to defining an effective Hamiltonian which captures the effect of the Coulomb interaction but still can be written in a one-particle form.

4.1 Hartree-Fock approximation

One of the most interesting quantities to extract from a calculation is the total energy E of the system. The comparison of the total energies of two phases of the same system tells us which one is the most stable at zero Kelvin. The electronic contribution to E is obtained from the expectation value of the Hamiltonian

$$E[\widehat{\rho}] = \mathrm{Tr}\left(\widehat{\rho}\widehat{H}\right) = E_0[\widehat{\rho}] + \mathrm{Tr}\left(\widehat{\rho}\widehat{U}\right), \tag{4.1}$$

where $E_0[\widehat{\rho}] = \mathrm{Tr}(\widehat{\rho}\widehat{H}_0)$ is the energy contribution from the one-electron part of the Hamiltonian. The Coulomb interaction enters only in the form of an expectation value over $\widehat{U}$. The total energy of the system is therefore preserved if the operator $\widehat{U}$ can be replaced with an effective one-electron operator $\tilde{U}^{(1)}$ with the same expectation value as $\widehat{U}$,

$$\mathrm{Tr}\left(\widehat{\rho}\widehat{\Psi}^{\dagger}\tilde{U}^{(1)}\widehat{\Psi}\right) = \mathrm{Tr}\left(\widehat{\rho}\widehat{U}\right). \tag{4.2}$$

In the Hartree-Fock approximation[1] [12, 13] the effective operator $\tilde{U}^{(1)}$ is approximated by coupling two external one-electron states $|q_i\rangle\langle q_j|$ to one of the two interacting electrons in $\mathrm{Tr}(\widehat{\rho}\widehat{U})$,

$$\begin{aligned}
\widehat{U}^{HF} &= \sum_{ij}\frac{1}{2}\mathrm{Tr}\left(\widehat{\rho}\sum_{mn}\widehat{c}_m^{\dagger}\tilde{\mathrm{U}}_{minj}\widehat{c}_n - \widehat{c}_m^{\dagger}\tilde{\mathrm{U}}_{mijn}\widehat{c}_n\right)\widehat{c}_i^{\dagger}\widehat{c}_j \\
&= \sum_{ij}\frac{1}{2}\mathrm{Tr}(\widehat{\rho}\widehat{c}_m^{\dagger}\widehat{c}_n)\left[\tilde{\mathrm{U}}_{minj} - \tilde{\mathrm{U}}_{mijn}\right]\widehat{c}_i^{\dagger}\widehat{c}_j \qquad (4.3) \\
\tilde{\mathrm{U}}_{minj} &\equiv \left[\langle q_m|\otimes\langle q_i|\right]\tilde{U}\left[|q_n\rangle\otimes|q_j\rangle\right].
\end{aligned}$$

[1] We have here used a many-body density operator formalism. All the expressions reduce to the original ones if the density operator is set to be pure and separable.

The two terms $\tilde{U}_{minj}$ and $\tilde{U}_{mijn}$ comes from coupling the one-electron states $|q_i\rangle\langle q_j|$ to the same particle label or to different particle labels, respectively.

$\widehat{U}^{HF}$ gives the correct expectation value if the density operator can be represented by a pure separable state, i.e. $\widehat{\rho} = \widehat{\Lambda}_\nu^\dagger|0\rangle\langle 0|\widehat{\Lambda}_\nu$. However, as pointed out in section 3.4, the ground state of a system of interacting particles at finite temperature is in general neither pure nor separable. The problem of not being able to describe an entangled ground state was nevertheless already introduced in the concept of an effective Hamiltonian in a single-particle form. As we saw in section 3.1.5, all the eigenstates of a Hamiltonian describing non-interacting particles are always separable.

Even if the temperature is set to zero and the ground state is assumed to be a pure separable state we still have to deal with the problem that $\widehat{U}^{HF}$ depends on the state of the system through $\widehat{\rho}$. Thus, in order to find a correct ground state we must use the operator $\widehat{U}^{HF}$ that in itself depends on the ground state we are out to find. The most common way to deal with this problem is to start from a trial density operator $\widehat{\rho}_0$, construct $\widehat{U}^{HF}$, find the ground state $\widehat{\rho}_{gs}$, make a new trial density operator $\widehat{\rho}_1$ from a mixture of $\widehat{\rho}_0$ and $\widehat{\rho}_{gs}$, and repeat until the trial density operator stops changing. Due to this algorithm the Hartree-Fock method is often called the self-consistent field method in literature.

4.2 Density Functional Theory

Density Functional Theory (DFT) is centered around the electron density

$$\rho(\mathbf{r}) = \mathrm{Tr}[\widehat{\rho}\widehat{n}(\mathbf{r})] \equiv \mathrm{Tr}[\widehat{\rho}\widehat{\Psi}^\dagger|\mathbf{r}\rangle\langle\mathbf{r}|\widehat{\Psi}], \tag{4.4}$$

and is based on two theorems first formulated[2] by Hohenberg and Kohn [14]. DFT in the Hohenberg-Kohn formulation is an exact theory but with an extremely computationally expensive energy functional [15, 16].

4.2.1 Hohenberg-Kohn theorems

Theorem 1

If two external potentials $\widehat{V}_1$ and $\widehat{V}_2$ give the same ground-state electron density $\rho_0(\mathbf{r}) \equiv \mathrm{Tr}[\widehat{\rho}_1\widehat{n}(\mathbf{r})] = \mathrm{Tr}[\widehat{\rho}_2\widehat{n}(\mathbf{r})]$, then their ground state density operators $\widehat{\rho}_1$ and $\widehat{\rho}_2$ will be degenerate, i.e., $\mathrm{Tr}(\widehat{\rho}_1\widehat{H}_1) = \mathrm{Tr}(\widehat{\rho}_2\widehat{H}_1)$ and $\mathrm{Tr}(\widehat{\rho}_1\widehat{H}_2) = \mathrm{Tr}(\widehat{\rho}_2\widehat{H}_2)$.

Theorem 2

There is a universal energy functional $F[\rho]$, independent of $\widehat{V}$, which is minimized by the ground state density $\rho_0(\mathbf{r})$. The ground state energy of an elec-

[2]Here we have generalized the theorems to deal with density operators and allow for degeneracies in the ground state.

tron density $\rho(\mathbf{r})$ is given by $E[\rho] \equiv F[\rho] + \int V(\mathbf{r})\rho(\mathbf{r})d\mathbf{r}$.

Before we prove these theorems, let us first separate out the external potential $\widehat{V} \equiv \widehat{\Psi}^{\dagger} V(\tilde{\mathbf{r}})\widehat{\Psi}$ from $\widehat{H}_0$,

$$\widehat{H}_0' \equiv \widehat{H}_0 - \widehat{V}. \tag{4.5}$$

Furthermore, in the following proofs we assume that any relativistic terms in the Hamiltonian can be neglected. All proofs are, however, identical if we consider a many-body representation $\widehat{H}$ of the fully relativistic Hamiltonian $\tilde{H}$ in Eq. (2.2) plus a Coulomb interaction term $\widehat{U}$.

Proof 1
Take two external potentials $\widehat{V}_1$ and $\widehat{V}_2$ and construct two Hamiltonians $\widehat{H}_1 = \widehat{H}_0' + \widehat{U} + \widehat{V}_1$ and $\widehat{H}_2 = \widehat{H}_0' + \widehat{U} + \widehat{V}_2$. The two Hamiltonians give rise to two density operators $\widehat{\rho}_1$ and $\widehat{\rho}_2$ corresponding to the ground state[3] of the system. Let us now restrict ourselves to the potentials fulfilling the condition stated in the theorem: $\rho(\mathbf{r}) = \mathrm{Tr}[\widehat{\rho}_1\widehat{n}(\mathbf{r})] = \mathrm{Tr}[\widehat{\rho}_2\widehat{n}(\mathbf{r})]$. Given this condition the ground state energies can be written as

$$E_1 = \mathrm{Tr}(\widehat{\rho}_1\widehat{H}_1) \leq \mathrm{Tr}(\widehat{\rho}_2\widehat{H}_1) = \mathrm{Tr}\left(\widehat{\rho}_2[\widehat{H}_0' + \widehat{U}]\right) + \int V_1(\mathbf{r})\rho(\mathbf{r})d\mathbf{r}, \tag{4.6}$$

$$E_2 = \mathrm{Tr}(\widehat{\rho}_2\widehat{H}_2) \leq \mathrm{Tr}(\widehat{\rho}_1\widehat{H}_2) = \mathrm{Tr}\left(\widehat{\rho}_1[\widehat{H}_0' + \widehat{U}]\right) + \int V_2(\mathbf{r})\rho(\mathbf{r})d\mathbf{r}, \tag{4.7}$$

Suppose now that $\widehat{\rho}_1$ and $\widehat{\rho}_2$ are not degenerate, i.e.,

$$\mathrm{Tr}(\widehat{\rho}_1\widehat{H}_1) < \mathrm{Tr}(\widehat{\rho}_2\widehat{H}_1) \tag{4.8}$$

and/or

$$\mathrm{Tr}(\widehat{\rho}_2\widehat{H}_2) < \mathrm{Tr}(\widehat{\rho}_1\widehat{H}_2). \tag{4.9}$$

This assumption changes the less-or-equal sign in Eq. (4.6) and/or (4.7) into a strictly-less-than sign. Adding Eq. (4.6) and (4.7) then yields

$$\begin{aligned} E_1 + E_2 &< \mathrm{Tr}\left(\widehat{\rho}_2[\widehat{H}_0' + \widehat{U}]\right) + \mathrm{Tr}\left(\widehat{\rho}_1[\widehat{H}_0' + \widehat{U}]\right) + \int [V_1(\mathbf{r}) + V_2(\mathbf{r})]\rho(\mathbf{r})d\mathbf{r} \\ &= \mathrm{Tr}(\widehat{\rho}_1\widehat{H}_1) + \mathrm{Tr}(\widehat{\rho}_2\widehat{H}_2) = E_1 + E_2. \end{aligned} \tag{4.10}$$

Eq. (4.10) is a contradiction, and this proves that our assumption that $\widehat{\rho}_1$ and $\widehat{\rho}_2$ are not degenerate is false.

Proof 2
The ground state density operator $\widehat{\rho}_0$ is obtained by minimizing the total energy $E = \mathrm{Tr}(\widehat{\rho}\widehat{H})$ with respect to all variables in $\widehat{\rho}$. However, instead of doing

[3]The ground state of a system at finite temperature is given by the thermal density operator defined in Eq. (3.37)

this minimization in just one step one can start by restricting the minimization to those density operators $\widehat{\rho}$ which give a certain electron density [15, 16] $\rho(\mathbf{r})$, giving

$$\begin{aligned} E[\rho] &= \min_{\widehat{\rho}\to\rho} \mathrm{Tr}\left[\widehat{\rho}(\widehat{H}_0' + \widehat{U} + \widehat{V}(\tilde{\mathbf{r}}))\right] \\ &= \min_{\widehat{\rho}\to\rho} \mathrm{Tr}\left[\widehat{\rho}(\widehat{H}_0' + \widehat{U})\right] + \int V(\mathbf{r})\rho(\mathbf{r})d\mathbf{r} \\ &= F[\rho] + \int V(\mathbf{r})\rho(\mathbf{r})d\mathbf{r}, \end{aligned} \tag{4.11}$$

where $\widehat{\rho}\to\rho$ implies $\widehat{\rho}\in\{\widehat{\rho};\mathrm{Tr}[\widehat{\rho}\widehat{n}(\mathbf{r})]=\rho(\mathbf{r})\}$. The energy is minimized in a second step with respect to $\rho(\mathbf{r})$ to get the total energy

$$E = \min_{\rho} E[\rho]. \tag{4.12}$$

If the minimization procedure in Eq. (4.12) tries to evaluate $E[\rho]$ for some unphysical electron density, not describable by any density operator, the constraint in the minimization procedure in Eq. (4.11) sets $E[\rho]$ to an infinitely high value.

4.2.2 Kohn-Sham formulation

The proof of the second theorem gives an explicit form of the universal functional F, but the minimization procedure involved is as computational demanding as the original many-body problem. The aim of the Kohn-Sham method [17] is to extract those terms from the universal functional F that are known to give a large contribution in the Hartree-Fock method, and then approximate the remaining term with a computationally inexpensive functional. Since the Hartree-Fock method works with density operators $\widehat{\rho}$ and not electron densities $\rho(\mathbf{r})$, there is no direct connection between the terms in

$$E^{HF}[\widehat{\rho}] = \mathrm{Tr}\left[\widehat{\rho}\widehat{H}^{HF}\right] = \mathrm{Tr}\left[\widehat{\rho}(\widehat{H}_0 + \widehat{U}^{HF})\right] \tag{4.13}$$

and $E[\rho]$ in Eq. (4.12). Kohn and Sham realized that one first needs to change the minimization from $\rho(\mathbf{r})$ to $\widehat{\rho}$, giving

$$E = \min_{\rho} E[\rho] = \min_{\widehat{\rho}} E^{KS}[\widehat{\rho}] \equiv \min_{\widehat{\rho}} E[\mathrm{Tr}(\widehat{n}(\mathbf{r})\widehat{\rho})]. \tag{4.14}$$

The change of minimization parameter does not change the value of E because the functional $E[\rho]$ takes its minimum value for a physical $\rho(\mathbf{r})$ obtained for some $\widehat{\rho}$. Since $E^{KS}[\widehat{\rho}]$ depends on $\widehat{\rho}$ we can now easily extract parts of $\mathrm{Tr}\left[\widehat{\rho}\widehat{H}^{HF}\right]$,

$$E^{KS}[\widehat{\rho}] = \mathrm{Tr}(\widehat{\rho}\widehat{H}_0) + E_H[\widehat{\rho}] + E_{XC}[\widehat{\rho}], \tag{4.15}$$

$$E_{XC}[\widehat{\rho}] \equiv E[\mathrm{Tr}(\widehat{n}(\mathbf{r})\widehat{\rho})] - \mathrm{Tr}(\widehat{\rho}\widehat{H}_0') - E_H[\widehat{\rho}]. \tag{4.16}$$

The first term on the right hand side in Eq. (4.15) is the expectation value of the one-electron operators, including the external potential. The second term is the Hartree functional $E_H[\rho]$ which is defined as

$$E_H[\widehat{\rho}] = \sum_{ijmn} \frac{1}{2} \mathrm{Tr}\left[\widehat{\rho}\widehat{c}_m^\dagger \widehat{c}_n\right] \tilde{\mathrm{U}}_{minj} \mathrm{Tr}\left[\widehat{c}_i^\dagger \widehat{c}_j \widehat{\rho}\right] \tag{4.17}$$

$E_H[\rho]$ corresponds to the expectation value of the $\tilde{\mathrm{U}}_{minj}$ (Hartree) term in Eq. (4.3). The exchange term $\tilde{\mathrm{U}}_{mijn}$ is not extracted but is allowed to remain in the exchange-correlation term $E_{XC}[\widehat{\rho}]$.

E_{XC} can be returned to a density functional by a second minimization procedure

$$E_{XC}[\widehat{\rho}] \to E_{XC}[\rho]|_{\rho(\mathbf{r})=\mathrm{Tr}[\widehat{\rho}\widehat{n}(\mathbf{r})]} = E[\rho] - \min_{\widehat{\rho}\to\rho} \left(\mathrm{Tr}[\widehat{\rho}\widehat{H}_0] + E_H[\widehat{\rho}]\right). \tag{4.18}$$

The new Kohn-Sham term, given by

$$E_{full}^{KS}[\widehat{\rho}] = \mathrm{Tr}(\widehat{\rho}\widehat{H}_0) + E_H[\widehat{\rho}] + E_{XC}[\rho]|_{\rho(\mathbf{r})=\mathrm{Tr}[\widehat{\rho}\widehat{n}(\mathbf{r})]}, \tag{4.19}$$

does not give the ground state energy corresponding to the electron density ρ unless $\widehat{\rho}$ minimizes $\mathrm{Tr}(\widehat{\rho}\widehat{H}_0) + E_H[\widehat{\rho}]$. This is not a problem, however, since the density operator that minimizes E^{KS} also must minimize the two Hartree-Fock terms $\mathrm{Tr}(\widehat{\rho}\widehat{H}_0)$ and $E_H[\widehat{\rho}]$, for a given electron density ρ.

No approximations have been done so far, but nothing has been gained in terms of computational complexity either. It is therefore time to introduce the first approximation in the Kohn-Sham scheme. Instead of minimizing over all density operators we restrict the search space of the minimization procedure in Eq. (4.14) and (4.18) to pure separable states, i.e., $\widehat{\rho} = |\nu\rangle\langle\nu| = \widehat{\Lambda}_\nu^\dagger|0\rangle\langle 0|\widehat{\Lambda}_\nu$, where $\langle\nu|\nu\rangle = 1$ and $\langle\nu|\widehat{n}|\nu\rangle = N$. Equation (4.14) can then be written as

$$\min_{\substack{\widehat{\rho}=|\nu\rangle\langle\nu| \\ \langle\nu|\nu\rangle=1 \\ \langle\nu|\widehat{n}|\nu\rangle=N}} E^{KS}[\widehat{\rho}] = \min_{\substack{|\nu\rangle \\ \langle\nu|\nu\rangle=1 \\ \langle\nu|\widehat{n}|\nu\rangle=N}} \langle\nu| \left(\widehat{H}_0 + \frac{1}{2}\int \frac{\widehat{n}(\mathbf{r})\widehat{n}(\mathbf{r}')}{|\mathbf{r}-\mathbf{r}'|} d\mathbf{r}d\mathbf{r}'\right) |\nu\rangle + E_{XC}[\rho] \tag{4.20}$$

The restriction to pure separable states is in principle not an approximation as long as the corresponding electron densities span the same space as the electron densities from the full many-body states. The reason for this is that the exact universal function F is still embedded in E_{XC} and will minimize over all many-body states, not just the pure separable ones. It is important to note the particles that are represented by $|\nu\rangle$ do not behave as electrons. The condition that $|\nu\rangle$ must be pure and separable implies that they instead act like non-interacting particles, and we will therefore refer to them as Kohn-Sham particles.

The minimization procedure can now be carried out using ε as a Lagrangian multiplier for the $\langle \nu|\nu\rangle = 1$ constraint, and[4] μ for $\langle \nu|\widehat{n}|\nu\rangle = N$, giving

$$\frac{\delta}{\delta\langle\nu|}\left[\langle\nu|\widehat{H}_0 + \frac{1}{2}\int\frac{\widehat{n}(\mathbf{r})\widehat{n}(\mathbf{r}')}{|\mathbf{r}-\mathbf{r}'|}d\mathbf{r}d\mathbf{r}' - \varepsilon - \mu\widehat{n}|\nu\rangle + E_{XC}[\rho]\right] = 0. \tag{4.21}$$

Performing the derivation in Eq. (4.21) gives

$$\left[\widehat{H}_0 + \int\frac{\rho(\mathbf{r})\widehat{n}(\mathbf{r}')}{|\mathbf{r}-\mathbf{r}'|}d\mathbf{r}d\mathbf{r}' - \varepsilon - \mu\widehat{n}\right]|\nu\rangle + \frac{\delta E_{XC}}{\delta\langle\nu|} = 0, \tag{4.22}$$

where we have used that

$$\frac{\delta}{\delta\langle\nu|}\langle\nu|\widehat{n}(\mathbf{r})\widehat{n}(\mathbf{r}')|\nu\rangle = [\rho(\mathbf{r})\widehat{n}(\mathbf{r}') + \widehat{n}(\mathbf{r})\rho(\mathbf{r}')]|\nu\rangle. \tag{4.23}$$

The second approximation in the Kohn-Sham scheme is to replace the exact but computationally cumbersome E_{XC} functional with some approximate but less demanding functional. One of the most popular choices, introduced already in the original paper by Kohn and Sham [17], is the exchange-correlation functional of the Local Density Approximation,

$$E_{XC}^{LDA}[\rho] = \int\rho(\mathbf{r})\varepsilon(\rho(\mathbf{r}))d\mathbf{r}, \tag{4.24}$$

$$\frac{\delta E_{XC}}{\delta\langle\nu|} = \int\widehat{n}(\mathbf{r})\varepsilon(\rho(\mathbf{r})) + \rho(\mathbf{r})\widehat{n}(\mathbf{r})\left.\frac{d\varepsilon}{dx}\right|_{x=\rho(\mathbf{r})}d\mathbf{r}|\nu\rangle. \tag{4.25}$$

The function ε is parameterized to give the exact exchange-correlation energy for a homogeneous electron gas with electron density $\rho = \rho(\mathbf{r})$. Substituting Eq. (4.25) into (4.22) gives

$$\left[\widehat{H}_0 + \int\left(\frac{\rho(\mathbf{r}')}{|\mathbf{r}-\mathbf{r}'|}d\mathbf{r}' + \varepsilon(\rho(\mathbf{r})) + \rho(\mathbf{r})\frac{d\varepsilon}{dx}\right)\widehat{n}(\mathbf{r})d\mathbf{r} - \varepsilon\right]|\nu\rangle = 0, \tag{4.26}$$

where $\mu\widehat{n}$ has been (re)added to $\widehat{H}_0$. Equation (4.26) is an eigenvalue problem, and the minimization procedure in this case corresponds to finding the eigenvector $|\nu_0\rangle$ with the smallest eigenvalue ε_0. Equation (4.26) contains only one-electron operators and can be written as

$$\widehat{H}^{KS}|\nu\rangle \equiv \widehat{\Psi}^\dagger\tilde{H}^{KS}\widehat{\Psi}|\nu\rangle = \varepsilon|\nu\rangle. \tag{4.27}$$

The ground state of $\widehat{H}^{KS}$ can easily be found by diagonalizing $\tilde{H}^{KS}$ as shown in Sec. 3.1.5. Since $\widehat{H}^{KS}$ contains the electron density which depends on $|\nu_0\rangle$ one needs to solve Eq. (4.26) self-consistently together with

$$\rho(\mathbf{r}) = \langle\nu_0|\widehat{n}(\mathbf{r})|\nu_0\rangle, \tag{4.28}$$

$$N = \langle\nu_0|\widehat{n}|\nu_0\rangle, \tag{4.29}$$

[4]Those of you who still remember our 'lightened' notation may extract $\mu\widehat{n}$ from $\widehat{H}_0$ instead of adding it twice.

where the number of electrons N can be adjusted using the chemical potential μ in $\widehat{H}_0$. The self-consistent value of ε_0 corresponds to $E^{KS}[\rho_0]$. The Kohn-Sham Hamiltonian $\widehat{H}^{KS}$ has a very different starting point compared to the Hartree-Fock Hamiltonian $\widehat{H}^{HF}$. However, when looking at Eq. (4.1) and (4.15) we see that it is possible to interpret the Hartree plus exchange-correlation term as just another way to approximate $\widehat{U}^{(1)}$ in Eq. (4.2). It should nevertheless be clearly stated that the approximation of the exchange-correlation functional does not reduce KS-DFT to a simple mean-field approximation like Hartree-Fock. Hence, there is nothing in the theory that says that the non-interacting KS particles used in the minimization should be interpreted as electrons, or even that the KS excitation spectra should represent electronic excitations. This point is affirmed by the sharp contrast between experimental photoemission data and the corresponding KS excitation spectrum often seen for localized d- and f-electrons. That said, there is often a surprisingly good agreement between the two quantities for delocalized s- and p-electrons. We have now the option to either discard all the KS particle data, or to use them as a starting point in a scheme aimed to produce a proper electronic excitation spectra. The latter choice implies that we stray a bit from the path of theoretical rigor and actually interpret the KS excitation spectrum as a mean-field-like description of the electronic excitation energies. In the remaining part of this thesis we will explore the second option, and pursue techniques to improve the lacking correspondence for the localized states.

5. Single Impurity Anderson Model

Both HF and KS-DFT map the many-body Hamiltonian $\widehat{H}$ directly to a one-particle form $\tilde{H}^{MF}$. The resulting ground state and excited states are therefore always separable[1]. However, as we saw in section 3.4 electrons in partially filled localized orbitals tend to become entangled due to the Coulomb interaction, making HF and KS-DFT unsuitable[2] to describe these states. For simplicity, let us analyze this problem by considering just a single set of localized orbitals $\mathscr{A}$ (an impurity), spanned by $\{|q_i\rangle\}_{i\in A}$, in a system (the host) otherwise well described by an effective one-particle Hamiltonian $\widehat{H}^{MF} = \widehat{\Psi}^{\dagger}(\tilde{H}_0 + \tilde{U}^{MF})\widehat{\Psi}$. This kind of system corresponds to a Single Impurity Anderson Model [18, 10] (SIAM). To simplify the notation we introduce a subspace index according to the following rules

$$\widehat{\Psi}_A \equiv \tilde{P}_A\widehat{\Psi}, \tag{5.1}$$

$$\tilde{V}_{AB} \equiv \tilde{P}_A\tilde{V}\tilde{P}_B, \tag{5.2}$$

$$\tilde{U}_{ABCD} \equiv \left(\tilde{P}_A \otimes \tilde{P}_B\right)\tilde{U}\left(\tilde{P}_C \otimes \tilde{P}_D\right), \tag{5.3}$$

$$\widehat{V}_{AB} \equiv \widehat{\Psi}^{\dagger}\tilde{V}_{AB}\widehat{\Psi} \equiv \widehat{\Psi}_A^{\dagger}\tilde{V}\widehat{\Psi}_B, \tag{5.4}$$

$$\widehat{U}_{ABCD} \equiv \widehat{\Psi}^{(2)\dagger}\tilde{U}_{ABCD}\widehat{\Psi}^{(2)}. \tag{5.5}$$

Here B, C, and D are index sets corresponding to the orbitals $\mathscr{B}$,$\mathscr{C}$, and $\mathscr{D}$, and the projection operator $\tilde{P}_A$ is defined as

$$\tilde{P}_A \equiv \sum_{i\in A} |q_i\rangle\langle q_i|. \tag{5.6}$$

The SIAM Hamiltonian can now be written as

$$\widehat{H}^{SIAM} = \widehat{T} + \widehat{U}^{SIAM}_{AAAA} \tag{5.7}$$

where $\widehat{U}^{SIAM}_{AAAA}$ describes the Coulomb interaction between the electrons on the impurity and $\widehat{T}$ gives the hopping of the electrons between different orbitals. For our system $\widehat{U}^{SIAM}_{AAAA}$ is given by screened Coulomb interaction $\widehat{U}^{eff}_{AAAA}$, and

[1]The separability of the states in KS-DFT is with respect to the KS particles, not the electrons hiding in an ill-defined way in the approximated exchange-correlation functionals.

[2]The exact functional in Eq. (4.18) could in principle yield the correct total energy, but it would correspond to solving the full many-body problem and then throwing away all the information except the total energy. The resulting KS excitation spectra would still not correspond to the proper electronic excitation spectra, making it the most unsuitable method of them all.

the hopping parameters are given by $\widehat{H}^{MF} - \widehat{U}^{DC}_{AA}$, where $\widehat{U}^{DC}_{AA}$ is the so called double counting correction, giving

$$\widehat{H}^{SIAM} = \widehat{H}^{MF} + \widehat{U}^{eff}_{AAAA} - \widehat{U}^{DC}_{AA}. \tag{5.8}$$

We will return to the definition of $\widehat{U}^{eff}_{AAAA}$ and $\widehat{U}^{DC}_{AA}$ in sections 5.2 and 5.3, respectively, but before that we need to introduce the concept of Green's functions.

5.1 Green's function formalism

There are two ways of handling a one-electron operator $\tilde{A}$ in a many-body system. We have already encountered the first one in section 3.1.4, where the field operator $\widehat{\Psi}$ offered a direct way to map $\tilde{A}$ into a many-body representation

$$\widehat{A} = \widehat{\Psi}^{\dagger}\tilde{A}\widehat{\Psi}. \tag{5.9}$$

The many-body operator $\widehat{A}$ can now directly act upon the density operator $\widehat{\rho}$ and be subject to the dynamics of the Hamiltonian $\widehat{H}$. The second way is to keep $\tilde{A}$ in the one-electron representation but to represent $\widehat{\rho}$ and the dynamics of $\widehat{H}$ using a one-particle Green's function [9]

$$\begin{aligned}\tilde{G}^{S}(t,t') &\equiv -i\sum_{ij}\left\langle S[\widehat{c}_i(t)\widehat{c}^{\dagger}_j(t')]\right\rangle |q_i\rangle\langle q_j| \\ &\equiv -i\mathrm{Tr}(\widehat{\rho}S[\widehat{\Psi}(t)\widehat{\Psi}^{\dagger}(t')]),\end{aligned} \tag{5.10}$$

where the trace runs over all many-body states and $\widehat{\rho}$ is a density operator, for example the thermal density operator taken from Eq. (3.37). The superoperator S is either a time-ordering T, advanced-ordering A, or retarded-ordering R operator defined as

$$T[\widehat{c}(t)\widehat{c}^{\dagger}(t')] \equiv +\theta(t-t')\widehat{c}(t)\widehat{c}^{\dagger}(t') - \theta(t'-t)\widehat{c}^{\dagger}(t')\widehat{c}(t), \tag{5.11}$$

$$A[\widehat{c}(t)\widehat{c}^{\dagger}(t')] \equiv +\theta(t'-t)\left(\widehat{c}(t)\widehat{c}^{\dagger}(t') + \widehat{c}^{\dagger}(t')\widehat{c}(t)\right), \tag{5.12}$$

$$R[\widehat{c}(t)\widehat{c}^{\dagger}(t')] \equiv -\theta(t-t')\left(\widehat{c}(t)\widehat{c}^{\dagger}(t') + \widehat{c}^{\dagger}(t')\widehat{c}(t)\right), \tag{5.13}$$

where $\theta(\tau)$ is the unit step function. The different definitions of S are used for different problems. The advanced and retarded Green's function can for example describe the response of the system to different probes in Linear response theory [19]. The expectation value of the time-ordered Green's function $|\langle\nu_i(t)|\tilde{G}^{T}(t,t')|\nu_j(t')\rangle|^2$ describes for $t > t'$ ($t' > t$) the probability that the many-body system remains unchanged if a particle is added to (removed from) the single particle state $|\nu_j(t')\rangle$ at time t' and then is removed from (added to) the state $|\nu_i(t)\rangle$ at time t. Adding or removing a particle raises the energy of the system, which means that the time-ordered Green's function can be used

to look at the properties of the excited states. Nevertheless, it can also be used to calculate the one-particle reduced density operator

$$\tilde{\rho} \equiv \mathrm{Tr}(\widehat{\Psi}\widehat{\rho}\widehat{\Psi}^{\dagger}) = \sum_{ij} \mathrm{Tr}(\widehat{\rho}\widehat{c}_i^{\dagger}\widehat{c}_j)|q_i\rangle\langle q_j| = -i \lim_{t' \to t^+} \tilde{G}^T(t,t'). \tag{5.14}$$

$\tilde{\rho}$ can be used to obtain the expectation value of any one-particle operator

$$\mathrm{Tr}(\tilde{\rho}\tilde{J}) = \sum_{ij} \mathrm{Tr}(\widehat{\rho}\widehat{c}_i^{\dagger}\widehat{c}_j)\tilde{\mathrm{J}}_{ij} = \mathrm{Tr}(\widehat{\rho}\widehat{J}), \tag{5.15}$$

where $\widehat{J} = \sum_{ij} \tilde{\mathrm{J}}_{ij}\widehat{c}_i^{\dagger}\widehat{c}_j$. The trace on the left hand side of Eq. (5.15) is over the single-particle states while the trace in the middle and on the right hand side comes from the definition of $\tilde{\rho}$ and runs over all possible many-body states.

In the following sections we will focus on the time-ordered Green's function, unless otherwise stated.

5.1.1 Non-interacting Green's function

It can be difficult to use the definition in Eq. (5.10) to construct the Green's function $\tilde{G}^S(t,t')$ as it requires an explicit evaluation of the many-body density operator $\widehat{\rho}$. A solution to this problem is to instead focus on the time evolution of $\tilde{G}^S(t,t')$

$$\begin{aligned} i\frac{d}{dt}\tilde{G}^S(t,t') &= \left\langle \delta(t-t')\left\{\widehat{\Psi}(t)\widehat{\Psi}^{\dagger}(t)\right\} + S\left[\frac{d}{dt}\widehat{\Psi}(t)\widehat{\Psi}^{\dagger}(t')\right]\right\rangle \\ &= \delta(t-t')\tilde{1} + \left\langle S\left[\frac{d}{dt}\widehat{\Psi}(t)\widehat{\Psi}^{\dagger}(t')\right]\right\rangle \qquad (5.16) \\ &= \delta(t-t')\tilde{1} + i\left\langle S\left[[\widehat{H},\widehat{\Psi}(t)]\widehat{\Psi}^{\dagger}(t')\right]\right\rangle, \qquad (5.17) \end{aligned}$$

where we have used the Heisenberg equation

$$\frac{d}{dt}\widehat{\Psi}(t) = i[\widehat{H},\widehat{\Psi}(t)]. \tag{5.18}$$

If the dynamics of the system is governed by a single-particle Hamiltonian $\tilde{H}$ the commutator with the field operator $\widehat{\Psi}(t)$ reduces to

$$[\widehat{H},\widehat{\Psi}(t)] = -\tilde{H}\widehat{\Psi}(t). \tag{5.19}$$

Substituting Eq. (5.19) into Eq. (5.17) yields the differential equation

$$\left(i\frac{d}{dt} - \tilde{H}\right)\tilde{G}_0^S(t,t') = \tilde{1}\delta(t-t'). \tag{5.20}$$

where we have added the subscript 0 to emphasize that $\tilde{G}_0^S(t,t')$ describes non-interacting particles. Taking the Fourier transform of Eq. (5.20) with respect to the complex variable ω and $\tau = t - t'$ gives

$$\left(\omega - \tilde{H}\right)\tilde{G}_0(\omega) = \tilde{1}, \tag{5.21}$$

which has the formal solution

$$\tilde{G}_0(\omega) = \sum_i \frac{|q_i'\rangle\langle q_i'|}{\omega - E_i^{(1)}}. \tag{5.22}$$

where $E_j^{(1)}$ and $|q_j'\rangle$ are the one-particle eigenvalues and eigenstates of $\tilde{H}$, respectively. The matrix element $\langle q_i'|\tilde{G}_0(\omega)|q_i'\rangle$ is undefined for $\omega = E_i^{(1)}$, but is analytical elsewhere. It might seem odd that Eq. (5.22) does not contain any reference to the many-body density operator $\widehat{\rho}$. However, since $\tilde{G}_0(\omega)$ only describes the propagation of added non-interacting particles or holes, it does not depend on the current state of the system but only on the single-particle Hamiltonian that gives the single-particle dynamics.

5.1.2 Density of states

The single-particle density of states (DOS) $\rho(E)$ can be obtained from $\tilde{G}_0(\omega)$ in Eq. (5.22) by letting ω approach the real axis from both the upper and the lower half-plane,

$$\begin{aligned}
\rho(E) &= \lim_{\delta\to 0^+} \frac{-1}{2\pi}\Im\mathrm{Tr}\left[\tilde{G}_0(E+i\delta) - \tilde{G}_0(E-i\delta)\right] \\
&= \lim_{\delta\to 0^+} \frac{-1}{2\pi}\Im\sum_j \underbrace{\left[\frac{1}{E+i\delta-E_j^{(1)}} - \frac{1}{E-i\delta-E_j^{(1)}}\right]}_{\frac{-2i\delta}{(E-E_j^{(1)})^2+\delta^2}} \\
&= \frac{-1}{2\pi}\Im\left[-2i\pi\sum_j \delta(E-E_j^{(1)})\right] = \sum_j \delta(E-E_j^{(1)}).
\end{aligned} \tag{5.23}$$

As $\tilde{G}_0(E+i\delta)$ ($\tilde{G}_0(E-i\delta)$) is only evaluated in the complex upper (lower) half-plane it can be replaced by the Fourier transform of $\tilde{G}_0^R(t,t')$ ($\tilde{G}_0^A(t,t')$). Since $\Im\tilde{G}_0(E+i\delta) = -\Im\tilde{G}_0(E-i\delta)$ Eq. (5.23) simplifies to

$$\begin{aligned}
\rho(E) &= +\lim_{\delta\to 0^+} \frac{1}{\pi}\Im\mathrm{Tr}[\tilde{G}_0^A(E-i\delta)] \\
&= -\lim_{\delta\to 0^+} \frac{1}{\pi}\Im\mathrm{Tr}[\tilde{G}_0^R(E+i\delta)]
\end{aligned} \tag{5.24}$$

5.1.3 Thermal Green's function

$\tilde{G}(t,t')$ is called a thermal time-dependent one-particle Green's function if the density operator in Eq. (5.10) is taken from Eq. (3.37),

$$\begin{aligned}\tilde{G}(t,t') &= -i\mathrm{Tr}\left(\frac{e^{-\beta\widehat{H}}}{Z}T\left[\widehat{\Psi}(t)\widehat{\Psi}^{\dagger}(t')\right]\right)\\ &= \frac{-i}{Z}\sum_{ij}\langle\nu_i|\widehat{\Psi}|\nu_j\rangle\langle\nu_j|\widehat{\Psi}^{\dagger}|\nu_i\rangle e^{-i\tau(E_i^{(N)}-E_j^{(N)})}\times\\ &\quad\left[\theta(\tau)e^{-\beta E_i^{(N)}}-\theta(-\tau)e^{-\beta E_j^{(N)}}\right],\end{aligned} \tag{5.25}$$

where $\tau = t - t'$. Taking the Fourier transform of $\tilde{G}(t,t')$ in Eq. (5.25) gives the Lehmann representation

$$\begin{aligned}\tilde{G}(\omega) = \frac{1}{Z}\sum_{ij}&\langle\nu_i|\widehat{\Psi}|\nu_j\rangle\langle\nu_j|\widehat{\Psi}^{\dagger}|\nu_i\rangle\\ &\left(\frac{e^{-\beta E_i^{(N)}}}{\omega - E_i^{(N)} + E_j^{(N)} + i\delta} - \frac{e^{-\beta E_j^{(N)}}}{\omega - E_i^{(N)} + E_j^{(N)} - i\delta}\right).\end{aligned} \tag{5.26}$$

5.1.4 Hybridization

Up to now all systems have been considered isolated from any quantum mechanical environment. In practice any realistic system is part of some larger quantum mechanical system. The interaction between the system and its environment needs to be addressed before the basic machinery introduced in the previous sections can be applied.

Let us consider a system of non-interacting particles, and divide its states into two orthogonal subspaces, $\mathscr{A}$ spanned by $\{|q_i\rangle\}_{i\in A}$ and $\mathscr{B}$ spanned by $\{|q_i\rangle\}_{i\in B}$. The Hamiltonian of the system can be written as

$$\tilde{H} = \tilde{H}_{AA} + \tilde{H}_{BB} + \tilde{H}_{AB} + \tilde{H}_{BA}. \tag{5.27}$$

where we have used the projection notation introduced in Eq. (5.2). Substituting Eq. (5.27) into Eq. (5.21) yields

$$(\omega\tilde{1}_{AA} - \tilde{H}_{AA})\tilde{G}_{AA}(\omega) = \tilde{1}_{AA} + \tilde{H}_{AB}\tilde{G}_{BA}(\omega), \tag{5.28}$$

$$(\omega\tilde{1}_{BB} - \tilde{H}_{BB})\tilde{G}_{BA}(\omega) = \tilde{H}_{BA}\tilde{G}_{AA}(\omega). \tag{5.29}$$

Substituting $\tilde{G}_{BA}$ from Eq. (5.29) into (5.28) finally gives

$$\left[\omega\tilde{1}_{AA} - \tilde{H}_{AA} - \tilde{H}_{AB}(\omega\tilde{1}_{BB} - \tilde{H}_{BB})^{-1}\tilde{H}_{BA}\right]\tilde{G}_{AA}(\omega) = \tilde{1}_{AA}. \tag{5.30}$$

A comparison between Eq. (5.21) and (5.30) shows that in the case of non-interacting particles, the only difference between an isolated system and a subsystem is the hybridization function

$$\tilde{\Delta}_{AA}(\omega) \equiv \tilde{H}_{AB}(\omega \tilde{1}_{BB} - \tilde{H}_{BB})^{-1}\tilde{H}_{BA}. \tag{5.31}$$

$\tilde{\Delta}_{AA}(\omega)$ has the same analytical properties as $\tilde{G}_0(\omega)$, which means that we can define a hybridization spectral density $\rho_\Delta(E)$ in analogy with Eq. (5.24) as

$$\rho_\Delta(E) = -\lim_{\delta\to 0^+}\frac{1}{\pi}\Im\mathrm{Tr}[\tilde{\Delta}_{AA}(E+i\delta)]. \tag{5.32}$$

$\rho_\Delta(E)$ shows how strongly the orbitals in subspace $\mathscr{A}$ hybridize with the rest of the system at a given energy E. Instead of constructing $\tilde{\Delta}_{AA}(\omega)$ from Eq. (5.31), it is often more convenient to extract it from the inverse of the projected Green's function

$$\tilde{\Delta}_{AA}(\omega) = \omega\tilde{1}_{AA} - \tilde{H}_{AA} - [\tilde{G}_{AA}(\omega)]^{-1}. \tag{5.33}$$

5.2 Screening

Let us now return to the SIAM Hamiltonian in Eq. (5.8) and the definition of $\widehat{U}^{eff}_{AAAA}$. Although it would seem natural to set $\widehat{U}^{eff}_{AAAA}$ equal to the (bare) $\widehat{U}_{AAAA}$ from Eq. (3.46), this choice would strongly overestimate the strength of the interaction between the electrons of the impurity. The missing ingredient is the strong screening induced by the (density-density) interaction with the bath electrons

$$\tilde{\mathrm{U}}^{eff}(t,t') = \tilde{\mathrm{U}}\delta(t-t') + \tilde{\mathrm{U}}\tilde{\chi}^A(t,t')\tilde{\mathrm{U}}. \tag{5.34}$$

where we have used the particle-hole four-index matrix notation

$$\tilde{\mathrm{A}}^{PH}_{\alpha\beta} = \tilde{\mathrm{A}}^{PH}_{\alpha_1\beta_1\alpha_2\beta_2}, \tag{5.35}$$

$$\left[\tilde{\mathrm{A}}^{PH}\tilde{\mathrm{B}}^{PH}\right]_{\alpha\beta} = \sum_\gamma \tilde{\mathrm{A}}^{PH}_{\alpha\gamma}\tilde{\mathrm{B}}^{PH}_{\gamma\beta} = \sum_{\gamma_1,\gamma_2}\tilde{\mathrm{A}}^{PH}_{\alpha_1\gamma_1\alpha_2\gamma_2}\tilde{\mathrm{B}}^{PH}_{\gamma_1\beta_1\gamma_2\beta_2}, \tag{5.36}$$

and defined

$$\begin{aligned}\tilde{\chi}^{PH}_{\alpha\beta}(t,t') = &-\mathrm{Tr}\left(\widehat{\rho}S[\widehat{c}^\dagger_{\alpha_1}(t)\widehat{c}_{\alpha_2}(t)\widehat{c}^\dagger_{\beta_1}(t')\widehat{c}_{\beta_2}(t')]\right)\\ &+\delta_{\alpha_1\alpha_2}\delta_{\beta_1\beta_2}\mathrm{Tr}\left(\widehat{\rho}\widehat{c}^\dagger_{\alpha_1}\widehat{c}_{\alpha_2}\right)\mathrm{Tr}\left(\widehat{\rho}\widehat{c}^\dagger_{\beta_1}\widehat{c}_{\beta_2}\right),\end{aligned} \tag{5.37}$$

$$\tilde{\chi}^A(t,t') = \tilde{\chi}^{PH}(t,t') - \tilde{\chi}^{PH}_{AAAA}(t,t'). \tag{5.38}$$

The operator $\tilde{\chi}^{PH}(t,t')$ is called the particle-hole susceptibility and describes the propagation of an electron-hole pair. In Eq. (5.38) $\tilde{\chi}^{PH}_{AAAA}(t,t')$ removes the self-induced screening of the impurity electrons, as $\widehat{U}^{eff}_{AAAA}$ in Eq. (5.8) takes this effect into account explicitly.

The constrained particle-hole susceptibility $\tilde{\chi}^A(t,t')$ involves mainly the weakly correlated bath states. It can therefore be approximated by means of the constrained random phase approximation (cRPA) [20, 21, 22]

$$\tilde{\chi}^A(t,t') = \tilde{\mathrm{P}}^A(t,t') + \int \tilde{\mathrm{P}}^A(t,t'')\tilde{\mathrm{U}}\tilde{\chi}^A(t'',t')dt'' \tag{5.39}$$

where we have used the particle-hole four-index matrix notation and defined the particle-hole polarization bubble

$$\begin{aligned}
\tilde{P}^{PH}(t,t') &= -\tilde{G}(t,t') \otimes \tilde{G}(t',t) \\
&= \mathrm{Tr}\left(\widehat{\rho} T[\widehat{\Psi}(t)\widehat{\Psi}^\dagger(t')]\right) \otimes \mathrm{Tr}\left(\widehat{\rho} T[\widehat{\Psi}(t')\widehat{\Psi}^\dagger(t)]\right), \qquad (5.40) \\
\tilde{P}^A(t,t') &= \tilde{P}^{PH}(t,t') - \tilde{P}^{PH}_{AA}(t,t') \qquad (5.41)
\end{aligned}$$

Taking the Fourier transform of Eq. (5.34) and (5.39) gives

$$\begin{aligned}
\tilde{\mathrm{U}}^{eff}(\omega) &= \tilde{\mathrm{U}} + \tilde{\mathrm{U}}\tilde{\chi}^A(\omega)\tilde{\mathrm{U}}, \qquad (5.42) \\
\tilde{\chi}^A(\omega) &= \tilde{\mathrm{P}}^A_0(\omega) + \tilde{\mathrm{P}}^A_0(\omega)\tilde{\mathrm{U}}\tilde{\chi}^A(\omega). \qquad (5.43)
\end{aligned}$$

Substituting Eq. (5.43) into Eq. (5.42) and solving for $\tilde{\mathrm{U}}^{eff}$ yields

$$\tilde{\mathrm{U}}^{eff}(\omega) = (\tilde{\mathrm{I}} - \tilde{\mathrm{P}}^A_0(\omega)\tilde{\mathrm{U}})^{-1}\tilde{\mathrm{U}}. \tag{5.44}$$

Finally, due to the difficulties in treating the fully dynamical interaction term $\tilde{\mathrm{U}}^{eff}(\omega)$ [22], it is common to consider the limit $\omega \to 0$ and project upon $\mathscr{A}$ to obtain

$$\tilde{\mathrm{U}}^{eff}_{AAAA} = [(\tilde{\mathrm{I}} - \tilde{\mathrm{P}}^A_0(0)\tilde{\mathrm{U}})^{-1}\tilde{\mathrm{U}}]_{AAAA}. \tag{5.45}$$

This static approximation is often adequate if we are not focusing on the high energy excitation spectrum.

5.3 Double counting corrections

Given the expression for the screened Coulomb interaction $\tilde{\mathrm{U}}^{eff}_{AAAA}$ in Eq. (5.45), we are now ready to deal with the double counting (DC) correction term $\widehat{U}^{DC}_{AA}$ introduced in Eq. (5.8). $\widehat{U}^{DC}_{AA}$ is supposed to cancel the Coulomb interaction contributions which are taken into account both in $\tilde{\mathrm{U}}^{eff}_{AAAA}$ and in $\widehat{H}^{MF}$. The first problem is to determine the on-site Coulomb interaction $\widehat{U}^{MF}_{AA}$ included in $\widehat{H}^{MF}$, since without a proper description of $\widehat{U}^{MF}_{AA}$ it is not possible to identify the extra contributions.

5.3.1 Hartree-Fock

In the case $\widehat{H}^{MF}$ is obtained from the Hartree-Fock approximation $\widehat{U}^{MF}_{AA}$ is given by $\widehat{U}^{HF}_{AA}$ from Eq. (4.3). Since $\tilde{\mathrm{U}}^{eff}_{AAAA}$ was constructed to improve the

mean-field description, a natural approach to the double counting problem would be to remove $\widehat{U}_{AA}^{HF}$ from $\widehat{H}^{MF}$. Unfortunately this choice would not be correct, again due to a lack of screening in $\widehat{U}^{HF}$. Replacing $\widehat{U}_{AA}^{HF}$ with a much weaker $\tilde{\mathrm{U}}_{AAAA}^{eff}$ would result in that the correlated orbitals would fill up with electrons. We are now left with two options: we can either include the (RPA) screening also in the host material, i.e. perform a GW calculation instead of HF[22], or remove the mean-field part of the screened $\tilde{\mathrm{U}}_{AAAA}^{eff}$. The latter choice gives the screened Hartree-Fock (SHF) double counting term

$$\widehat{U}_{AA}^{SHF} = [\tilde{\mathrm{U}}_{AAAA}^{eff}]^{HF} = \sum_{ij\in A} \frac{1}{2}\tilde{\rho}_{nm}\left[\tilde{\mathrm{U}}_{minj}^{eff} - \tilde{\mathrm{U}}_{mijn}^{eff}\right]\widehat{c}_i^{\dagger}\widehat{c}_j. \tag{5.46}$$

5.3.2 KS-DFT

While it is possible to obtain $\widehat{U}_{AA}^{MF}$ in the case of Hartree-Fock, major complications arise when $\widehat{H}^{MF}$ is given by the KS Hamiltonian $\widehat{H}^{KS}$ from Eq. (4.27). As we saw in section 4.2.2, the exchange-correlation functional in KS-DFT is defined with respect to the total electron density. The non-linearity of the functional makes it impossible to directly extract the contribution coming from just the Coulomb interaction between the electrons in the correlated orbitals[3]. This lack of a proper definition has paved the way for several more or less hand-waving approximations. It is however interesting to note that the two most commonly used double counting corrections, Around Mean-Field (AMF) and Fully Localized Limit (FFL), are actually strongly related to the type of correlations present in $\widehat{\rho}$. To see this we must make a detailed derivation starting from the effective Hartree-Fock energy correction

$$E_{HF}^{eff} = \mathrm{Tr}(\tilde{U}_{AA}^{SHF}\tilde{\rho}), \tag{5.47}$$

where $\tilde{\rho}$ is the one-particle reduced density operator from Eq. (5.14). Expanding Eq. (5.47) in the eigenbasis of $\tilde{\rho}$ (Löwdin's natural orbitals) gives

$$E_{HF}^{eff} = \sum_{ij}\frac{1}{2}\left[\tilde{\mathrm{U}}_{ijij}^{eff} - \tilde{\mathrm{U}}_{ijji}^{eff}\right](\tilde{\mathrm{n}}_i\tilde{\mathrm{n}}_j - \tilde{\mathrm{n}}_i^2\delta_{ij}), \tag{5.48}$$

where the $\tilde{\mathrm{n}}_i^2\delta_{ij}$ term is trivially zero in the previous sum, but is introduced to take care of the self-interaction arising from the following approximations. If for a moment we forget the spin-orbit coupling, the terms in Eq. (5.48) can be rearranged according to spin up ($\uparrow$) and spin down ($\downarrow$) contributions

$$\begin{aligned} E_{HF}^{eff} = &\sum_{ab}\left[\tilde{\mathrm{U}}_{abab}^{eff} - \tilde{\mathrm{U}}_{abba}^{eff}\right](\tilde{\mathrm{n}}_{a\uparrow}\tilde{\mathrm{n}}_{b\uparrow} + \tilde{\mathrm{n}}_{a\downarrow}\tilde{\mathrm{n}}_{b\downarrow} - [\tilde{\mathrm{n}}_{a\uparrow}^2 + \tilde{\mathrm{n}}_{a\downarrow}^2]\delta_{ab}) \\ &+\tilde{\mathrm{U}}_{abab}^{eff}(\tilde{\mathrm{n}}_{a\uparrow}\tilde{\mathrm{n}}_{b\downarrow} + \tilde{\mathrm{n}}_{a\downarrow}\tilde{\mathrm{n}}_{b\uparrow}), \end{aligned} \tag{5.49}$$

[3]This fact also calls into question the standard implementation of the Self-Interaction Correction which applies the exchange-correlation functional to partial electron densities.

where the indices a, b run over the non-spin degrees of freedom. The next step is to take the spherical average of the effective Coulomb interaction terms in Eq. (5.49), giving

$$E^{eff}_{AHF} = \left\langle \tilde{U} - \tilde{J} \right\rangle \sum_{ab} (\tilde{\mathrm{n}}_{a\uparrow}\tilde{\mathrm{n}}_{b\uparrow} + \tilde{\mathrm{n}}_{a\downarrow}\tilde{\mathrm{n}}_{b\downarrow}) - \left\langle \tilde{U} - \tilde{J} \right\rangle \mathrm{Tr}(\tilde{\rho}^2) \\ \left\langle \tilde{U} \right\rangle (\tilde{\mathrm{n}}_{a\uparrow}\tilde{\mathrm{n}}_{b\downarrow} + \tilde{\mathrm{n}}_{a\downarrow}\tilde{\mathrm{n}}_{b\uparrow}), \tag{5.50}$$

where

$$\left\langle \tilde{U} - \tilde{J} \right\rangle \equiv \frac{\sum_{ab} \left[\tilde{\mathrm{U}}^{eff}_{abab} - \tilde{\mathrm{U}}^{eff}_{abba} \right]}{D^2}, \tag{5.51}$$

$$\left\langle \tilde{U} \right\rangle \equiv \frac{\sum_{ab} \tilde{\mathrm{U}}^{eff}_{abab}}{D^2}, \tag{5.52}$$

and $D = \sum_a 1$. Evaluating the sums in Eq. (5.50) yields

$$E^{eff}_{AHF} = \frac{1}{2} \left[\left\langle \tilde{U} - \tilde{J} \right\rangle \frac{N^2 + M^2}{2} + \left\langle \tilde{U} \right\rangle \frac{N^2 - M^2}{2} \right] - \frac{1}{2} \left\langle \tilde{U} - \tilde{J} \right\rangle \mathrm{Tr}(\tilde{\rho}^2), \tag{5.53}$$

where $N = \sum_a (\tilde{\mathrm{n}}_{a\uparrow} + \tilde{\mathrm{n}}_{a\downarrow})$ and $M = \sum_a (\tilde{\mathrm{n}}_{a\uparrow} - \tilde{\mathrm{n}}_{a\downarrow})$. The term $\mathrm{Tr}(\tilde{\rho}^2)$ is proportional to the linear entropy, and is therefore sensitive to both the classical and quantum correlations in the state. The expression for FLL is obtained by assuming that $\widehat{\rho}$ is pure and separable, i.e. that $\tilde{\rho}$ is idempotent, giving

$$E^{eff}_{FLL} = \frac{1}{2} \left[\left\langle \tilde{U} - \tilde{J} \right\rangle \frac{N^2 + M^2}{2} + \left\langle \tilde{U} \right\rangle \frac{N^2 - M^2}{2} \right] - \frac{1}{2} \left\langle \tilde{U} - \tilde{J} \right\rangle N. \tag{5.54}$$

The AMF double counting assumes that $\widehat{\rho}$ is maximally mixed for a given value of M, i.e. $\mathrm{Tr}(\tilde{\rho}^2) \approx (N^2 + M^2)/D$, giving

$$E^{eff}_{AMF} = \frac{1}{2} \left[\left\langle \tilde{U} - \tilde{J} \right\rangle \frac{N^2 + M^2}{2} + \left\langle \tilde{U} \right\rangle \frac{N^2 - M^2}{2} \right] - \frac{1}{2} \left\langle \tilde{U} - \tilde{J} \right\rangle (N^2 + M^2)/D. \tag{5.55}$$

A third option is to replace $\mathrm{Tr}(\tilde{\rho}^2)$ with the linear interpolation of these two limits

$$\mathrm{Tr}(\tilde{\rho}^2) = x \left(\frac{N^2 + M^2}{D} \right) + (1 - x)N \Rightarrow x \equiv \frac{\mathrm{Tr}(\tilde{\rho}^2) - N}{(N^2 + M^2)D^{-1} - N}, \tag{5.56}$$

giving

$$E^{eff}_{x} = x E^{eff}_{AMF} + (1 - x) E^{eff}_{FLL}. \tag{5.57}$$

The corresponding double counting corrections are given by the derivatives of E^{eff} with respect to N and M.

The AMF, FLL, and interpolation DC corrections offers a heuristic solution to the screening problem by starting from the effective Hartree-Fock energy.

However, this treatment results in a rough estimate of the double counting correction as it ignores the double counting in the correlation part of the KS energy functional.

When the correlated orbitals are almost equally occupied and the recipes above give too crude estimates of the double counting correction, one can resort to the empirical chemical potential double counting. It defines $\widehat{U}^{DC}_{AA} = \mu_{DC}\widehat{n}_A$, so that the double counting parameter μ_{DC} can act as a chemical potential in the impurity problem. μ_{DC} is then essentially treated as a free parameter and is set according to experimental photoemission data. The theoretical justification for such a procedure is simply that the correct double counting should give the correct experimental chemical potential, and since the double counting is unknown we might as well set it to the correct value by hand. The obvious drawback is that it requires experimental data.

Finally a fifth option is to take the average hermitian part of the self-energy $\tilde{\Sigma}_{AA}(\omega = 0)$ introduced in the next section, to enforce Fermi-liquid behavior.

It is hard to say which KS-DFT double counting correction is better than another since the double counting problem is so ill-posed. However, from the derivations of FLL and AMF one could expect that FLL is suitable for localized electrons in a low temperature ferromagnetic phase, while AMF works better for rather delocalized electrons in high temperature paramagnetic phases.

5.4 Self-energy

It is time to introduce one of the main advantages the Green's function formalism has to offer, the possibility to go beyond a non-interacting particle description while still remaining in the one-particle Hilbert space. This is made possible by the so called self-energy correction $\tilde{\Sigma}(\tau)$.

Substituting $\widehat{H}^{SIAM}$ into Eq. (5.17) gives

$$\begin{aligned} i\frac{d}{dt}\tilde{G}^S(t,t') = {} & \delta(t-t')\tilde{1} + i\left\langle S\left[[\widehat{H}^{MF} - \widehat{U}^{DC}_{AA}, \widehat{\Psi}](t)\widehat{\Psi}^\dagger(t')\right]\right\rangle \\ & + i\left\langle S\left[[\widehat{U}_{AAAA}, \widehat{\Psi}](t)\widehat{\Psi}^\dagger(t')\right]\right\rangle . \end{aligned} \tag{5.58}$$

Like in Eq. (5.19) the second term on the right hand side in Eq. (5.58) reduces to

$$i\left\langle S\left[[\widehat{H}^{MF} - \widehat{U}^{DC}_{AA}, \widehat{\Psi}](t)\widehat{\Psi}^\dagger(t')\right]\right\rangle = (\widehat{H}^{MF} - \widehat{U}^{DC}_{AA})\tilde{G}^S(t,t'). \tag{5.59}$$

While the commutator in the third term is zero except for local impurity states

$$i\left\langle S[[\widehat{U}_{AAAA}, \widehat{\Psi}](t)\widehat{\Psi}^\dagger(t')]\right\rangle = i\tilde{P}_A\left\langle S[[\widehat{U}_{AAAA}, \widehat{\Psi}_A](t)\widehat{\Psi}^\dagger(t')]\right\rangle , \tag{5.60}$$

it is still hard to evaluate due to the many-body nature of $\widehat{U}_{AAAA}$. We postpone this problem by simply defining the self-energy $\tilde{\Sigma}^S_{AA}(\tau)$ as the local one-particle operator that makes $\tilde{G}^S(t,t')$ fulfill

$$i\tilde{P}_A \left\langle S[[\widehat{U}_{AAAA}, \widehat{\Psi}_A](t)\widehat{\Psi}^\dagger(t')] \right\rangle = \left(\tilde{\Sigma}^S_{AA} * \tilde{G}^S\right)(t,t') \tag{5.61}$$

where $*$ denotes the convolution operation

$$(f*g)(x,y) \equiv \int_{-\infty}^{\infty} f(z)g(x-z,y)dz. \tag{5.62}$$

Substituting Eq. (5.61) into Eq. (5.58) yields

$$\left(\frac{d}{dt} - \tilde{H}^{MF} + \tilde{U}^{DC}_{AA}\right)\tilde{G}^S(t,t') - \left(\tilde{\Sigma}^S_{AA} * \tilde{G}^S\right)(t,t') = \tilde{1}\,\delta(t-t'). \tag{5.63}$$

The Green's function $\tilde{G}^S(t,t')$ depends only on the time difference $\tau = t-t'$, which allows us to take the Fourier transform on both sides of Eq. (5.63) to obtain the well-known Dyson equation [9, 10]

$$\left[\tilde{G}_0^{-1}(\omega) - \tilde{\Sigma}_{AA}(\omega)\right]\tilde{G}(\omega) = \tilde{1}, \tag{5.64}$$

where

$$\tilde{G}_0(\omega) = \left(\omega\tilde{1} - \tilde{H}^{MF} + \tilde{U}^{DC}_{AA}\right)^{-1}. \tag{5.65}$$

$\tilde{G}(\omega)$ is given by $\tilde{G}^R(\omega)$ for $\Im\omega > 0$ and $\tilde{G}^A(\omega)$ for $\Im\omega < 0$. Rearranging and projecting the terms in Eq. (5.64) gives an explicit definition of the self-energy

$$\tilde{\Sigma}_{AA}(\omega) = [\tilde{G}_{0AA}(\omega)]^{-1} - [\tilde{G}_{AA}(\omega)]^{-1}. \tag{5.66}$$

In order to calculate $\Sigma_{AA}(\omega)$ of a thermal system using Eq. (5.66), we first need to know the thermal one-particle Green's function $\tilde{G}(\omega)$. The definition of $\tilde{G}(\omega)$ in Eq. (5.26) requires the eigenvalues and eigenstates of $\widehat{H}^{SIAM}$, which makes it intractable for all but the smallest of systems. Fortunately, there are various techniques – impurity solvers – that allow us to calculate the self-energy without explicitly constructing $\tilde{G}(\omega)$ for the entire system. We will mainly focus on three of these impurity solvers: the Hubbard-I Approximation, Exact Diagonalization, and Spin-Polarized T-matrix Fluctuation Exchange. However, before we dive into the nuts and bolts of these impurity solvers, there is another fundamental issue of self-consistency needs to be addressed.

Once the self-energy has been calculated it contains a refined description of the electronic interaction in the correlated orbitals. This information is passed from the self-energy to the global Green's function $\tilde{G}(\omega)$ through Eq. (5.64). However, as the system is updated the mean-field part of the Hamiltonian needs to be recalculated, which requires the one-particle reduced density operator from Eq. (5.14) (See section 5.6). The updated Hamiltonian gives rise to a new Green's function which in turn generates a new self-energy. This chain of updates forms a self-consistency cycle analogous to that of Hartree-Fock or KS-DFT.

5.5 Impurity solvers

5.5.1 Hubbard-I Approximation

The Hubbard-I approximation [23, 24] (HIA) completely neglects the hybridization between the local orbitals and the bath. The SIAM Hamiltonian and bath Green's function are then reduced to

$$\widehat{H}^{SIAM} \xrightarrow{\Delta=0} \widehat{H}^{HIA}_{AA} = \widehat{H}^{MF}_{AA} + \widehat{U}_{AAAA} - \widehat{U}^{MF}_{AA}, \tag{5.67}$$

$$\tilde{G}_0(\omega) \xrightarrow{\Delta=0} \tilde{G}^{HIA}_{0AA}(\omega) = [\omega\tilde{1}_{AA} - \widehat{H}^{MF}_{AA} - \widehat{U}^{MF}_{AA}]^{-1}. \tag{5.68}$$

Since the Hubbard-I Hamiltonian $\widehat{H}^{HIA}$ describes a system with just a few orbitals and electrons it can be written in a many-body basis and diagonalized numerically. The eigenvalues $E_i^{(N)}$ and eigenvectors $|\nu_i\rangle$ of $\widehat{H}^{HIA}$ are used in Eq. (5.26) to produce $\tilde{G}^{HIA}_{AA}(\omega)$. $\tilde{G}^{HIA}_{0AA}(\omega)$ and $\tilde{G}^{HIA}_{AA}(\omega)$ are then substituted into Eq. (5.66) to yield $\tilde{\Sigma}_{AA}(\omega)$.

HIA is in some ways the simplest of the impurity solvers, as it does not treat the hybridization with the bath at all. On the other hand, it treats all interactions between the local electrons exactly, and produces an analytical self-energy for arbitrary frequencies ω. The HIA self-energy gives therefore often a highly accurate spectral density when the correlated orbitals are very localized. Nevertheless, even a tiny hybridization can give rise to an extra quasiparticle peak in the low energy part of the spectrum at sufficiently low temperatures. This resonance is due the Kondo effect, a collective screening of the magnetic moment of the impurity by the electrons in the bath. Since HIA does not capture this effect one must proceed with care when comparing the spectral density with experimental photoemission data taken at low temperatures.

5.5.2 Exact Diagonalization

Exact Diagonalization (ED) is a natural extension of HIA in the sense that it reduces the system to a finite size, but also takes into account a significant part of the hybridization. It does so by not only including the correlated subspace $\mathscr{A}$, like in HIA, but also an auxiliary subspace $\mathscr{B}$ spanned by a few fictitious bath states $\{|q_i^{ED}\rangle\}_{i\in B}$. The Hamiltonian of this extended system has the form

$$\widehat{H}^{ED} = \widehat{H}^{HIA}_{AA} + \widehat{H}^{ED}_{AB} + \widehat{H}^{ED}_{AB} + \widehat{H}^{ED}_{BB}, \tag{5.69}$$

where $\widehat{H}^{ED}_{AB} = \widehat{\Psi}^\dagger \tilde{H}^{ED}_{AB} \widehat{\Psi}$ and $\widehat{H}^{ED}_{BB} = \widehat{\Psi}^\dagger \tilde{H}^{ED}_{BB} \widehat{\Psi}$ represent the hybridization strength between the bath and the correlated orbitals, and the bath Hamiltonian, respectively. $\tilde{H}^{ED}_{AB}$ and $\tilde{H}^{ED}_{BB}$ are fitted to reproduce the hybridization function $\Delta_{AA}(\omega)$ from Eq. (5.33) as close as possible. In Paper V we performed the fitting by minimizing the cost function

$$F(\tilde{H}^{ED}_{AB}, \tilde{H}^{ED}_{BB}) = \sum_n W_n \left\| \tilde{H}^{ED}_{AB}[i\omega_n\tilde{1} - \tilde{H}^{ED}_{BB}]^{-1}\tilde{H}^{ED}_{BA} - \tilde{\Delta}_{AA}(i\omega_n) \right\|_F^2, \tag{5.70}$$

where $i\omega_n = i\pi T(2n+1)$ is a Matsubara frequency [10], $\{W_n\}$ is a set of weights and $\|\tilde{A}\|_F^2 = \mathrm{Tr}(\tilde{A}^\dagger \tilde{A})$ is the Frobenius norm. The use of Matsubara frequencies makes $\tilde{\Delta}_{AA}(i\omega_n)$ rather smooth, which reduces the risk of getting stuck in a local minimum. Once $\widehat{H}^{ED}$ has been constructed the rest of the procedure is identical to that of the HIA solver.

5.5.2.1 Technical considerations

An important technical issue in the implementation of ED is constructing the matrix representation of the Hamiltonian with respect to the many-body basis. This step is greatly simplified if the basis vectors are defined as pure separable states (single Slater determinants) in some one-particle basis. As we saw in section 3.1.2 the Slater determinants can be visualized in the occupation number formalism. For example 5 electrons in a 10 orbital manifold can form the following many-body states:

$$\begin{aligned}
|\Psi_1^5\rangle &= |1111100000\rangle, \\
|\Psi_2^5\rangle &= |1111010000\rangle, \\
|\Psi_3^5\rangle &= |1111001000\rangle, \\
&\vdots \\
|\Psi_{M-1}^5\rangle &= |0000101111\rangle, \\
|\Psi_M^5\rangle &= |0000011111\rangle.
\end{aligned}$$

Here M is the number of possible many-body states, i.e. the binomial coefficient of 10 over 5. When the creation and annihilation operators are given in the same one-particle basis as $|\Psi_i^N\rangle$, then their action becomes a simple remapping of the indices $N \to N \pm 1, i \to j$ and a multiplication of a phase factor (± 1).

The size of the many-body basis explodes with the number of orbitals and electrons, as shown in Eq. (3.4), so even for a moderate number of orbitals and electrons the Hilbert space becomes too large to handle in practice. However often the system under consideration possesses useful symmetries, which can be used to find some criteria to *a priori* identify a block structure in the Hamiltonian. These blocks can then be treated separately which saves a lot of computational resources.

A general way to obtain these criteria is to define the many-body basis vectors as the eigenvectors of a set of commuting observables $\{\widehat{A}^k\}$, and then determine how the states mix under the action of the Hamiltonian. Since the basis vectors should be representable by single Slater determinants, only commuting one-electron observables

$$\widehat{A}^k = \sum_{ij} \tilde{A}_{ij}^k \widehat{c}_i^\dagger \widehat{c}_j, \tag{5.71}$$

should to be considered. Furthermore, to keep the calculation of the mixing rather simple we impose an additional condition that the observables should

commute with $\widehat{U}$. These two restrictions reduce the list of potential observables $\{\widehat{A}^k\}$ for the correlated orbitals to $\widehat{S}_z$ and $\widehat{L}_z$ (or alternatively $\widehat{S}_x$ and $\widehat{L}_x$ and $\widehat{S}_y$ and $\widehat{L}_y$). The auxiliary bath orbitals are not directly affected by $\widehat{U}$, so each bath spin-orbital m can be assigned an observable $\widehat{n}^m = \widehat{c}^\dagger_m \widehat{c}_m$ that measures its occupation.

Each spin-orbital j can be transformed into a common eigenstate of all these observables and assigned a vector of eigenvalues $\vec{a}^j$. A many-body basis vector $|\Psi^N_i\rangle$, defined as a single Slater determinant with respect to these orbitals, is trivially an eigenstate of the observables in $\{\widehat{A}^k\}$, with an eigenvalue vector

$$\vec{A}^i = \sum_{j=1}^{K} \langle \Psi^N_i | \widehat{c}^\dagger_j \widehat{c}_j | \Psi^N_i \rangle \vec{a}^j. \tag{5.72}$$

Obtaining these eigenvalue vectors is not enough to determine the block structure of $\widehat{H}^{ED}$, as the one-electron Hamiltonian $\widehat{H}^0$ does not in general commute with the observables in $\{\widehat{A}^k\}$. In particular, the hybridization with the bath orbitals rarely commute with $\tilde{L}_z$. The off-diagonal elements of $\tilde{H}^0$ determine how the blocks will form. Each non-zero off-diagonal element $\tilde{H}^0_{mn} \widehat{c}^\dagger_m \widehat{c}_n$ allows a many-body basis vector $|\Psi_i\rangle$ to couple to a basis vector $|\Psi_j\rangle$ if the following condition is fulfilled

$$\vec{A}^j - \vec{A}^i = \vec{a}^m - \vec{a}^n. \tag{5.73}$$

The problem of generating a block structure can now be transformed into finding the connected components of an undirected graph, where the vertices are defined by $\{\vec{A}^i\}$ and the edges by $\{\vec{a}^m - \vec{a}^n, 0\}$ for all n and m through Eq. (5.73). This problem can be solved efficiently through the use of sparse logical square matrix multiplication[4], in the following steps:

1. Map each vertex to a matrix index, and each edge to a true element in the logical matrix T.
2. Multiply T with itself, until it remains constant. This procedure makes the connected components complete.
3. The true elements in a row or column in T gives the indices of all the vertices of a connected component.

This algorithm can be further improved by contracting any dense region in the graph before T is defined. Additionally, the second step can be performed even more efficiently through the use of an update matrix V:

1. $V \leftarrow T$
2. While $V \neq 0$
   a) $T \leftarrow T$ .or. V
   b) $V \leftarrow$ (.not. T) .and. $T.V$

[4]Notice that our tests have shown that the intrinsic Fortran function MATMUL for large dense logical matrices is extremely inefficient. In order to test our procedure we strongly suggest to look for alternative solutions for matrix multiplications.

The Hamiltonian is now finally ready to be block diagonalized by grouping all the many-body basis vectors with quantum number vectors $\{\vec{A}^i\}$ matching a given connected component.

Further technical considerations, like how the choice of local orbitals affects the hybridization function, can be found in the supplemental material of Paper V.

5.5.3 Spin-Polarized T-matrix Fluctuation-exchange

Spin-Polarized T-matrix Fluctuation-exchange (SPTF) solver is a diagrammatic approach based on the perturbation of the Green's function with respect to $\widehat{U}^{eff}_{AAAA} - \widehat{U}^{DC}_{AA}$. The first step in deriving the SPTF contributions is to construct the local particle-particle susceptibility from the RPA expression

$$\tilde{\chi}^{PP}_{AA}(t,t') = \tilde{P}^{PP}_{AA}(t,t') + \int \tilde{P}^{PP}_{AA}(t,t'')\tilde{\mathrm{U}}^{eff}_{AA}\tilde{\chi}^{PP}_{AA}(t'',t')dt'' \tag{5.74}$$

where

$$\begin{aligned}\tilde{P}^{PP}_{AA}(t,t') &= -\tilde{G}_{AA}(t,t') \otimes \tilde{G}_{AA}(t,t') \\ &= \mathrm{Tr}\left(\widehat{\rho}T[\widehat{\Psi}_A(t)\widehat{\Psi}^{\dagger}_A(t')]\right) \otimes \mathrm{Tr}\left(\widehat{\rho}T[\widehat{\Psi}_A(t)\widehat{\Psi}^{\dagger}_A(t')]\right).\end{aligned} \tag{5.75}$$

It should be noted that it is not the particle-hole four-index matrix notation defined in Eq. (5.35) that is used in Eq. (5.74) but rather the corresponding particle-particle notation

$$\tilde{\mathrm{V}}^{PP}_{\alpha\beta} = \tilde{\mathrm{V}}^{PP}_{\alpha_1\alpha_2\beta_1\beta_2}. \tag{5.76}$$

The bare particle-particle polarization $\tilde{P}^{PP}_{AA}(t,t')$ describes the independent propagation of two electrons, while $\tilde{P}(t,t')$ in Eq. (5.40) describes an electron and a hole. The constrained particle-hole susceptibility $\tilde{\chi}^{A}(t,t')$ was used in Eq. (5.42) to account for the screening of the bare interaction $\tilde{U}_{AA}$ by the bath electrons, giving the effective interaction $\tilde{U}^{eff}$. The local particle-particle susceptibility $\tilde{\chi}^{PP}_{AA}(t,t')$ plays a similar role in the SPTF method. It is used to construct the T-matrix $\tilde{T}_{AA}(t,t')$ which describes the particle-particle screening of effective interaction $\tilde{U}^{eff}$ by the correlated electrons themselves

$$\tilde{\mathrm{T}}_{AA}(t,t') = \tilde{\mathrm{U}}^{eff}_{AA}\delta(t-t') + \tilde{\mathrm{U}}^{eff}_{AA}\tilde{\chi}^{PP}_{AA}(t,t')\tilde{\mathrm{U}}^{eff}_{AA}, \tag{5.77}$$

where we again have used the particle-particle four index matrix notation.

The second part of the SPTF scheme is to construct an effective particle-hole interaction. The starting point is the static anti-symmetrized vertex

$$\tilde{U}^{AS}_{\alpha\beta} = \tilde{\mathrm{T}}_{\alpha_1\beta_1\alpha_2\beta_2}(\omega)\big|_{\omega=0} - \tilde{\mathrm{T}}_{\alpha_1\beta_1\beta_2\alpha_2}(\omega)\big|_{\omega=0}, \tag{5.78}$$

where $\tilde{\mathrm{T}}_{AA}(\omega)$ is the Fourier transform of $\tilde{\mathrm{T}}_{AA}(t,t')$ from Eq. (5.77). The anti-symmetrized vertex give rise to a new RPA particle-hole susceptibility

$$\tilde{\chi}^{AS}_{AA}(t,t') = \tilde{\mathrm{P}}^{PH}_{AA}(t,t') + \int \tilde{\mathrm{P}}^{PH}_{AA}(t,t'')\tilde{\mathrm{U}}^{AS}_{AA}\tilde{\chi}^{AS}_{AA}(t'',t')dt''. \tag{5.79}$$

$\tilde{\chi}^{AS}_{AA}(t,t')$ is then used to obtain the particle-hole effective interaction

$$\tilde{\mathrm{W}}^{AS}_{AA}(t,t') = \tilde{U}^{AS}_{AA} + \tilde{\mathrm{U}}^{AS}_{AA}\tilde{\chi}^{AS}_{AA}(t,t')\tilde{\mathrm{U}}^{AS}_{AA}. \tag{5.80}$$

The SPTF self-energy is given by the Fourier transforms of the effective interaction $\tilde{\mathrm{W}}^{AS}_{AA}(\omega)$ and the Hartree-Fock approximation of $\tilde{\mathrm{T}}_{AA}(\omega)$ combined with the Green's function in a GW form

$$\tilde{\Sigma}^{SPTF}_{ij}(\omega) = \mathrm{Tr}\left([(\tilde{W}^{AS}_{iAjA} + \tilde{T}_{iAjA} - \tilde{T}_{iAAj} - \tilde{W}^{DC}_{AA}) * \tilde{G}_{AA}](\omega)\right). \tag{5.81}$$

where the convolution is defined in Eq. (5.62). The double counting term $\tilde{W}^{DC}_{AA}(\omega)$ is given by

$$\tilde{W}^{DC}_{AA}(\omega) = \tilde{U}^{AS}_{AA} + \tilde{\mathrm{U}}^{AS}_{AA}\tilde{\mathrm{P}}^{PH}_{AA}(\omega)\tilde{\mathrm{U}}^{AS}_{AA}. \tag{5.82}$$

It cancels the parts which are included both in the T-matrix and in the W-matrix.

5.6 One-particle reduced density operator

A large part of the work dedicated to this thesis went into solving technical problems related to the implementation of our methods. This is reflected in the following two sections, which will deal with the asymptotic summation of the Green's function over the Matsubara frequencies[5].

The one-particle reduced density operator $\tilde{\rho}$ defined in Eq. (5.14) is obtained from $\lim_{\tau\to 0-}\tilde{G}(\tau)$. However, the self-energy update in Eq. (5.64) generates $\tilde{G}(i\omega_n)$ in the (Matsubara) frequency domain. This means that the calculation of $\tilde{\rho}$ requires a Fourier transform of $\tilde{G}(i\omega_n)$ in the limit $\tau \to 0^-$

$$\tilde{\rho} = \lim_{\tau\to 0^-}\lim_{N\to\infty}\frac{1}{\beta}\sum_{n=-N}^{N}\tilde{G}(i\omega_n)e^{-i\omega_n\tau}. \tag{5.83}$$

The asymptotic behavior of $\tilde{G}(i\omega_n)$ goes as $1/(i\omega_n)$. This makes the partial sum in Eq. (5.83) only point wise convergent and not uniformly convergent with respect to τ, and means that the limits can not be interchanged. One way around this problem is to use that the Dyson equation in Eq. (5.66) ensures that the self-energy matrix[6] takes the analytical form

$$\tilde{\Sigma}(i\omega_n) = \tilde{\Sigma}(\infty) + \tilde{\Sigma}^d(i\omega_n), \tag{5.84}$$

$$\tilde{\Sigma}^d(i\omega_n) = \tilde{\mathrm{V}}^\dagger[i\omega_n\tilde{1} - \tilde{\mathrm{D}}]^{-1}\tilde{\mathrm{V}}, \tag{5.85}$$

[5] These sections will likely require your full attention, so before we continue may I suggest a quick coffee break?

[6] From here on we drop any SIAM superscript and the explicit local projections as the following procedure is general.

where $\tilde{\mathrm{D}}$ is a diagonal matrix. Substituting Eq. (5.84) into Eq. (5.64) gives

$$\begin{aligned}\tilde{\mathrm{G}}(i\omega_n) &= \left[i\omega_n\tilde{\mathrm{I}} - \tilde{\mathrm{H}}^{stat} - \tilde{\Sigma}^d(i\omega_n)\right]^{-1} \\ &= \tilde{\mathrm{W}}^\dagger\left[i\omega_n\tilde{\mathrm{I}} - \tilde{\mathrm{E}} - \tilde{\mathrm{W}}\tilde{\Sigma}^d(i\omega_n)\tilde{\mathrm{W}}^\dagger\right]^{-1}\tilde{\mathrm{W}}, \end{aligned} \tag{5.86}$$

where the diagonal matrix $\tilde{\mathrm{E}}$ contains the eigenvalues and the unitary matrix $\tilde{\mathrm{W}}$ contains the eigenvectors of the static Hamiltonian

$$\tilde{\mathrm{H}}^{stat} = \tilde{\mathrm{H}}^{MF} - \sum_i \tilde{\mathrm{U}}^{DC}_{A_iA_i} + \tilde{\Sigma}(\infty). \tag{5.87}$$

$\tilde{\Sigma}^d(i\omega_n)$ can be expanded in the limit of large ω_n as

$$\tilde{\mathrm{W}}\tilde{\Sigma}^d(i\omega_n)\tilde{\mathrm{W}}^\dagger = \sum_{j=0}^{\infty}\frac{\tilde{\mathrm{W}}\tilde{\mathrm{V}}^\dagger\tilde{\mathrm{D}}^j\tilde{\mathrm{V}}\tilde{\mathrm{W}}^\dagger}{(i\omega_n)^{j+1}} = \sqrt{\tilde{\mathrm{A}}}[i\omega_n\tilde{\mathrm{I}} - \tilde{\mathrm{B}}]^{-1}\sqrt{\tilde{\mathrm{A}}} + O(\frac{1}{\omega_n^3}). \tag{5.88}$$

where

$$\tilde{\mathrm{A}} \equiv \tilde{\mathrm{W}}\tilde{\mathrm{V}}^\dagger\tilde{\mathrm{V}}\tilde{\mathrm{W}}^\dagger, \tag{5.89}$$

$$\tilde{\mathrm{B}} \equiv \tilde{\mathrm{A}}^{-1/2}\tilde{\mathrm{W}}\tilde{\mathrm{V}}^\dagger\tilde{\mathrm{D}}\tilde{\mathrm{V}}\tilde{\mathrm{W}}^\dagger\tilde{\mathrm{A}}^{-1/2}. \tag{5.90}$$

The Green's function can now be decomposed into a numerical part and an analytical part

$$\begin{aligned}\tilde{G}^{an}(i\omega_n) &= \left[i\omega_n\tilde{\mathrm{I}} - \tilde{\mathrm{E}} - \frac{\tilde{\mathrm{A}}'}{i\omega_n\tilde{\mathrm{I}} - \tilde{\mathrm{B}}'}\right]^{-1} \\ &= \frac{i\omega_n\tilde{\mathrm{I}} - \tilde{\mathrm{B}}'}{(i\omega_n\tilde{\mathrm{I}} - \tilde{\mathrm{E}})(i\omega_n\tilde{\mathrm{I}} - \tilde{\mathrm{B}}') - \tilde{\mathrm{A}}'} \end{aligned} \tag{5.91}$$

$$\tilde{G}^{num}(i\omega_n) = \tilde{G}(i\omega_n) - \tilde{\mathrm{W}}^\dagger\tilde{G}^{an}(i\omega_n)\tilde{\mathrm{W}}, \tag{5.92}$$

where we have rotated the analytical part into the eigenbasis of $\tilde{\mathrm{H}}^{stat}$, and $\tilde{\mathrm{A}}'$ and $\tilde{\mathrm{B}}'$ are the diagonal components of $\tilde{\mathrm{A}}$ and $\tilde{\mathrm{B}}$, respectively. It should be states that $\tilde{\mathrm{A}}'$ and $\tilde{\mathrm{B}}'$ are in practice obtained by fitting the asymptotic part of the self-energy with a model function, and not from Eq. (5.88). The construction in Eq. (5.91) makes $\tilde{G}^{an}(i\omega_n)$ diagonal, with simple poles at

$$z_\pm = \frac{\tilde{\mathrm{E}} + \tilde{\mathrm{B}}'}{2} \pm \frac{1}{2}\sqrt{(\tilde{\mathrm{E}} - \tilde{\mathrm{B}}')^2 + 4\tilde{\mathrm{A}}'}. \tag{5.93}$$

The density operator can now also be split into an analytical and numerical part

$$\tilde{\rho} = \tilde{\mathrm{W}}^\dagger\tilde{\rho}^{an}\tilde{\mathrm{W}} + \tilde{\rho}^{num}, \tag{5.94}$$

$$\tilde{\rho}^{an} = \lim_{\tau\to 0^-}\lim_{N\to\infty}\frac{1}{\beta}\sum_{n=-N}^{N}\tilde{G}^{an}(i\omega_n)e^{-i\omega_n\tau}, \tag{5.95}$$

$$\tilde{\rho}^{num} = \lim_{\tau\to 0^-}\lim_{N\to\infty}\frac{1}{\beta}\sum_{n=0}^{N}\left[\tilde{\mathrm{G}}^{num}(i\omega_n)e^{-i\omega_n\tau} + \tilde{\mathrm{G}}^{num\dagger}(i\omega_n)e^{i\omega_n\tau}\right], \tag{5.96}$$

where we have used that $\tilde{G}(i\omega_n) = [\tilde{G}(-i\omega_n)]^\dagger$ to restrict the numerical summation to positive Matsubara frequencies.

The numerical part $\widehat{\rho}^{num}$ converges uniformly with respect to ω_n [25] which allows the order of the limits in Eq. (5.96) to be interchanged. With a minimal loss of accuracy the resulting sum can be truncated at some large cut-off Matsubara frequency $N_{\max}$, giving

$$\tilde{\rho}^{num} \approx \sum_{n=0}^{N_{\max}} \frac{1}{\beta} \left[\tilde{G}^{num}(i\omega_n) + \tilde{G}^{num\dagger}(i\omega_n) \right]. \tag{5.97}$$

The analytical part $\widehat{\rho}^{an}$ has a simple form but contains the logarithmic divergence of $\widehat{\rho}$. However, the convenient simple pole structure allows the summation to be transformed into a complex contour integral through the use of Cauchy's residue theorem

$$\begin{aligned} &\lim_{\tau\to 0^-} \lim_{R\to\infty} \frac{1}{2\pi i} \oint_R \frac{e^{-\tau z}\tilde{\mathrm{G}}^{an}(z)}{e^{\beta z}+1} dz = \\ &= -\lim_{\tau\to 0^-} \lim_{R\to\infty} \frac{1}{\beta} \sum_{n=-N}^{N} \tilde{\mathrm{G}}^{an}(i\omega_n) e^{-i\tau\omega_n} + \sum_{j=\pm} \frac{\mathrm{Res}_{z=\tilde{z}_j}[\tilde{\mathrm{G}}^{an}(z)]}{e^{\beta\tilde{z}_j}+\tilde{1}} = 0 \end{aligned} \tag{5.98}$$

where we have used that

$$\mathrm{Res}_{z=i\omega_n}\left[\frac{1}{e^{\beta z}+1}\right] = -\frac{1}{\beta}, \tag{5.99}$$

and that the circular contour is zero for $-\beta < \tau < 0, 0 \le \theta < 2\pi$ as

$$\lim_{R\to\infty} \frac{e^{-\tau R e^{i\theta}}}{e^{\beta R e^{i\theta}}+1} = 0. \tag{5.100}$$

Eq. (5.98) implies that

$$\tilde{\rho}^{an} = \sum_{j=\pm} \frac{\mathrm{Res}_{z=\tilde{z}_j}[\tilde{\mathrm{G}}^{an}(z)]}{e^{\beta\tilde{z}_j}+\tilde{1}} = \frac{\tilde{\mathrm{Q}}^G_+}{e^{\beta\tilde{z}_+}+\tilde{1}} + \frac{\tilde{\mathrm{Q}}^G_-}{e^{\beta\tilde{z}_-}+\tilde{1}} \tag{5.101}$$

where the residues $\tilde{\mathrm{Q}}^G_\pm$ are given by

$$\tilde{\mathrm{Q}}^G_\pm = \frac{\tilde{1}}{2} \pm \frac{\tilde{\mathrm{E}} - \tilde{\mathrm{B}}'}{2\sqrt{(\tilde{\mathrm{E}}-\tilde{\mathrm{B}}')^2 + 4\tilde{\mathrm{A}}'}}. \tag{5.102}$$

The final expression for the density operator $\tilde{\rho}$ is obtained by substituting Eq. (5.101) and (5.97) into Eq. (5.94).

5.7 Total energy correction

Another important quantity is the total energy correction ΔE_{HGM} which is the sum of the Galitskii-Migdal contribution [26, 27], and the expectation value

of $\tilde{H}^{MF}$ and the double counting correction $\tilde{\mathrm{U}}^{EDC}$ given by

$$\tilde{\mathrm{U}}^{EDC} \equiv \sum_i \tilde{\mathrm{U}}^{(1)DC}_{A_iA_i} + \frac{1}{2}\sum_i \tilde{\mathrm{U}}^{(2)DC}_{A_iA_i}, \tag{5.103}$$

$$\Delta E_{HGM} = \lim_{\tau\to 0^-}\lim_{N\to\infty}\sum_{n=-N}^{N}\mathrm{Tr}\left[\left(\tilde{H}^{MF} - \tilde{\mathrm{U}}^{EDC} + \frac{\tilde{\Sigma}(i\omega_n)}{2}\right)\frac{\tilde{G}(i\omega_n)e^{-i\omega_n\tau}}{\beta}\right] \tag{5.104}$$

where $\tilde{\mathrm{U}}^{(1)DC}_{A_iA_i}$ and $\tilde{\mathrm{U}}^{(2)DC}_{A_iA_i}$ are the parts of the double counting that represents one particle potentials and two particle interactions, respectively. The asymptotic behavior of the summation in ΔE_{HGM} is proportional to that of $\tilde{\rho}$ in Eq. (5.83). As we saw in Eq. (5.86), $\tilde{G}(i\omega_n)$ becomes diagonal in the eigenbasis of $\tilde{H}^{stat}$ in the asymptotic limit. To take advantage of this we extract parts of the Hamiltonian and the double-counting correction from Eq. (5.104), giving

$$\begin{aligned}\Delta E_{HGM} = &\lim_{\tau\to 0^-}\lim_{N\to\infty}\frac{1}{2\beta}\sum_{n=-N}^{N}\mathrm{Tr}\left[\left(\tilde{H}^{stat} + \tilde{\Sigma}^{d}(i\omega_n)\right)\tilde{G}(i\omega_n)e^{-i\omega_n\tau}\right] \\ &+\frac{1}{2}\mathrm{Tr}\left[\tilde{H}^{MF}\tilde{\rho}\right] - \frac{1}{2}\sum_i \mathrm{Tr}\left[\tilde{\mathrm{U}}^{(1)DC}_{A_iA_i}\tilde{\rho}_{A_iA_i}\right],\end{aligned} \tag{5.105}$$

where $\tilde{\rho}$ is given by Eq. (5.94). Following the same procedure as for $\tilde{\rho}$ in the previous section, we can now define the analytical and numerical parts using Eq. (5.88) and (5.91)

$$\Delta E_{HGM} = \Delta E^{an}_{HGM} + \Delta E^{num}_{GM} + \Delta E^{MF}_{HGM}, \tag{5.106}$$

$$\Delta E^{MF}_{HGM} = \mathrm{Tr}\left[\tilde{H}^{MF}\tilde{\rho}\right] - \frac{1}{2}\sum_i \mathrm{Tr}\left[\tilde{\mathrm{U}}^{(1)DC}_{A_iA_i}\tilde{\rho}_{A_iA_i}\right], \tag{5.107}$$

$$\begin{aligned}\Delta E^{an}_{HGM} &= \lim_{\tau\to 0^-}\lim_{N\to\infty}\frac{1}{2\beta}\sum_{n=-N}^{N}\mathrm{Tr}\left[\left(\tilde{E} + \frac{\tilde{\mathrm{A}}'}{i\omega_n\tilde{\mathrm{I}} - \tilde{\mathrm{B}}'}\right)\tilde{G}^{an}(i\omega_n)e^{-i\omega_n\tau}\right] \\ &= \lim_{\tau\to 0^-}\lim_{N\to\infty}\frac{1}{2\beta}\sum_{n=-N}^{N}\mathrm{Tr}\left[\frac{e^{-i\omega_n\tau}\tilde{\mathrm{A}}'}{(i\omega_n\tilde{\mathrm{I}} - \tilde{\mathrm{E}})(i\omega_n\tilde{\mathrm{I}} - \tilde{\mathrm{B}}') - \tilde{\mathrm{A}}'}\right] \\ &\quad +\frac{1}{2}\mathrm{Tr}\left[\tilde{E}\tilde{\rho}^{an}\right],\end{aligned} \tag{5.108}$$

$$\Delta E^{num}_{GM} = \Delta E_{GM} - \Delta E^{an}_{GM} - \Delta E^{MF}_{HGM}. \tag{5.109}$$

The evaluation of ΔE^{MF}_{HGM} poses no difficulties apart from that it requires the density operator $\tilde{\rho}$. ΔE^{num}_{GM} converges uniformly with respect to ω_n and can therefore be treated in the same way as $\tilde{\rho}^{num}$. The static part of ΔE^{an}_{HGM}, i.e. the second term in Eq. (5.108), is readily evaluated once $\tilde{\rho}^{an}$ has been calculated. The only remaining term in Eq. (5.106) to evaluate is the dynamical part of ΔE^{an}_{HGM}, which can be treated in the same way as $\tilde{G}^{an}(z)$. The part within the

trace has the same simple poles $z_{\pm}$, but its residues are given by

$$\tilde{\mathrm{Q}}_{\pm}^{HGM} = \frac{\pm\tilde{\mathrm{A}}'}{\sqrt{(\tilde{\mathrm{E}}-\tilde{\mathrm{B}}')^2+4\tilde{\mathrm{A}}'}}. \tag{5.110}$$

Applying Cauchy's residue theorem to ΔE_{HGM}^{an} gives

$$\Delta E_{HGM}^{an} = \frac{1}{2}\mathrm{Tr}\left[\tilde{E}\tilde{\rho}^{an}\right] + \frac{1}{2}\mathrm{Tr}\left[\frac{\tilde{\mathrm{Q}}_{+}^{HGM}}{e^{\beta\tilde{z}_{+}}+\tilde{1}} + \frac{\tilde{\mathrm{Q}}_{-}^{HGM}}{e^{\beta\tilde{z}_{-}}+\tilde{1}}\right]. \tag{5.111}$$

This method of evaluating the total energy correction and the density operator can in principle be extended by replacing the one pole approximation of $\tilde{\Sigma}^{d}(i\omega_n)$ with an m-pole approximation, and use a root solver to find the poles of the analytical Green's function. This would allow the numerical cutoff frequency $N_{\max}$ to be reduced even further, and thereby save even more computational resources.

6. Periodic Anderson Model

While the Single Impurity Anderson Model presented in the previous chapter offers a great insight in how to improve a mean-field description, it is limited to systems containing just a single impurity[1]. The Periodic Anderson Model (PAM) offers a closer description of a correlated material as it allows the impurities to form a periodic lattice. However, the model is not completely general as the electrons in the localized orbitals $\mathscr{A}_i$ at impurity i are only allowed to interact with the electrons in impurity j through the hopping term, and not through the two-particle operator U-term

$$\widehat{H}^{PAM} = \widehat{T} + \sum_i \widehat{U}^{PAM}_{A_iA_iA_iA_i}. \tag{6.1}$$

If we once more identify the model parameters with the mean-field Hamiltonian and effective Coulomb interaction, like we did in Eq. (5.8), we get

$$\widehat{H}^{PAM} = \widehat{H}^{MF} + \sum_i (\widehat{U}^{eff}_{A_iA_iA_iA_i} - \widehat{U}^{DC}_{A_iA_i}), \tag{6.2}$$

where $\widehat{U}^{eff}_{A_iA_iA_iA_i}$ and $\widehat{U}^{DC}_{A_iA_i}$ are defined in section 5.2 and 5.3, respectively. The PAM Green's function $\tilde{G}^{PAM}(\omega)$ is given by

$$\left(\omega\tilde{1} - \tilde{H}^{MF} + \sum_i \tilde{U}^{DC}_{A_iA_i} - \tilde{\Sigma}^{PAM}(\omega)\right)\tilde{G}^{PAM}(\omega) = \tilde{1}, \tag{6.3}$$

where the PAM self-energy $\tilde{\Sigma}^{PAM}(\omega)$ in general is non-local.

6.1 Dynamical Mean Field Theory

Dynamical Mean Field Theory [28, 29, 30, 31, 32] (DMFT) is built around the mapping of the Periodic Anderson Model to several Single Impurity Anderson Models, one for each impurity, schematically depicted in Fig. 6.1. The mapping is defined[2] through the locally projected Hamiltonians

$$\widehat{H}^{SIAM}_{A_iA_iA_iA_i} \equiv \widehat{H}^{PAM}_{A_iA_iA_iA_i} \tag{6.4}$$

[1] Or at least to systems with very low impurity concentrations, so that all impurity interactions may be completely neglected.

[2] The following equations can also be obtained by setting $\tilde{G}^{SIAM}_{A_iA_i}(\omega) = \tilde{G}^{PAM}_{A_iA_i}(\omega)$, $\tilde{\Sigma}^{SIAM}_{A_iA_i}(\omega) = \tilde{\Sigma}^{PAM}_{A_iA_i}(\omega)$, $\tilde{U}^{SIAM}_{A_iA_iA_iA_i} = \tilde{U}^{PAM}_{A_iA_iA_iA_i}$, and then extracting $\tilde{H}^{MF}_{A_iA_i} - \tilde{U}^{DC}_{A_iA_i}$ in the limit $\omega \to \infty$.

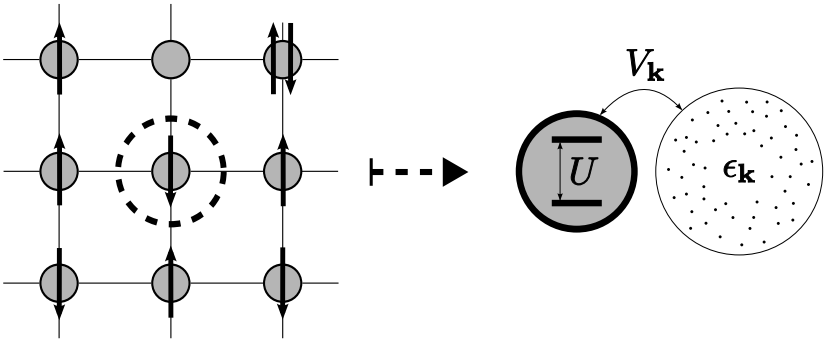

Figure 6.1. A schematical illustration of the mapping from the Periodic Anderson Model to a Single Impurity Anderson Model in the DMFT scheme. The bath parameters $V_{\mathbf{k}}$ and $\varepsilon_{\mathbf{k}}$ correspond to the off-diagonal (hopping) and diagonal (energy) elements of $\widehat{\mathrm{T}}$, respectively, and U symbolizes the $\widehat{U}^{SIAM}_{AAAA}$ term in Eq. (5.7).

and the SIAM hybridization function

$$\tilde{\Delta}^{SIAM}_{A_iA_i}(\omega) \equiv \tilde{\Delta}^{PAM}_{A_iA_i}(\omega) \equiv \omega\tilde{1} - \tilde{H}^{MF}_{A_iA_i} + \tilde{U}^{DC}_{A_iA_i} - \tilde{\Sigma}^{PAM}_{A_iA_i}(\omega) - [\tilde{G}^{PAM}_{A_iA_i}(\omega)]^{-1}. \tag{6.5}$$

Eq. (6.4) and (6.5) gives the SIAM bath Green's function

$$\tilde{G}^{SIAM}_{0A_iA_i}(\omega) = [\omega\tilde{1} - \tilde{H}^{MF}_{A_iA_i} + \tilde{U}^{DC}_{A_iA_i} - \tilde{\Delta}^{SIAM}_{A_iA_i}(\omega)]^{-1}, \tag{6.6}$$

which together with $\tilde{U}^{SIAM}_{A_iA_iA_iA_i} = \tilde{U}^{PAM}_{A_iA_iA_iA_i}$ from Eq. (6.4) fully determines the SIAM problem. Once the the SIAM problems are constructed they are solved by some appropriate impurity solvers to yield a set of self-energies $\{\tilde{\Sigma}^{SIAM}_{A_iA_i}(\omega)\}_i$. What is needed now is a way to relate this information to the PAM self-energy. DMFT provides this connection by approximating the PAM self-energy by its corresponding value in the limit of large coordination number, i.e. when the correlated orbitals are surrounded by a large number of hybridizing orbitals. In this limit the electrons are no longer allowed to form entangled states over clusters of impurities, which reduces the PAM self-energy to the sum of the local SIAM self-energies [28, 29, 30, 31, 32]

$$\tilde{\Sigma}^{PAM}(\omega) \approx \tilde{\Sigma}^{DMFT}(\omega) \equiv \sum_i \tilde{\Sigma}^{SIAM}_{A_iA_i}(\omega). \tag{6.7}$$

The DMFT scheme can be cast in the form of a loop which starts from a trial PAM self-energy, constructs $\tilde{G}^{PAM}$, performs the SIAM mapping to obtain $\{\tilde{\Sigma}^{SIAM}_{A_iA_i}(\omega)\}$, updates $\tilde{\Sigma}^{PAM}$ using Eq. (6.7), and then continues until self-consistency has been reached. This cycle is illustrated in the top of Fig. 6.2.

To make the procedure fully self-consistent it is important to also update the mean-field-like Hamiltonian. In the DFT+DMFT scheme the calculation

is divided into two cycles, the DFT cycle and the DMFT cycle, as shown in Fig. 6.2. In the DFT cycle the ground state of the system is approximated as a pure separable state and $\tilde{H}^{KS}$ is calculated. In the DMFT cycle $\tilde{H}^{KS}$ is kept fix while the self-energy is updated. The Green's function is then used to generate a new electron density and from that a new KS Hamiltonian.

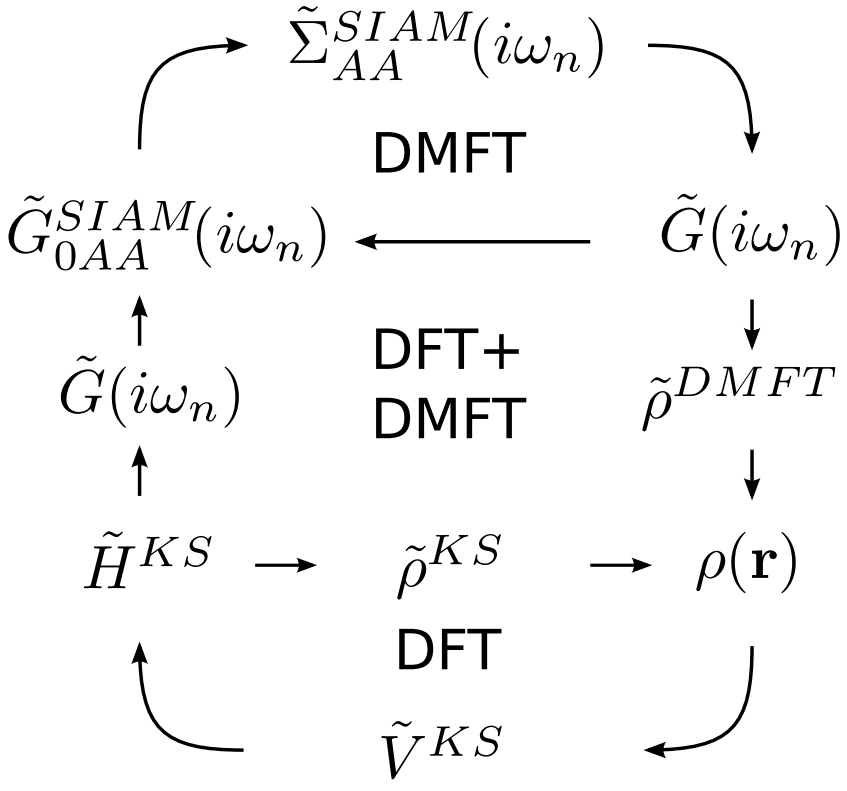

Figure 6.2. Schematic representation of the DFT+DMFT cycle. The first iteration starts in the DFT cycle where a trial electronic density is given as an input. The KS Hamiltonian is then set up and used in the construction of the Green's function $\tilde{G}(i\omega_n)$. The local Green's function $\tilde{G}_{AA}(i\omega_n)$ is obtained by projecting $\tilde{G}(i\omega_n)$ onto a correlated orbitals $\mathscr{A}$. $\tilde{G}_{AA}(i\omega_n)$ gives the impurity bath Green's function $\tilde{G}_{0AA}(i\omega_n)$ which is then fed to an impurity solver. The resulting impurity self-energies are then summed to produce the total self-energy used to update $\tilde{G}(i\omega_n)$. Once the basic DMFT cycle has converged a new electron density is constructed and the loop continues until full self-consistency.

7. Results

7.1 Intermediate valence compounds

Intermediate valence (IV) systems [33, 34, 35] have ground states where the localized d- or f-manifold is in a mixed state containing both f^n and f^{n+1} configurations. The principal interest in these materials is due to the interaction between these localized electrons and the itinerant conduction electrons, which manifests itself in exotic material properties [36]. Usually IV systems are metallic, albeit poorly conducting, down to very low temperatures with ground states which can be described as paramagnetic Fermi liquids [37, 38], but the compounds investigated in Papers I, II, and III all show unusual temperature dependencies.

$YbInCu_4$ undergoes a first-order isostructural electronic phase transition at $T_c \approx 40$ K, associated with a change in the valence state of Yb ions, which causes the electrical resistivity and the effective magnetic moment to drop by an order of magnitude [39]. YbB_{12} and SmB_6, on the other hand, are classical examples of narrow-gap semiconductors which develop a band gap on the order of 10 meV as the temperature is lowered [36]. From a theoretical point of view they are considered excitonic insulators [40, 41, 42] or Kondo insulators [36]. The heavy fermion material $SmSn_3$ shows anomalies in the specific heat [43] and electric resistivity [44] with two sharp peaks at 9.3 and 9.6 K, and one broad peaks at and 10.8 K. While the latter is attributed to an antiferromagnetic phase transition, the first two peaks are still of unknown origin, although multipole magnetic order was suggested to play a key role [43]. Also the temperature dependence of the electric resistivity and specific heat of Yb_2Pd_2Sn reveal signatures of a non-Fermi liquid ground state, with two maxima at 200 and 11 K. $YbPd_2Sn$ exhibits coexistence of superconductivity ($T_c = 2.3$ K) and antiferromagnetism ($T_N = 0.28$ K).

Although the anomalous properties of many of these materials have been known for decades [48, 49, 50, 51, 39] the underlying mechanism and relation to the IV ground state is still unclear [52, 53, 41, 42, 54, 55, 56, 57, 58]. Most of the theoretical studies have focused on the the interaction between the localized f-electrons and the itinerant electrons in the meV energy scale close to the Fermi level, using primarily model Hamiltonian approaches [59, 60, 61, 56, 62, 58, 63]. The theoretical calculations in Paper I, II, and III are aimed to complement these studies with an accurate description of the multiplet spectra of the localized f-electrons. To this end we used the LDA+DMFT approach with the Hubbard-I Approximation impurity solver (see section 6.1) integrated

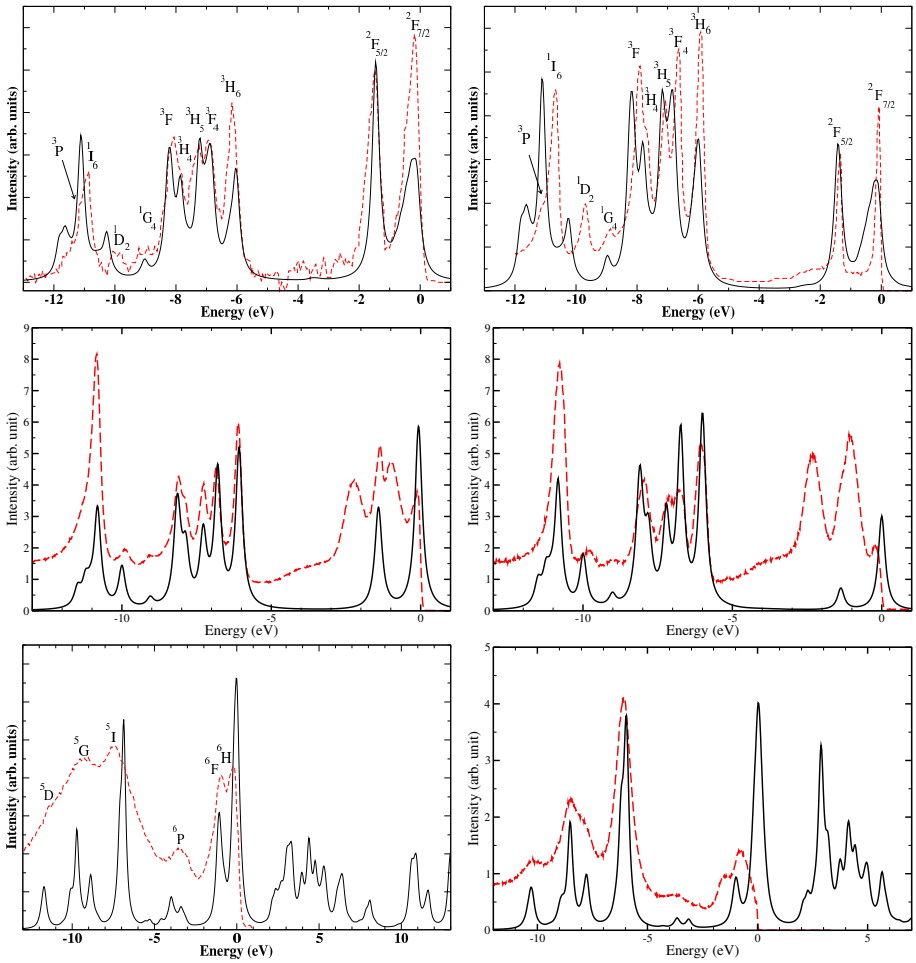

Figure 7.1. Partial Yb 4f or Sm 4f density of states from LDA+DMFT[HIA] (full lines) and experimental photoemission spectrum from Refs. [45, 46, 47] and Paper III and II (dashed lines). Upper left: $YbInCu_4$, upper right: YbB_{12}, middle left: Yb_2Pd_2Sn, middle right: $YbPd_2Sn$, lower left: SmB_6, lower right: $SmSn_3$.

in the FP-LMTO code RSPt [64]. While the Hubbard-I approximation does not take into account the hybridization between the correlated f-orbitals and the bath, and therefore can not produce any quasiparticle peak associated with the Kondo effect, it still gives a very accurate description of the highly localized f-electrons. The results, in form of 4f-partial densities of states, are shown in Fig. 7.1 along with the corresponding experimental photoemission spectra.

The theoretical partial densities of the correlated states and the measured photoemission spectra show an overall excellent agreement. All major peaks are reproduced and their positions lie within a few tenths of an electron volt of

the experimental positions. This data clearly support the use of the Hubbard-I approximation for localized 4f-electrons. However, to include the Kondo physics it is necessary to refine the theoretical description even further, e.g. by using the atomic HIA data as input to simulations based on the Continuous Time Quantum Monte Carlo method.

7.2 Hard permanent magnets

Hard permanent magnets are materials characterized by their huge coercive fields. They are of crucial technical importance and can be found in such diverse applications as electric motors, magnetic recording media, and in the mining industry, where they are used in mineral separation processes. The strongest magnetic materials known today are alloys of rare earth elements, e.g. $Nd_2Fe_{14}B$ and $SmCo_5$. While it is known that the coercivity arises from a coupling between the localized rare-earth f-electrons and the itinerant transition metal d-electrons, the details of this interaction and how it influences the crystal field splitting in the f-manifold is still an outstanding problem. In Paper IV we calculate the electronic structure of $SmCo_5$ using LSDA+DMFT. We treat the localized Sm-4f electrons with the HIA solver and the weakly correlated Co-3d electrons with the SPTF solver in the full conserving formulation (See Paper VIII).

The inclusion of spin-polarization in the LSDA part of the DFT+DMFT cycle makes the double counting problem even more complicated. We used the double counting correction $\tilde{H}^{DC} = \mu^{DC}\tilde{1} + \tilde{H}^{X}$ for the Sm 4f states, where the double counting parameter μ^{DC} acts as an atomic chemical potential, and H^X is introduced to remove the local intra-orbital LDA exchange splitting. An estimate of the inter-orbital LDA exchange splitting was obtained from a separate charge self-consistent calculation, but where the Sm 4f electrons were constrained to stay paramagnetic. This approach works under the assumption that the Sm 4f inter-orbital LDA exchange splitting is only slightly perturbed by the polarization of the Sm 4f-states. In the main calculation H^X was adjusted to remove any intra-orbital LDA exchange splitting from the projected LDA Hamiltonian, while keeping the previously estimated inter-orbital LDA exchange splitting constant. The charge self-consistency is fundamental in this approach as a one-shot calculation would completely neglect the effect of the SPTF self-energy on inter-orbital exchange splitting.

The inclusion of the full Coulomb interaction drastically improves the correspondence between the calculated spectral properties and the experimental data, as seen in Fig. 7.2. Moreover, the magnetic properties are strongly influenced by the inclusion of the LDA+DMFT self-energy, as shown in Table 7.1. In the one-particle band picture the magnetic moment driven by a large exchange-splitting, which gives a very large spin-moment but severely underestimates the orbital moment. In the atomic-like picture, given by the HIA

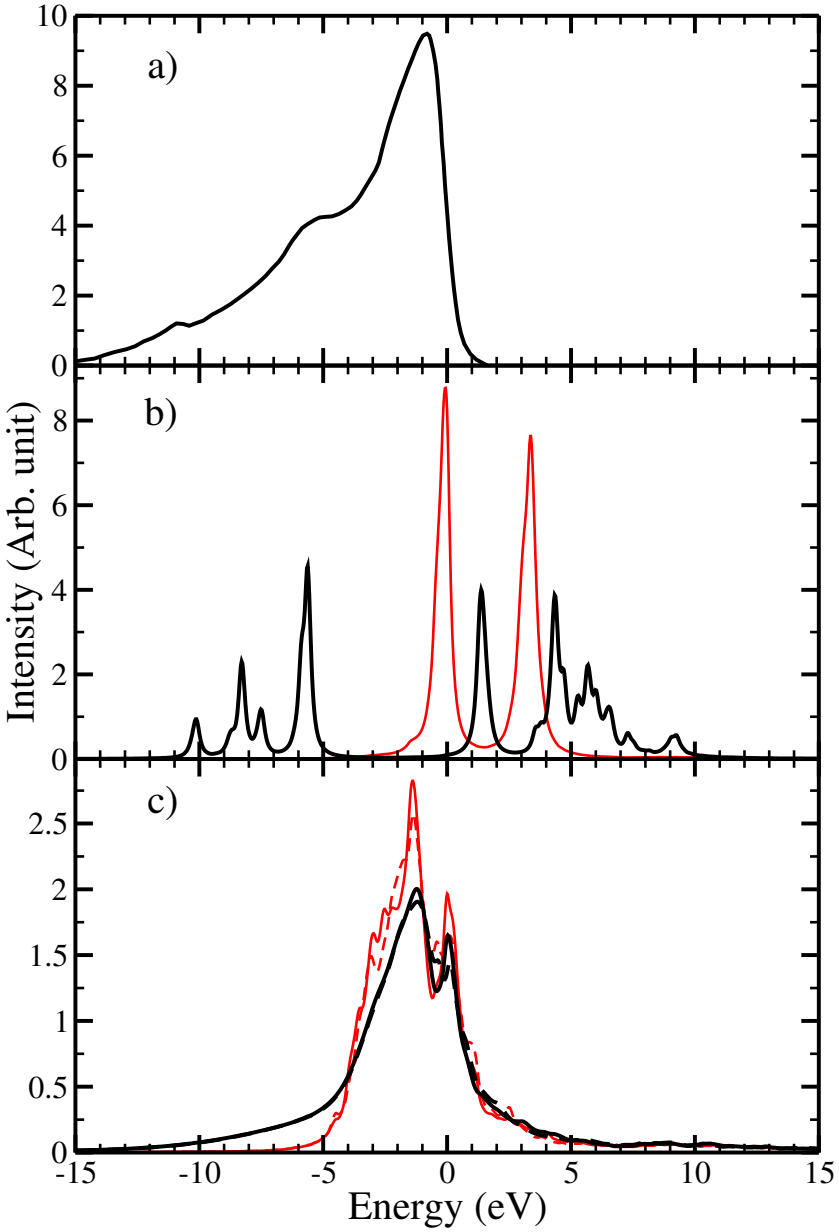

Figure 7.2. Experimental and calculated spectra of $SmCo_5$. The calculated LDA values are represented with thin lines while the LDA+DMFT values are given by thick lines. (a) Experimental x-ray photoemission spectrum from Ref. [65]. The small peak at -11 eV is an Ar 2p artifact from the sample cleaning procedure. (b) Calculated projected density of states of Sm 4f orbitals. (c) Calculated projected density of states of Co 3d states for Wyckoff position 2c (solid lines) and 3g (dashed lines). The Fermi level is at zero energy.

Table 7.1. *Spin (m_s), orbital (m_o), and total (m_{tot}) moment of $SmCo_5$. The total moment also includes the contribution from the interstitial region. All the magnetic moments are given in units of μ_B.*

	Sm		Co (2c)		Co (3g)		Total
Method	m_s	m_o	m_s	m_o	m_s	m_o	m_{tot}
LSDA (100 K)	-5.48	1.81	1.58	0.06	1.55	0.10	4.04
LSDA+DMFT (100 K)	-4.38	4.45	1.54	0.21	1.53	0.18	8.24
LSDA+DMFT (400 K)	-3.47	3.26	1.54	0.22	1.52	0.18	8.02
Exp.	–	–	–	–	–	–	8.9

solver, there is a large set of almost degenerate many-body eigenstates with different magnetization directions. The inter-orbital exchange introduces a small energy bias in favor of a certain magnetization direction which increases the weights of the favored states in the many-body density operator. This small energy is on the same order as the thermal energy fluctuations ($\approx k_B T$), which gives the magnetic moment a proper temperature dependence.

7.3 Electronic entanglement in the late transition metal monoxides

The electronic structure of the late transition metal monoxides (TMO) – MnO, FeO, CoO and NiO – has been the topic of much discussion for a long time [66, 67]. The surge in interest arose when it stood clear that single Slater determinant band structure calculations [68] predict these oxides to be metallic, while experiments showed that they are wide-gap insulators with band gaps of 2 – 4 eV. Mott and Peierls identified the strong on-site Coulomb repulsion between the electrons in the TM-3d orbitals as the driving force behind the formation of the band gap [69, 70]. Later, a set of refined experiments showed that there is also a strong hybridization between the TM-3d and O-2p states [71, 72], which places the TMOs in the intermediate regime between Mott insulators and charge-transfer insulators in the Zaneen, Sawatzky and Allen classification scheme [73].

Over the years numerous computational schemes have been used to describe the spectral properties of the TMOs; density functional theory (DFT) in local (LDA) or semi-local (GGA) approximations [74, 75], self-interaction corrections [76] and LDA+U [77, 78], combinations between GW and LDA+U [79, 80], and between GW and hybrid functionals [81]. The inclusion of type II antiferromagnetic order is vital to get the correct shape of the excitation spectrum in these studies, while experiments have shown that spectral properties are insensitive to the magnetic order [82]. This discrepancy can be traced to the one-single Slater determinant (pure separable state) nature of these approaches. Methods based on describing the electrons in the TM-3d orbitals using a general mixed and entangled many-body state, like finite cluster ap-

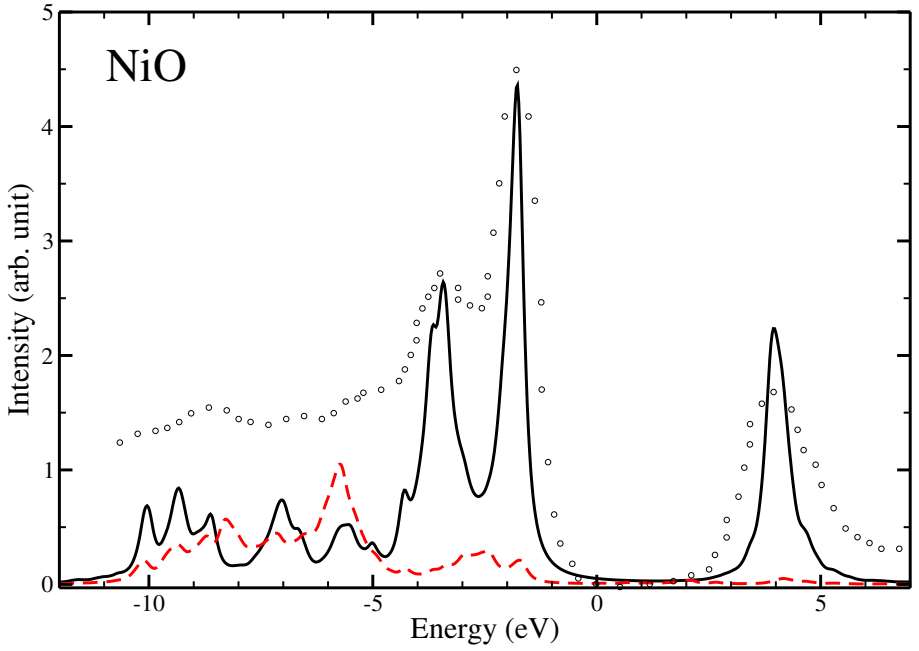

Figure 7.3. PDOS of the Ni 3d states (thick lines) and O 2p states (dashed lines) in NiO, and corresponding XPS/BIS data (black circles). The Fermi level is at zero energy.

proximations [83, 84] and LDA+DMFT [85, 86, 87, 88, 89, 90, 91] do not have this drawback. Unfortunately, it has been difficult for the above mentioned LDA+DMFT studies to reproduce experimental photoemission spectra. This might in part be due to the use of various technical approximations, in particular the three-pole approximation, the maximum entropy method, a lack of charge self-consistency, and the density-density approximation of the Coulomb interaction matrix.

In Paper V we present the LDA+DMFT results obtained with our newly implemented ED impurity solver, free of the technical approximations mentioned above. While the quality of the calculations are affirmed through comparison with experimental photoemission experiments (XPS/BIS), as shown for NiO in Fig. 7.3, the main focus of the letter is the entanglement between the electrons in the impurity problem.

7.3.1 Entanglement measures

Entanglement between distinguishable particles has been studied in great detail both theoretically and experimentally [92]. As the particles are distinguishable they can be labelled and partitioned into different subspaces of the Hilbert space using tensor products ($\otimes$). A pure state $|\Psi'\rangle$ of N distinguish-

able particles is then defined as being separable if it can be written as a single product state

$$|\Psi'\rangle = \bigotimes_{j=1}^{N} |\Psi'_j\rangle \equiv |\Psi'_1\rangle \otimes |\Psi'_2\rangle \otimes \cdots \otimes |\Psi'_N\rangle. \tag{7.1}$$

The representation of an entangled state $|\Psi\rangle$ requires at least a superposition of two product states

$$|\Psi\rangle = \sum_{i=1}^{M\geq 2} \bigotimes_{j=1}^{N} |\Psi^i_j\rangle. \tag{7.2}$$

The fixed partitioning of the Hilbert space makes it natural to ask whether or not the particles in a composite partition A are entangled with the particles not in A (composite partition B). The standard way to investigate this for a pure state $|\Psi\rangle$ is to construct a reduced N_A-particle density operator by taking the partial trace over the subspace B

$$\tilde{\rho}_A = \mathrm{Tr}_B\left[\tilde{\rho}\right] \equiv \sum_i \langle \Psi^i_{(B)} | \tilde{\rho}_N | \Psi^i_{(B)} \rangle \tag{7.3}$$

where

$$|\Psi^i_{(B)}\rangle = \tilde{1} \otimes |\Psi^j_{b_1}\rangle \otimes \tilde{1} \otimes \cdots \otimes |\Psi^j_{b_2}\rangle \otimes \cdots \otimes |\Psi^j_{b_{N_B}}\rangle \otimes \tilde{1}, \tag{7.4}$$

and $b_1, \ldots, b_{N_B}$ are the indices of the partitions included in B. The particles are entangled if $\tilde{\rho}^i_{N-1}$ is a mixed state, which can be checked using the von Neumann entropy

$$S_{vN} = \mathrm{Tr}\left[\tilde{\rho}^i_{N-1} \ln(\tilde{\rho}^i_{N-1})\right]. \tag{7.5}$$

The bipartitioning procedure measures the entanglement between two given subspaces, but it does not give a value of the total entanglement in the system. This quantity can be evaluated through a geometric entanglement measure [93]

$$E_G[|\Psi\rangle\langle\Psi|] = 1 - \max_{|\Psi'\rangle} \left|\langle\Psi'|\Psi\rangle\right|^2, \tag{7.6}$$

where $|\Psi'\rangle$ is restricted to be separable. E_G measures the distance between $|\Psi\rangle$ and the closest possible separable state $|\Psi'\rangle$. Although it is trivial to calculate the overlap, it is far from easy to perform the minimization over all separable states due to the large variational space. A practical alternative to a brute force numerical optimization is the search function F, schematically presented in pseudocode form in Fig. 7.4.

The situation is rather similar when the particles are indistinguishable, apart from that there is no natural partitioning of the Hilbert space. It is still possible to define a bipartition, as shown in Eq. (3.49), but the number of particles in each partition is in general not fixed. In Paper V we instead focus on the one-particle reduced density matrix defined in Eq. (5.14), and an analogous search

function F is:
input: pure state $|\Psi\rangle$, partitioning if the Hilbert space $\{\mathscr{A}_m\}^M$, current maximal overlap O'_{max}

1. *#Detect single-particle states:*
   if $(|\{\mathscr{A}_m\}| = 1)$ **return** $\langle\Psi|\Psi\rangle$
2. *#Measurement optimization*:
   Diagonalize the one-particle density matrices of each partition $\tilde{\rho}^{(m)} = \tilde{\mathrm{V}}^{(m)}\tilde{\mathrm{D}}^{(m)}\tilde{\mathrm{V}}^{(m)\dagger}$, where $\tilde{\rho}^{(m)} = \mathrm{Tr}_{\mathscr{H}\setminus\mathscr{A}_m}(|\Psi\rangle\langle\Psi|)$.
3. Label the eigenvalues $\tilde{\mathrm{D}}^{(m)}_{ii}$ from largest to smallest such that $\tilde{\mathrm{D}}^{(m_k)}_{i_k i_k} \geq \tilde{\mathrm{D}}^{(m_l)}_{i_l i_l}$ for $k \leq l$. Define $|\Psi^k\rangle = \sum_j \tilde{\mathrm{V}}^{(m_k)}_{i_k j}|\Psi^{(m_k)}_j\rangle$.
4. *#Perform the measurement and add another one-particle detector:*
   for $k = 1, 2, \cdots$, total number of states
   if $(\tilde{D}^{(}m_k)_{i_k i_k} > O'_{max})$ then
   $\tilde{P}_k \leftarrow \bigotimes_{i=1}^{m_k-1} \tilde{1} \otimes \langle\Psi^k| \bigotimes_{i=m_k+1}^{M} \tilde{1}$
   $O'_{max} \leftarrow \max\left(O'_{max}, F\left[\tilde{P}_k|\Psi\rangle, \{\mathscr{A}_m\}_{m\neq m_k}, O'_{max}\right]\right)$
   end if
   done
5. **return** O'_{max}

end F

Figure 7.4. A pseudocode representation of the recursive depth first search function $F\,[|\Psi\rangle, \{\mathscr{A}_m\}, O'_{max}]$. Note that the state $|\Psi\rangle$ is not renormalized after each measurement, and that the initial value of O'_{max} can be set to zero. Comments are given in italic.

algorithm to the one presented in Fig. 7.4 is derived. We also considers the entanglement in mixed states, in particular in the paramagnetic phase where the ground state is composed by a large number of degenerate many-body states. Although the presence of classical correlations makes it much more difficult to extract the strength of the entanglement, the use of spin coherent operators allowed us to obtain a practical expression for the paramagnetic mixed state entanglement as well.

The entanglement measures presented in Paper V finally make it possible to study the role of the entanglement in more exotic systems as complex actinides or Fe based superconductors, and see how it relates to their unconventional properties. We are just beginning to explore this promising new path of research.

7.4 Magnetically doped semiconductors

Diluted magnetic semiconductors (DMS) are obtained by doping standard semiconductors with a small amount of magnetic impurities, which results

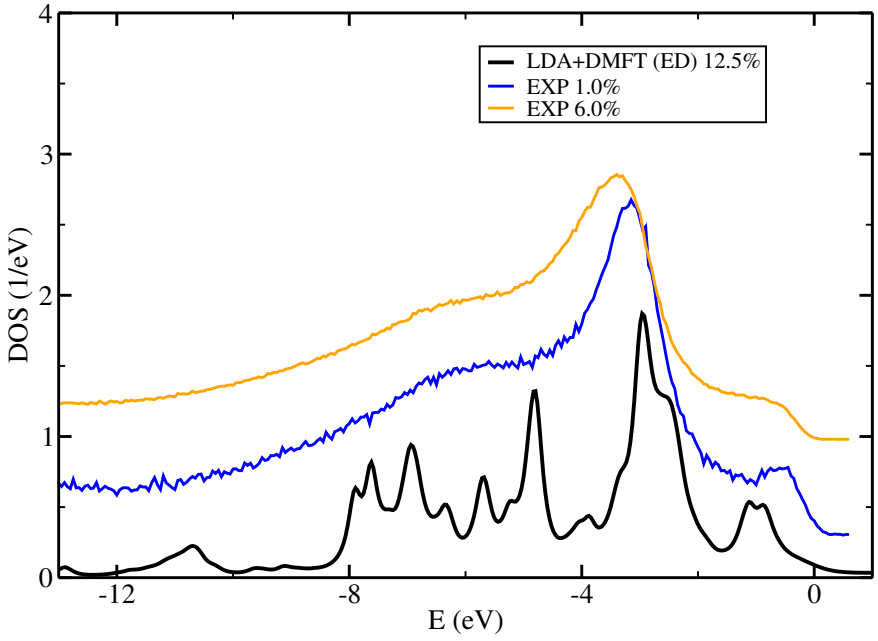

Figure 7.5. Resonant photoemission spectrum of Mn-3d states in Mn doped GaAs at several concentrations compared to the Mn-3d projected density of states from LDA+DMFT with the ED solver. The Fermi level is at zero energy, and no artificial shifts have been applied between theoretical and experimental curves. In the inset the ferromagnetic (FM) and non-magnetic (NM) LDA results are shown.

in a ferromagnetic order. These materials are of prime interest in the emerging field of spintronics, where they are used in electrical circuits to manipulate the spin of the transported electrons. In practical applications, an ordering temperature above room temperature is needed, but none of the claimed candidate materials, like Mn or Co doped ZnO, have so far hold up to scrutiny. The study of DMS materials based on ZnO has been hampered by difficulties in synthesizing samples with a homogeneous distribution of dopants. Mn doped GaAs offers a considerably more robust situation, and substitutional Mn doping at the Ga sites can reach concentrations up to 6-8 % resulting in ordering temperatures as high as 170 K. In Paper VI we calculate the spectral properties of Mn doped GaAs using the LDA+DMFT approach and the ED impurity solver. The multiplet-like spectrum compares well with the experimental photoemission data, as shown in Fig. 7.5, which indicates that the Mn 3d-electrons are localized in nature although they are strongly influenced by the hybridization with the host material.

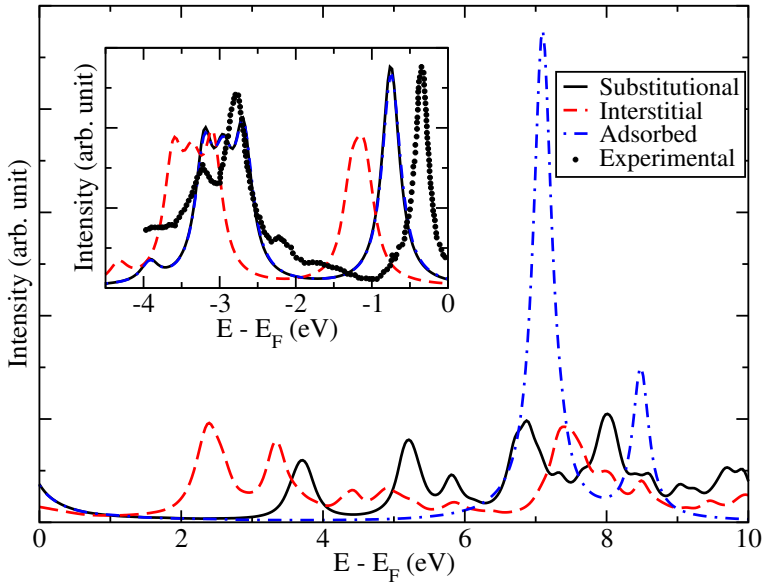

Figure 7.6. Calculated Fe 3d excitation spectrum for different impurity sites: substitutional position in the Cs bulk (solid line), interstitial position in the first sub layer of the Cs surface (dashed line), and adsorbed position on top of the Cs surface (dashed dotted line). The experimental photoemission spectrum [94] is shown for comparison (circles).

7.5 Iron impurities in Cesium

In Paper VII we investigate Fe impurities in Cs, and how the local environment of the Fe atoms affects the excitation spectrum using LDA+DMFT[ED]. This study was motivated by a report by Carbone *et al.* [94] who analyzed the deposition of Fe impurities on different alkali metal surfaces (Cs, K, Na and Li). Their photoemission spectroscopy data show two different correlation regimes. The Fe atoms deposited on the Cs surface display a rich multiplet spectrum, indicating strong correlations, while a more band-like behavior of the Fe impurities is seen in the case of the Li surface. In their paper Carbone *et al.* suggest that the photoemission signal comes from the impurities adsorbed on the surface. However, often impurities do not adsorb on surfaces but rather diffuse into the material, e.g. into interstitial positions or even change place with the host atoms in substitutional positions. Through a series of calculations we show that it is hard to distinguish among the substitutional, interstitial and adsorbed sites by probing the occupied part of the excitation spectrum, corresponding to an ordinary photoemission spectroscopy experiment. However, clear differences between the sites emerge in the unoccupied part of the excitation spectrum, as shown in Fig. 7.6. Therefore we conclude that an inverse photoemission experiment is likely able to determine the positions of the Fe impurities deposited on the Cs surface.

7.6 Magnetic moments in late transition metals

In Paper VIII we study three different formulations of SPTF and how they influence the magnetic moments and the spectra of the late transition metals Fe, Co, and Ni. All the formulations use the same SPTF equations presented in section 5.5.3, but they differ in the choice of Green's function used in the polarization bubbles in Eq. (5.40) and (5.75), and in the self-energy in Eq. (5.81). The symbol $\tilde{G}_{AA}(\omega)$ has the following meaning in the three formulations:

$\tilde{G}^{SIAM}_{0AA}(\omega)$	Standard formulation of SPTF in the bare Green's function (G0-SPTF)
$\tilde{G}^{SIAM}_{AA}(\omega)$	Fully conserving formulation of SPTF (Full G-SPTF)
$\tilde{G}^{HF}_{AA}(\omega)$	Partially conserving formulation of SPTF (GHF-SPTF)

The Green's function $\tilde{G}^{HF}_{AA}(\omega)$ used in GHF-SPTF is obtained from the Hartree-Fock self-energy

$$\tilde{\Sigma}^{HF}_{ij} = \frac{1}{2}\tilde{\rho}^{HF}_{nm}\left[\tilde{U}^{eff}_{minj} - \tilde{U}^{eff}_{mijn}\right], \tag{7.7}$$

and

$$[\tilde{G}^{HF}_{AA}(\omega)]^{-1} = [\tilde{G}^{SIAM}_{0AA}(\omega)]^{-1} + \tilde{\Sigma}^{HF}_{AA}. \tag{7.8}$$

The density operator $\tilde{\rho}^{HF}$ in Eq. (7.7) is obtained self-consistently from $\tilde{G}^{HF}_{AA}(\omega)$ and Eq. (5.14). GHF-SPTF is very close in spirit to LSDA+U+SPTF, the only difference between the two is that LDA+U+SPTF use $\tilde{\rho}_{AA}$ in Eq. (7.7) instead of $\tilde{\rho}^{HF}_{AA}$.

The results for the spectral density and magnetic moment of bcc Fe are shown in top and bottom panels of Fig. 7.7, respectively. The spectral properties are only minimally changed in the three different SPTF formulations. The main difference is that full G-SPTF leads to a strong smearing of the high-energy satellite. This extra smearing is closely related to the overscreening problem encountered in the fully self-consistent GW method. It stems from an overestimation of the polarization in Eq. (5.40) and (5.75), which overscreens the effective interactions and leads to a stronger imaginary component in the self-energy.

The magnetic moments show a larger difference between the three formulations, and the results obtained from full G-SPTF are intermediate to those of G0-SPTF and GHF-SPTF. This trend reveals that the screening is not the only factor influencing the electronic structure. The screening tends to quench the orbital polarization, so this effect alone would order the results according to G0-SPTF $>$ GHF-SPTF $>$ full G-SPTF. The competing effect is that the dressing of the Green's function pushes the orbital polarization via the construction of the self-energy in Eq. (5.81) and the use of the $\Sigma(0)$ double counting correction. In G0-SPTF there is little screening, but also no dressing of the Green's function, leading to a smaller orbital moment. The screening in GHF-SPTF is also small, but the inclusion of the Hartree-Fock self-energy in $\tilde{G}^{HF}_{AA}(\omega)$

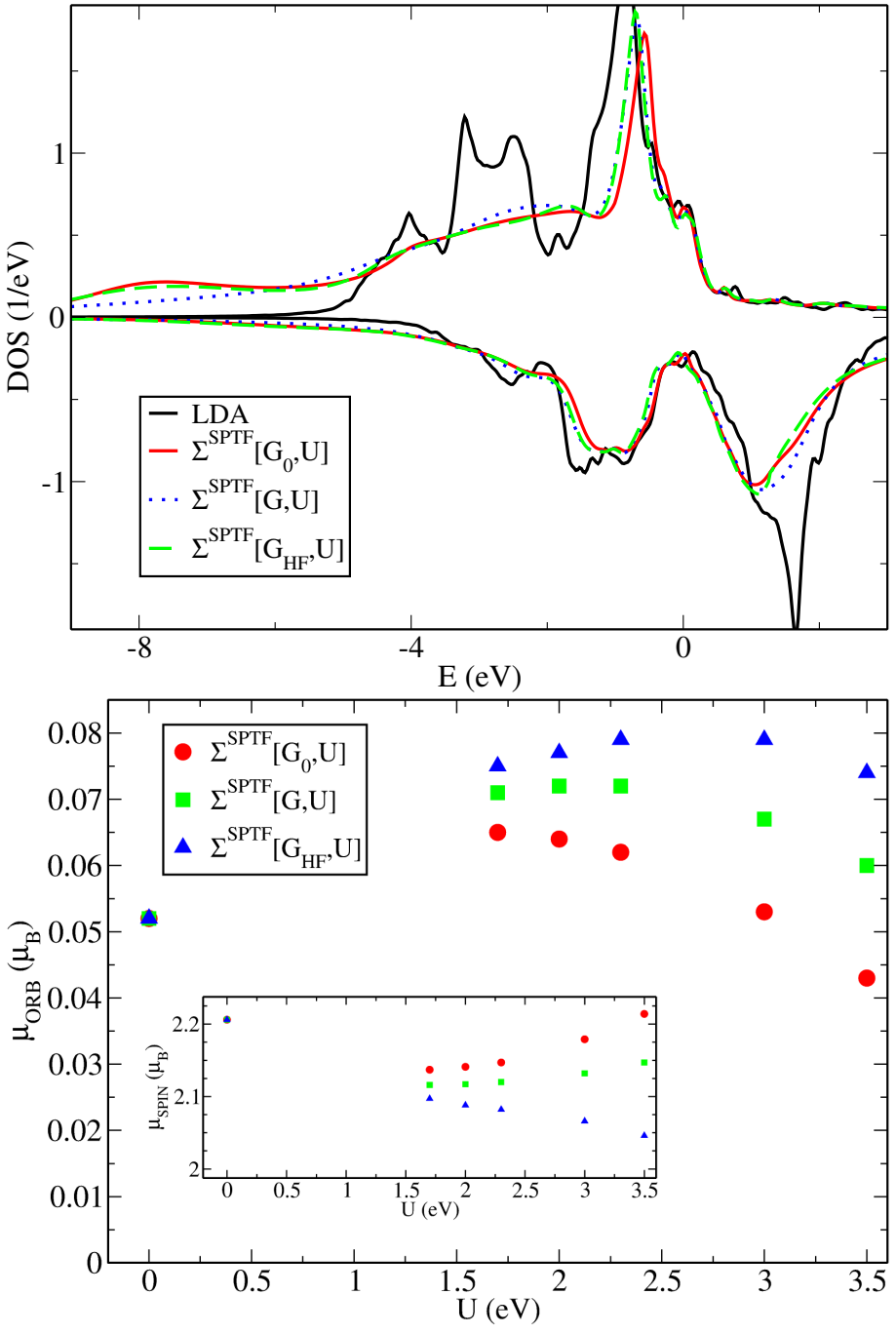

Figure 7.7. (top) Projected spectral density of Fe in the three different formulations of SPTF compared to LDA results. (bottom) Fe orbital and spin moments.

increases the orbital polarization. In full G-SPTF there is a large screening which compensates the orbital polarization given by $\tilde{G}^{SIAM}_{AA}(\omega)$, which explains the intermediate results. The results of Co and Ni follow the same trends. The experimental orbital moment of bcc Fe is 0.8-0.9 μ_B and the spin moment is 2.0-2.1 μ_B, which compares well to the results from the partially conserving formulation GHF-SPTF.

7.7 Spectral properties of NiS

By replacing the oxygen in NiO with larger and less electronegative sulfur atoms, the crystal structure becomes hexagonal and the correlation strength is reduced. NiS exhibits a first-order phase transition [95] at 260 K, accompanied by a 2% volume collapse and a transition from paramagnetism to antiferromagnetism. The high temperature paramagnetic phase is metallic while the low temperature antiferromagnetic phase displays a rather poor conductivity. To understand the role of correlation we have performed LDA+DMFT calculations for both these phases, and compared the calculated photoemission spectra with experimental data. The weak correlation strength, reflected in a rather small $\widehat{U}^{eff}_{AAAA}$ and a large and broad hybridization $\tilde{\Delta}_{AA}(\omega)$, allow us to use the SPTF impurity solver. The resulting self-energy shifts the main KS-DFT quasi-particle bands of the correlated Ni 3d orbitals closer to the Fermi level, and introduces a broadening of the spectral features, as shown in Fig. 7.8. The excitations at intermediate energies, caused by the hybridization with the S 3p orbitals, are also shifted but the main effect is a very strong broadening given by the large imaginary part of the self-energy. A comparison between LSDA+DMFT[SPTF], LSDA+U, and experimental data is shown in Fig. 7.8. The peak positions and spectral weights at the Fermi level are significantly improved due to the incorporation of the SPTF self-energy compared to the static Hartree-Fock self-energy in LSDA+U.

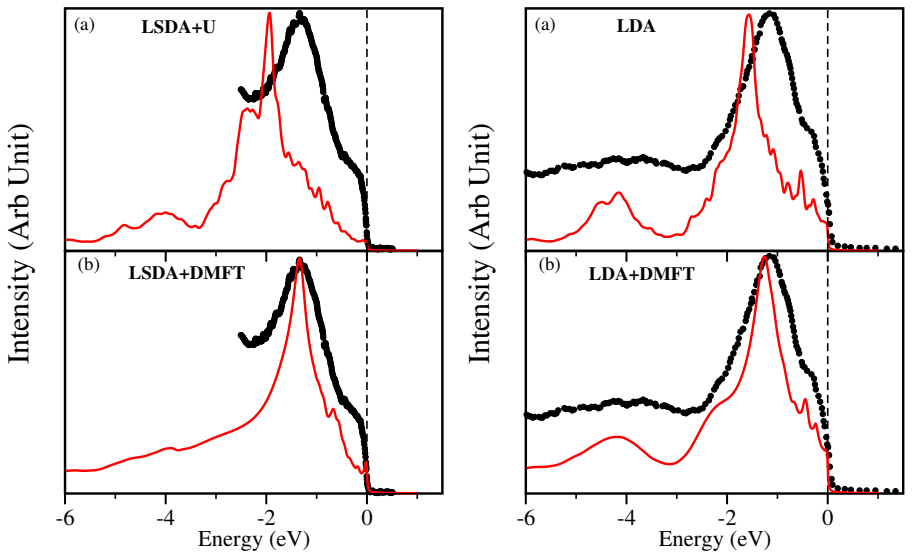

Figure 7.8. Theoretical (line) and experimental (circles) photoemission data for NiS. Left panel: AMF phase within (a) LSDA+U and (b) LSDA+DMFT for photon energy 21.2 eV at 150 K. Right panel: Non-magnetic phase within (a) LDA and (b) LDA+DMFT for photon energy 40.81 eV at 300 K.

8. Conclusions and outlook

The electrons in transition metal 3d-orbitals and lanthanide 4f-orbitals have a strong tendency to stay localized in various compounds and phases. The DFT+DMFT results presented in the previous chapter show that a proper many-body treatment on these localized electrons is essential to obtain the correct spectral weight redistribution and multiplet features in the excitation spectra. The many-body treatment gives a correct description of the paramagnetic phase, with $\langle \widehat{S}^2 \rangle \neq 0$ but $\langle \widehat{S}_z \rangle = 0$, and a proper temperature dependence of the ground state properties. However, there are still room for improvements. Most of these results where obtained from simulations where the screened on-site Coulomb interaction $\widehat{U}^{eff}_{AAAA}$ and the double counting correction $\widehat{U}^{DC}_{AA}$ were obtained in a semi-empirical way[1]. The self-consistent GW+DMFT scheme could potentially resolve these issues, but no fully self-consistent results have been presented so far. What is also missing is a canonical way to construct the correlated orbitals. This is closely related to the rather vague definition of the term 'strongly correlated' used in the quantum chemistry and condensed matter communities. The term is used to denote the electronic structure of those materials which KS-DFT or HF fail to describe even in a qualitative way. The lack of a quantitative definition of the strong correlation makes it very hard to define an optimal set of correlated orbitals aimed to capture its effects. Let us therefore end with some concluding remarks about the relation between the strong correlation and the well-defined classical and quantum correlations, in an attempt to shed some light on the subject.

The only trivial implication is that a mean-field description is separable. The reverse implication, that a separable ground state must be well described by KS-DFT or HF, is not true in general. Consider for example a material well described by the LDA+U method. The LDA+U Hamiltonian is identical to $\widehat{H}^{PAM}$ except that $\widehat{U}^{eff}_{AAAA}$ is replaced by the single-particle screened Hartree-Fock term $\widehat{U}^{SHF}_{AA}$. All the terms in the LDA+U Hamiltonian are single-particle terms which implies that the LDA+U ground state is separable, but it is of course still different from the KS-DFT ground state. This example shows also why it is essential to use a proper minimization procedure in a geometrical entanglement measure. The distance between a density operator obtained from LDA+U and any arbitrarily chosen separable reference state, like the DFT ground state of the same system, is always non-zero for a finite U, although

[1] The existence of more than 5 different double counting corrections makes the choice of correction almost a free parameter in itself.

both states are separable. It might be tempting to think of this distance as a measure of some strong correlations in the LDA+U ground state, but the connection to entanglement is then completely lost. Furthermore, since we add a Hartree-Fock term to the Hamiltonian in the LDA+U method, one could even argue that the LDA reference state is more correlated than the LDA+U state, at least in a DFT sense.

A finite classical correlation in the electronic structure of a thermal system implies the existence of nearly degenerate many-body states in the ground state density operator. These degeneracies are important in the description of temperature dependent properties, e.g. the magnetic moment. The standard KS-DFT and HF implementations take the classical correlations into account only in a rudimentary way. Their ground states are constructed from the single-particle eigenvectors of $\tilde{H}^{MF}$, occupied according to the Fermi-Dirac distribution of the corresponding eigenvalues. The main approximation is that the Hamiltonian $\tilde{H}^{MF}$ is obtained from a single, possibly symmetry-broken, electron density or one-particle reduced density operator. A proper treatment would instead require the use of several mean-field-like Hamiltonians of large supercells constructed from different starting points such that the crystal symmetry is fulfilled on average. However, it should be noted that even with a multi-Hamiltonian mean-field approach it is still not possible to describe a paramagnetic system. The reason is that the classical correlation related to the different local moments of the atoms is intrinsically coupled to the $\langle \widehat{S}^2 \rangle$ dependent entanglement described in Paper V.

The connection between entanglement and strong correlation in materials is still largely unexplored. A systematic study of the entanglement in the electronic structure of a set of strongly correlated materials would be highly interesting. The pair-hopping entanglement, described in Paper V and in Section 3.4, can simplify the study as it is present also in the pure ground states of magnetically ordered phases at zero Kelvin, as shown for CoO. However, as the name suggests, this form of entanglement requires that the pair-hopping terms in $\widehat{U}^{eff}_{AAAA}$ are included in the calculation, and not discarded as in the density-density approximation of the Coulomb interaction.

9. Sammanfattning

Eftersom elektroner är osärskiljbara fermioner beter de sig på ett väldigt annorlunda sätt än vanliga föremål i vår omgivning. Om flera elektroner befinner sig nära varandra går det, som namnet antyder, till exempel inte att avgöra vilken av elektronerna som är vilken. Om man ändå försöker beskriva elektrontillståndet genom att sätta en bestämd etikett på vardera elektron byter den matematiska beskrivningen av elektronerna tecken om man byter plats på två av elektronetiketterna. Detta gör det naturligt att försöka definiera tillståndet hos en samling elektroner med hjälp av en så kallad Slater-determinant som också delar denna egenskap. Snart visar det sig dock att det i många fall inte räcker med endast en Slater-determinant, utan att man behöver lägga ihop flera, antingen på ett klassiskt sätt med hjälp av sannolikheter, eller på ett kvantmekaniskt sätt med hjälp av linjärkombinationer (superpositioner). Om det endast behövs en Slater-determinant för att beskriva elektrontillståndet kallas det för ett rent och separabelt tillstånd. Om beskrivningen kräver klassiska sannolikheter är tillståndet inte längre rent utan kallas mixat. Om den behöver kvantmekaniska superpositioner kallas tillståndet sammanflätat istället för separabelt. För att helt säkert kunna säga vilken av ovanstående kategorier det totala elektrontillståndet tillhör räcker det inte med att undersöka en elektron åt gången utan man måste ta med förhållandet mellan alla elektroner på en gång. Redan på 50-talet bevisade Löwdin att den linjära entropin visar hur nära ett tillstånd är att vara rent och separabelt. Problemet vi brottas med än idag är dock att kunna bestämma storleken på den klassiska respektive den kvantmekaniska elektronkorrelationen var för sig. I Artikel V presenteras två olika metoder för att direkt kunna bestämma den kvantmekaniska sammanflätningen: det geometriska sammanflätningsmåttet och den korrigerade linjära entropin.

Standardmetoden för beräkningar av elektronstruktur, Kohn-Shams formulering av densitetsfunktionalteorin (KS-DFT), ger ofta en mycket bra beskrivning av ett materials egenskaper. Ibland blir dock vissa egenskaper, såsom elektrisk ledningsförmåga och magnetiskt moment, helt felaktiga för material med lokaliserade d- och f-elektroner. Att det behövs något utöver KS-DFT för att beskriva fotoemissionsspektra av dessa d- och f-elektroner är känt sedan länge. Detta har ofta avfärdats med att dessa data endast visar att det är de exciterade tillstånden och inte grundtillståndet som behöver korrigeras, om ens det. Om man dock tittar närmre på elektrontillstånden framträder bilden att KS-DFT ger en bra beskrivning av rena separabla elektrontillstånd, men att metoden tyvärr ofta faller ganska platt när det kommer till mixade

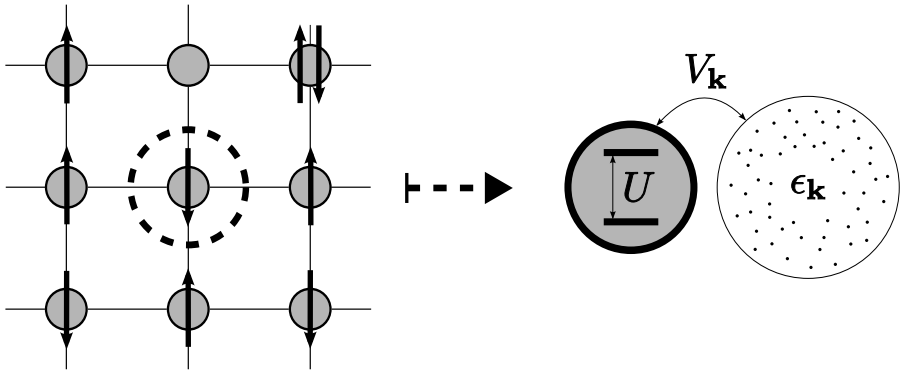

Figure 9.1. En schematisk illustration över hur atomerna i ett material beskrivs i DMFT med hjälp av en atom i ett elektronbad. Parametrarna $V_{\mathbf{k}}$ och $\varepsilon_{\mathbf{k}}$ beskriver hur lätt elektronerna kan hoppa mellan atomen och badet. Parametern U beskriver hur mycket extra energi det krävs för att ändra antalet elektroner hos atomen.

sammanflätade elektrontillstånd. En av de mest lovande metoderna för att förbättra DFT-resultaten är att inkludera dynamisk medelfältsteori (DMFT) i beräkningarna. I DMFT beskrivs de lokaliserade d- och f-orbitalerna med hjälp av en effektiv Andersonmodell som tillåter elektronerna att bli sammanflätade, vilket illustreras i Fig. 9.1. En betydande del av denna avhandling handlar om utveckling, implementation och användande av olika metoder för att lösa den effektiva Andersonmodellen i DMFT. Fokus ligger på Hubbard-I Approximationen (HIA), Exakt Diagonalisering (ED) och Spin-Polariserad T-matris-Fluktuation-utbytesväxelverkan[1] (SPTF).

I HIA tillåts inte elektonerna att lämna de lokaliserade orbitalerna. Detta motsvarar att sätta $V_{\mathbf{k}} = 0$ i Fig. 9.1. Detta förenklar problemet drastiskt, och gör det möjligt att att ta fram en exakt "atomär" lösning. Denna beskrivning visar sig stämma mycket bra för starkt lokaliserade 4f-elektroner i lantanoid-föreningar (Artikel I, II, III och IV).

I ED anpassas ett litet antal fiktiva orbitaler för att efterlikna effekten av elektronbadet i Andersonmodellen. Denna metod kan med framgång beskriva elektrontillstånden i övergångsmetallmonoxiderna MnO, FeO, CoO och NiO (Artikel V). Utöver excitationsspektra studerade vi även sammanflätningen hos elektrontillstånden. Det visade sig att CoO särskiljer sig från de andra övergångsmetallmonoxiderna genom att den har en extra intrikat form av elektronsammanflätning. Detta kunde förklaras genom en tävling mellan kristallfältsenergierna och Coloumb-repulsionen mellan 3d-elektronerna. Illustrationen på framsidan av denna avhandling visar hur två spin-upp elektroner i Co 3d-orbitalerna ger upphov till det sammanflätade tillståndet. Med

[1] I vardagligt tal kallar vi den bara för "Flex"

hjälp av ED har vi även studerat Mn inlöst i GaAs, ett material som tillhör klassen utspädda magnetiska halvledare, och Fe på en yta av Cs (Artikel VI och VII).

SPTF beskriver svagt växelverkande elektroner i mer delokaliserade orbitaler genom perturbationsteori. I Artikel VIII och IX studeras de magnetiska momenten och excitationsspektran hos Fe, Co, Ni och NiS. För de rena övergångsmetallerna analyseras även betydelsen av olika formuleringar av den perturbationsteori som används i SPFT.

Acknowledgments

First of all I would like to thank my main supervisor Olle Eriksson for introducing me to this fascinating research topic. I am very grateful for your support, guidance, and enthusiasm. Secondly, I wish to thank my office mate and favorite co-supervisor Igor Di Marco, we have had some great times together and I have learned a lot from you. I would also like to thank all the other coauthors I have had the pleasure to work with. Oscar and Torbjörn, without you guys there would be no DMFT Team. Marcio, you have been a great ED test pilot. Hitoshi, thank you for sharing you crisp experimental knowledge and photoemission data. Biplab, Barbara and Sumanta, thank you for your help with the macromolecules. Swarup, it was very nice working with you, and the visit to India was a true experience. I also wish to thank Sebastien Lebègue, Alexei Grechnev, Mikhail Katsnelson, and John Wills for sharing your programs and source codes with me, and for the hospitality you showed me when I was visiting.

I would probably not be writing this thesis, if it were not for all the support I have received from Erik Sjöquist, Johan Åberg, and Arnold Maliniak. You have been a great inspiration, and really I hope our ways will cross once more in the future!

I would also like to thank the people at the Division of Materials Theory. Misha, try not to create any monster codes while I'm away. Attila, you have taught me everything a man needs to know about J_{ij}. Baotian, forget about LDA+U, you will soon be the master of LDA+DMFT. Marco, thank you for producing the fancy orbitals on the cover page. I would also like to thank Pablo, Iulia, Cecilia, Leyla, Ralph, Corina, Wei Wei, Peter, Nina, Johan, Diana, Jan, Jonas, Annika, Anders, Ola, Bulten, and Petros for making my stay in Uppsala a pleasure.

Maggan and Janne, thank you for taking care of Karin while I was finalizing the thesis. Without your help this thesis would have been incomprehensible at best. A big thanks to my close friends Johan, Gerald, Pontus, Daniel, Marre, Erik, Sofie, Gustav, Malin, and Jojo for providing the perfect amount of distraction. And of course a big hug to my family for being there.

Finally, Karin and Emelie, your love and support is all that matters. You make my life complete.

References

[1] Dirac, P. (1928) *Proceedings of the Royal Society of London* **117**, 610 – 624.

[2] Bransden, B. and Joachin, C. (2000) Quantum mechanics, Pearson Education, .

[3] Koelling, D. D. and Harmon, B. N. (1977) *Journal of Physics C: Solid State Physics* **10(16)**, 3107–3114.

[4] Kennedy, W. (1988) *J. Phys. A, Math. Gen.* **21(13)**, 3021 – 3.

[5] Darwin, C. (1928/04/02) *Proc. Roy. Soc.* **118**, 654 – 680.

[6] Ashcroft, N. and Mermin, N. (1976) Solid State Physics, Cengage Learning, .

[7] Coleman, P. (2004) Lecture Notes, http://www.physics.rutgers.edu/˜coleman/, .

[8] Sakurai, J. (1994) Modern Quantum Mechanics, Addition Wesley Longman, .

[9] Inkson, J. (1984) Many-body theory of solids - An Introduction, Plenum Press, New York.

[10] Mahan, G. D. (1993) Many-Particle Physics, Plenum Press, New York and London.

[11] Benatti, F., Floreanini, R., and Marzolino, U. (2012) *Annals of Physics* **327(5)**, 1304 – 1319.

[12] Hartree, D. (1928/01/) *Proceedings of the Cambridge Philosophical Society* **24**, 89 – 132.

[13] Fock, V. (1930//) *Zeitschrift fur Physik* **61(1-2)**, 126 – 148.

[14] Hohenberg, P. and Kohn, W. (1964) *Phys. Rev.* **136**, B864.

[15] Levy, M. Sep 1982 *Phys. Rev. A* **26(3)**, 1200–1208.

[16] Lieb, E. (1983) *Int. J. Quantum Chem.* **24(3)**, 243.

[17] Kohn, W. and Sham, L. (1965) *Phys. Rev.* **140**, A1133.

[18] Anderson, P. W. (1961) *Phys. Rev.* **124**, 41.

[19] Uhrig, G. (2005) Correlated Fermionic Systems: Fermi Liquid and Luttinger Liquid, t1.physik.tu-dortmund.de/uhrig/teaching/liquids_ss2004/liquids_skript.pdf, .

[20] Aryasetiawan, F., Imada, M., Georges, A., Kotliar, G., Biermann, S., and Lichtenstein, A. I. (2004) *Phys. Rev. B* **70**, 195104.

[21] Aryasetiawan, F., Karlsson, K., Jepsen, O., and Schönberger, U. (2006) *Phys. Rev. B* **74**, 125106.

[22] Werner, P., Casula, M., Miyake, T., Aryasetiawan, F., Millis, A. J., and Biermann, S. (2012) *Nature Physics* , 1745 – 2481.

[23] Hubbard, J. (1963) *Proc. Roy. Soc.* **A 276**, 238.

[24] Lichtenstein, A. I. and Katsnelson, M. I. Mar 1998 *Phys. Rev. B* **57(12)**, 6884–6895.

[25] Bruus, H. and Flensberg, K. (2004) Many-body quantum theory in condensed matter physics: an introduction, Oxford University Press, USA, .

[26] Galitskii, V. M. and Migdal, A. B. (1958) *Zh. Eksp. Teor. Fiz.* **34**, 139 Sov. Phys. JETP **7**, 96 (1958).

[27] Di Marco, I., Minár, J., Chadov, S., Katsnelson, M. I., Ebert, H., and Lichtenstein, A. I. (2009) *Phys. Rev. B* **79(11)**, 115111.

[28] Georges, A., Kotliar, G., Krauth, W., and Rozenberg, M. J. (1996) *Rev. Mod. Phys.* **68**, 13.
[29] Held, K., Anisimov, V., Eyert, V., Keller, G., McMahan, A., Nekrasov, I., and Vollhardt, D. (2003) *Advances in Solid State Physics* **43**, 267–286.
[30] Kotliar, G. and Vollhardt, D. (2004) *Physics Today* **57(3)**, 53–59.
[31] Kotliar, G., Savrasov, S., Haule, K., Oudovenko, V., Parcollet, O., and Marianetti, C. (2006) *Rev. Mod. Phys.* **78**, 865.
[32] Held, K. (2007) *Advances in Physics* **56(6)**, 829–926.
[33] Parks, R. (1977) Valence Instabilities and Related Narrow-Band Phenomena, Plenum Press, New York.
[34] E. Müller-Hartmann, B. Roden, and D. Wohlleben, (ed.) Proceedings of the International Conference on Valence Fluctuations volume **47–48**, Elsevier B.V. (1985).
[35] Lawrence, J., Riseborough, P., and Parks, R. (1981) *Rep. Prog. Phys.* **44(1)**, 1–84.
[36] Riseborough, P. S. (2000) *Adv. Phys.* **49(3)**, 257–320.
[37] Varma, C. M. Apr 1976 *Rev. Mod. Phys.* **48(2)**, 219–238.
[38] Wachter, P. (1994) Intermediate valence and heavy fermions In Handbook on the Physics and Chemistry of Rare Earth volume **19**, pp. 177–382 Elsevier Science B.V.
[39] Felner, I. and Nowik, I. Jan 1986 *Phys. Rev. B* **33(1)**, 617–619.
[40] Stevens, K. W. H. (1976) *J. Phys. C* **9(8)**, 1417–1428.
[41] Irkhin, V. Y. and Katsnelson, M. I. (1984) *Journal of Physics C: Solid State Physics* **17(27)**, L699–L703.
[42] Irkhin, V. Y. and Katsnelson, M. I. (1986) *Solid State Commun.* **58(12)**, 881 – 884.
[43] Kasaya, M., Liu, B., Sera, M., Kasuya, T., Endoh, D., Goto, T., and Fujimura, T. (1985) *Journal of Magnetism and Magnetic Materials* **52(1)**, 289–292.
[44] Kletowski, Z. (1987) *Solid State Communications* **62(11)**, 745 – 747.
[45] Moreschini, L., Dallera, C., Joyce, J. J., Sarrao, J. L., Bauer, E. D., Fritsch, V., Bobev, S., Carpene, E., Huotari, S., Vankó, G., Monaco, G., Lacovig, P., Panaccione, G., Fondacaro, A., Paolicelli, G., Torelli, P., and Grioni, M. (2007) *Phys. Rev. B* **75(3)**, 035113.
[46] Chazalviel, J. N., Campagna, M., Wertheim, G. K., and Schmidt, P. H. Nov 1976 *Phys. Rev. B* **14(10)**, 4586–4592.
[47] Shigemoto, A., Imada, S., Sekiyama, A., Yamasaki, A., Irizawa, A., Muro, T., Saitoh, Y., Iga, F., Takabatake, T., and Suga, S. (2005) *J. Electron. Spectros. Relat. Phenom.* **144-147**, 671–673.
[48] Allen, G. C. and Hush, N. S. (1967) Intervalence-transfer absorption. part 1. qualitative evidence for intervalence-transfer absorption in inorganic systems in solution and in the solid state In Progr. Inorg. Chem. pp. 357–389 Wiley.
[49] Robin, M. B. and Day, P. (1968) Mixed valence chemistry-a survey and classification In Adv. Inorg. Chem. volume **10**, pp. 247–422 Elsevier B.V.
[50] Jayaraman, A., Narayanamurti, V., Bucher, E., and Maines, R. G. Aug 1970 *Phys. Rev. Lett.* **25(6)**, 368–370.
[51] Maple, M. B. and Wohlleben, D. Aug 1971 *Phys. Rev. Lett.* **27(8)**, 511–515.
[52] Falicov, L. M. and Kimball, J. C. May 1969 *Phys. Rev. Lett.* **22(19)**, 997–999.

[53] Martin, R. M. and Allen, J. W. (1979) *J. Appl. Phys.* **50(B11)**, 7561–7566.
[54] Bucher, B., Schlesinger, Z., Canfield, P. C., and Fisk, Z. Jan 1994 *Phys. Rev. Lett.* **72(4)**, 522–525.
[55] Cooley, J. C., Aronson, M. C., Fisk, Z., and Canfield, P. C. Feb 1995 *Phys. Rev. Lett.* **74(9)**, 1629–1632.
[56] Kasuya, T. (1996) *Phys. B: Condens. Matter.* **223-224**, 402–408.
[57] Nemkovski, K. S., Mignot, J.-M., Alekseev, P. A., Ivanov, A. S., Nefeodova, E. V., Rybina, A. V., Regnault, L.-P., Iga, F., and Takabatake, T. (2007) *Phys. Rev. Lett.* **99(13)**, 137204.
[58] Yamaoka, H., Tsujii, N., Yamamoto, K., Vlaicu, A. M., Oohashi, H., Yoshikawa, H., Tochio, T., Ito, Y., Chainani, A., and Shin, S. (2008) *Phys. Rev. B* **78(4)**, 045127.
[59] Saso, T. and Harima, H. (2003) *J. Phys. Soc. Jpn.* **72**, 1131–1137.
[60] Dallera, C., Grioni, M., Shukla, A., Vankó, G., Sarrao, J. L., Rueff, J. P., and Cox, D. L. Apr 2002 *Phys. Rev. Lett.* **88(19)**, 196403.
[61] Antonov, V. N., Harmon, B. N., and Yaresko, A. N. Oct 2002 *Phys. Rev. B* **66(16)**, 165209.
[62] Takegahara, K. and Kasuya, T. (1990) *J. Phys. Soc. Jpn.* **59(9)**, 3299–3306.
[63] Yanase, A. and Harima, H. (1992) *Prog. Theor. Phys. Suppl.* **108**, 19–25.
[64] Wills, J., Eriksson, O., Alouani, M., and Price, D. (2000) Full-potential lmto total energy and force calculations In Hugues Dreysse, (ed.), Electronic Structure and Physical Properies of Solids, pp. 148–167 Springer Verlag.
[65] Cuthill, J. R., McAlister, A. J., Erickson, N. E., and Watson, R. E. (1974) *AIP Conference Proceedings* **18(1)**, 1039–1043.
[66] Brandow, B. (1977) *Advances in Physics* **26(5)**, 651–808.
[67] Imada, M., Fujimori, A., and Tokura, Y. (1998) *Rev. Mod. Phys.* **70**, 1039.
[68] deBoer, J. H. and Verwey, E. J. W. (1937) *Proceedings of the Physical Society* **49(4S)**, 59.
[69] Mott, N. F. and Peierls, R. (1937) *Proceedings of the Physical Society* **49(4S)**, 72.
[70] Mott, N. F. (1949) *Proc. Phys. Soc. A* **62**, 416.
[71] Shen, Z.-X., List, R. S., Dessau, D. S., Wells, B. O., Jepsen, O., Arko, A. J., Barttlet, R., Shih, C. K., Parmigiani, F., Huang, J. C., and Lindberg, P. A. P. (1991) *Phys. Rev. B* **44**, 3604–3626.
[72] Shen, Z.-X. and Dessau, D. (1995) *Physics Reports* **253(1-3)**, 1 – 162.
[73] Zaanen, J., Sawatzky, G. A., and Allen, J. W. (1985) *Phys. Rev. Lett.* **55**, 418–421.
[74] Andersen, O. K., Skriver, H. L., Nohl, H., and Johansson, B. (1980) *Journal of Pure and Applied Chemistry* **52(1)**, 93–118.
[75] Dufek, P., Blaha, P., Sliwko, V., and Schwarz, K. (1994) *Phys. Rev. B* **49**, 10170–10175.
[76] Svane, A. and Gunnarsson, O. (1990) *Phys. Rev. Lett.* **65**, 1148.
[77] Anisimov, V. I., Zaanen, J., and Andersen, O. K. (1991) *Phys. Rev. B* **44**, 943–954.
[78] Anisimov, V. I., Solovyev, I. V., Korotin, M. A., Czyżyk, M. T., and Sawatzky, G. A. (1993) *Phys. Rev. B* **48**, 16929–16934.
[79] Kobayashi, S., Nohara, Y., Yamamoto, S., and Fujiwara, T. (2008) *Phys. Rev. B*

78, 155112.
[80] Jiang, H., Gomez-Abal, R. I., Rinke, P., and Scheffler, M. (2010) *Phys. Rev. B* **82**, 045108.
[81] Rödl, C., Fuchs, F., Furthmüller, J., and Bechstedt, F. (2009) *Phys. Rev. B* **79**, 235114.
[82] Tjernberg, O., Söderholm, S., Chiaia, G., Girard, R., Karlsson, U. O., Nylén, H., and Lindau, I. (1996) *Phys. Rev. B* **54**, 10245–10248.
[83] Fujimori, A., Minami, F., and Sugano, S. (1984) *Phys. Rev. B* **29**, 5225–5227.
[84] Eder, R. (2008) *Phys. Rev. B* **78**, 115111.
[85] Ren, X., Leonov, I., Keller, G., Kollar, M., Nekrasov, I., and Vollhardt, D. (2006) *Phys. Rev. B* **74(19)**, 195114.
[86] Kuneš, J., Anisimov, V. I., Lukoyanov, A. V., and Vollhardt, D. (2007) *Phys. Rev. B* **75(16)**, 165115.
[87] Kuneš, J., Anisimov, V. I., Skornyakov, S. L., Lukoyanov, A. V., and Vollhardt, D. (2007) *Phys. Rev. Lett.* **99(15)**, 156404.
[88] Yin, Q., Gordienko, A., Wan, X., and Savrasov, S. Y. (2008) *Phys. Rev. Lett.* **100**, 066406.
[89] Kuneš, J., Lukoyanov, A. V., Anisimov, V. I., Scalettar, R. T., and Pickett, W. E. (2008) *Nat. Mater.* **7**, 198–202.
[90] Korotin, D., Kozhevnikov, A., Skornyakov, S., Leonov, I., Binggeli, N., Anisimov, V., and Trimarchi, G. (2008) *The European Physical Journal B* **65**, 91–98.
[91] Karolak, M., Ulm, G., Wehling, T., Mazurenko, V., Poteryaev, A., and Lichtenstein, A. (2010) *Journal of Electron Spectroscopy and Related Phenomena* **181(1)**, 11 – 15.
[92] Amico, L., Fazio, R., Osterloh, A., and Vedral, V. (2008) *Rev. Mod. Phys.* **80**, 517–576.
[93] Vedral, V., Plenio, M. B., Rippin, M. A., and Knight, P. L. (1997) *Phys. Rev. Lett.* **78**, 2275–2279.
[94] Carbone, C., Veronese, M., Moras, P., Gardonio, S., Grazioli, C., Zhou, P. H., Rader, O., Varykhalov, A., Krull, C., Balashov, T., Mugarza, A., Gambardella, P., Lebègue, S., Eriksson, O., Katsnelson, M. I., and Lichtenstein, A. I. Mar 2010 *Phys. Rev. Lett.* **104**, 117601.
[95] Trahan, J., Goodrich, R. G., and Watkins, S. F. Oct 1970 *Phys. Rev. B* **2**, 2859–2863.

Acta Universitatis Upsaliensis

Digital Comprehensive Summaries of Uppsala Dissertations from the Faculty of Science and Technology 936

Editor: The Dean of the Faculty of Science and Technology

A doctoral dissertation from the Faculty of Science and Technology, Uppsala University, is usually a summary of a number of papers. A few copies of the complete dissertation are kept at major Swedish research libraries, while the summary alone is distributed internationally through the series Digital Comprehensive Summaries of Uppsala Dissertations from the Faculty of Science and Technology.

Distribution: publications.uu.se
urn:nbn:se:uu:diva-173300

ACTA
UNIVERSITATIS
UPSALIENSIS
UPPSALA
2012